Final Report
Volume 1-Final Summary Report
(Item 2199; ORA 125-4262)

Resilient Moduli of Raw and Stabilized Aggregate Bases and Evaluation of Layer Coefficients for AASHTO Flexible Pavement Design

Submitted to:
Lawrence J. Senkowski
Assistant Division Engineer
Research, Development and Technology Transfer
Oklahoma Department of Transportation
200 N.E. 21st Street, Oklahoma City, Oklahoma 73105-3204

Prepared by:
Musharraf M. Zaman
Joakim G. Laguros
Ping Tian
Jianhua Zhu
Kundan K. Pandey

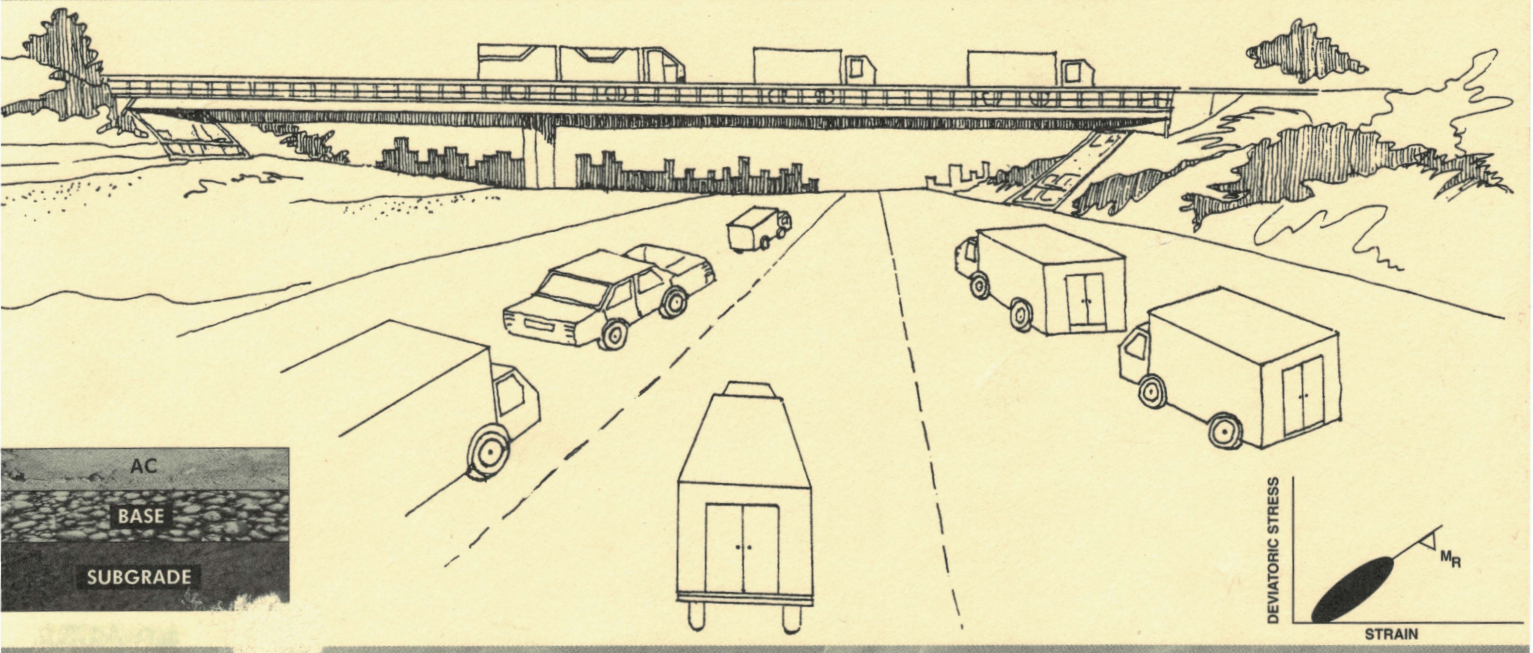

From: School of Civil Engineering and Environmental Science, and The Office of Research Administration,
The University of Oklahoma, Norman, Oklahoma 73019
August 1998

RESILIENT MODULI OF RAW AND STABILIZED AGGREGATE BASES AND EVALUATION OF LAYER COEFFICIENTS FOR AASHTO FLEXIBLE PAVEMENT DESIGN

FINAL SUMMARY REPORT
(Item 2199; ORA 125-4262)

VOLUME I

Submitted to:
Lawrence J. Senkowski
Assistant Division Engineer
Research, Development and Technology Transfer
Oklahoma Department of Transportation
200 N.E. 21st Street
Oklahoma City, Oklahoma 73105-3204

Prepared by:

Musharraf M. Zaman
Joakim G. Laguros
Ping Tian
Jianhua Zhu
Kundan K. Pandey

School of Civil Engineering and Environmental Science
The University of Oklahoma
Norman, Oklahoma 73019

From:
The Office of Research Administration
The University of Oklahoma
Norman, Oklahoma 73019

August 1998

TECHNICAL REPORT STANDARD TITLE PAGE

1. REPORT NO.	2. GOVERNMENT ACCESSION NO.	3. RECIPIENT'S CATALOG NO.
FHWA/OK 98(05)		

4. TITLE AND SUBTITLE	5. REPORT DATE
"Resilient Moduli of Raw and Stabilized Aggregate Bases and Evaluation of Layer Coefficients for AASHTO Flexible Pavement Design" Volume I	August 1998
	6. PERFORMING ORGANIZATION CODE
7. AUTHOR(S) Musharraf M. Zaman, Joakim G. Laguros, Ping Tian, Jianhua Zhu, Kundan K. Pandey	8. PERFORMING ORGANIZATION REPORT ORA 125-4262
	10. WORK UNIT NO.
9. PERFORMING ORGANIZATION AND ADDRESS The University of Oklahoma Norman, Oklahoma 73019	11. CONTRACT OR GRANT NO. Item No. 2199
	13. TYPE OF REPORT AND PERIOD COVERED Final Report (Oct. 1994 – Aug. 1998)
12. SPONSORING AGENCY NAME AND ADDRESS Oklahoma Department of Transportation Research, Development and Technology Transfer 200 N.E. 21st Street, Oklahoma City, OK 73105	14. SPONSORING AGENCY CODE

15. SUPPLEMENTARY NOTES
Performed in cooperation with the U.S. Department of Transportation and the Federal Highway Administration.

16. ABSTRACT

A comprehensive study involving laboratory testing of resilient moduli (M_R) of aggregate materials, determination of layer coefficients, and their application in AASHTO flexible pavement design was conducted. Three coarse aggregates, namely, Richard Spur (RS), Sawyer, and Meridian, that are commonly used as subbase/base of roadway pavements in Oklahoma were selected. Based on the Los Angeles abrasion values, the RS and the Sawyer aggregates are considered good quality aggregates, whereas the Meridian is considered a marginal aggregate.

A series of laboratory tests was conducted on the RS and the Sawyer aggregates to investigate the effect of testing procedure, gradation, moisture content, and drainage condition on the M_R values. For the marginal (Meridian) aggregate, the effect of stabilization on the M_R values was investigated in terms of different amount of stabilizing agents and different curing periods. Three different industrial by-products (Class C fly ash, Fluidized bed ash, and Cement-kiln-dust) were used for comparison. The variation in M_R values due to these effects was examined and the material parameters k_1 and k_2 required by the AASHTO design equation were evaluated

The AASHTO flexible pavement design methodology uses layer coefficients to relate the structural design of the pavement with its performance. Layer coefficient values (a_2) for the base course layer were determined for each combination of three different M_R values of asphalt concrete (AC) layer, three different AC layer thicknesses, and four different base layer thicknesses. Furthermore, the effects of gradation, moisture content, drainage condition, and different stabilizing agents on layer coefficients were investigated. Finally, regression equations for predicting the layer coefficients of base layers were developed for the selected aggregates and their applications in pavement design were illustrated through design examples.

17. KEY WORDS	18. DISTRIBUTION STATEMENT
Resilient Modulus, Aggregate Base, Gradation, Moisture, Drainage Condition, Stabilization, Fly Ash, Cement-Kiln-Dust.	No restrictions. This publication is available from the Office of Research, Oklahoma DOT.

19. SECURITY CLASSIF. (OF THIS REPORT)	20. SECURITY CLASSIF. (OF THIS PAGE)	21. NO. OF PAGES	22. PRICE
Unclassified	Unclassified	155	

DISCLAIMER

The contents of this report reflect the views of the authors who are responsible for the facts and the accuracy of the information presented herein. The contents do not necessarily reflect the official views of the Oklahoma Department of Transportation. This report does not constitute a standard, specification, or regulation.

ACKNOWLEDGMENTS

The authors would like to express their sincere appreciation to Mr. Lawrence Senkowski, Dr. James B. Nevels, Mr. Curtis Hayes, and Mr. Wilson Brewer from the Oklahoma Department of Transportation (ODOT), for their help and cooperation throughout the course of this study. Mr. Lawrence Senkowski provided the over-all direction for defining the project goals and objectives. Dr. James B. Nevels assisted in the experimental work and provided valuable suggestions during the research. Mr. Curtis Hayes and Mr. Wilson Brewer helped in locating quarries, sampling and transporting aggregate materials.

The authors are thankful to Mr. Mike Schmitz of the School of Civil Engineering and Environmental Science at the University of Oklahoma for his assistance whenever technical problems surfaced during the laboratory testing. Mr. Eddie Eckart and Mr. Kin-Lam Ng assisted the research team in specimen preparation and testing. Their help is greatly appreciated. The authors would also like to thank Dr. Dar-Hao Chen and Mr. Luping Yi for their help during the initial work of this research, and Ms. Kathy Maxie for typing this manuscript.

The authors are indebted to the Brazil Creek Minerals, Inc., in Fort Smith, Arkansas, and the Blue Circle Cement, Inc., in Tulsa, Oklahoma, for supplying the fly ash and the cement kiln dust as the stabilization agents for this research.

Finally, a word of thanks is due the ODOT panel members who provided suggestions during the conduct of this study and for critically reviewing this report.

TABLE OF CONTENTS

The report covered by this study is presented in four volumes, as indicated below:

- **Volume I: Final Summary Report**
- **Volume II: Richard Spur and Sawyer Aggregates**
- **Volume III: Meridian Aggregate Stabilized with Fly Ash and Fluidized Bed Ash**
- **Volume IV: Meridian Aggregate Stabilized with Cement-Kiln-Dust**

DISCLAIMER ..... **iii**
ACKNOWLEDGMENTS ..... **iv**
TABLE OF CONTENTS ..... **v**
LIST OF TABLES ..... **viii**
LIST OF FIGURES ..... **xi**
SUMMARY ..... **xiv**

CHAPTER 1 INTRODUCTION **1-1**
1.1 Problem Statement 1-1
1.2 Objectives and Tasks 1-4
1.3 Format of the Report 1-6

CHAPTER 2 MATERIALS USED IN THE STUDY AND THEIR FUNDAMENTAL PROPERTIES **2-1**
2.1 Introduction 2-1
2.2 Granular Base Aggregates 2-1
2.3 Fundamental Material Properties 2-2
2.3.1 Grain Size Distribution 2-2
2.3.2 Moisture-Density Relationship 2-3
2.3.3 Los Angles Abrasion 2-4
2.3.4 Specific Gravity 2-5
2.4 Stabilizing Agents 2-6
2.4.1 Class C Fly Ash 2-6
2.4.2 Fluidized Bed Ash 2-6
2.4.3 Cement-Kiln-Dust 2-7

CHAPTER 3 RESILIENT MODULUS AND LAYER COEFFICIENTS OF GOOD QUALITY AGGREGATES 3-1
3.1 Introduction 3-1
3.2 Preparation of Test Specimen 3-1
3.3 Testing Procedure and Equipment 3-3
3.4 Presentation and Discussion of Test Results 3-5
3.4.1 Effect of Testing Procedure 3-5
3.4.2 Effect of Gradation 3-11
3.4.3 Effect of Moisture Content 3-14
3.4.4 Effect of Drainage Condition 3-17
3.4.5 Variability of Experimental Results 3-20
3.5 Statistical Correlations 3-22
3.5.1 Determination of Material Model Parameters 3-22
3.5.2 Multiple Linear Regression Model 3-23
3.6 Evaluation of Layer Coefficient 3-28
3.6.1 Layer Coefficients 3-28
3.6.2 Determination of Equivalent Layer Bulk Stress (ELBK) 3-29
3.6.3 Determination of Layer Coefficients 3-30
3.7 Design of AASHTO Flexible Pavements 3-34

CHAPTER 4 RESILIENT MODULUS AND LAYER COEFFICIENTS OF STABILIZED AGGREGATES 4-1
4.1 Introduction 4-1
4.2 State-of-the-Art of Stabilization of Highway Bases and Subbases 4-1
4.3 Laboratory Study of Stabilized and Raw Marginal Aggregate 4-4
4.3.1 Class C Fly-Ash (CFA) Stabilization 4-5
4.3.2 Fluidized Bed Ash (FBA) Stabilization 4-10
4.3.3 Cement-Kiln-Dust (CKD) Stabilization 4-11
4.4 Effect of Stabilizing Agent Type 4-13
4.5 Effect of Stabilization on Unconfined Compression Strength and Elastic Modulus 4-15
4.6 Variability of Strength Properties 4-18

4.7 Evaluation of Layer Coefficients 4-19
4.7.1 Effect of Amount of Stabilizing Agent 4-21
4.7.2 Effect of Curing Time 4-23
4.7.3 Effect of Stabilizing Agent Type 4-24
4.8 Design of an AASHTO Flexible Pavement 4-24

CHAPTER 5 MICROANALYSIS OF CHEMICALLY STABILIZED AGGREGATES 5-1
5.1 Introduction 5-1
5.2 Microanalysis Results 5-1
5.2.1 X-ray Diffraction 5-1
5.2.2 Scanning Electron Microscopy 5-2

CHAPTER 6 CONCLUSIONS AND RECOMMENDATIONS 6-1
6.1 Conclusions 6-1
6.2 Recommendations 6-5

REFERENCES 7-1

LIST OF TABLES

Table 2-1 The Optimum Moisture Content (OMC), Maximum Dry Density (MDD) of Raw and Stabilized Aggregates 2-8

Table 2-2 Chemical Composition of Stabilizing Agents Used 2-9

Table 3-1 Comparison of Different AASHTO Resilient Modulus Testing Procedures 3-38

Table 3-2 Unconfined Compressive Strength (U_c), Cohesion (C), and Friction Angle (ϕ) Measured for the RS and the Sawyer Aggregates 3-39

Table 3-3 Salient Features of AASHTO T 292-91I and T 294-94 Testing Procedures 3-40

Table 3-4 Measured Recoverable Deformations from the T 292-91I and T 294-94 Testing Methods 3-41

Table 3-5 Confidence Level Calculated from the Measured M_R Values (RS Aggregate at Median Gradation and 2% below OMC) 3-42

Table 3-6 Confidence Level Calculated from the Measured M_R Values (Sawyer Aggregate at Finer Limit Gradation and OMC) 3-43

Table 3-7 Material Parameters k_1 and k_2 of the RS and the Sawyer Aggregates 3-44

Table 3-8 Measure of Fit for Multiple M_R Models with Different Variables 3-45

Table 3-9 The Various Combinations of AC Layer Thickness (D_{ac}), AC Layer M_R (E_{ac}), Base Layer Thickness (D_2), and the Corresponding Case Numbers and ELBK 3-46

Table 3-10 Layer Coefficients (a_2) of the RS Aggregate at Different Gradations 3-47

Table 3-11 Layer Coefficients (a_2) of the RS Aggregate at Different Moisture Contents 3-48

Table 3-12 Layer Coefficients (a_2) of the RS Aggregate at Different Drainage Conditions 3-49

Table 3-13 Layer Coefficients (a_2) of the Sawyer Aggregate at Different Gradations 3-50

Table 3-14	Layer Coefficients (a_2) of the Sawyer Aggregate at Different Moisture Contents	3-51
Table 3-15	Layer Coefficients (a_2) of the Sawyer Aggregate at Different Drainage Conditions	3-52
Table 3-16	Measure of Fit for Layer Coefficient Models with Different Variables	3-53
Table 3-17	Comparison of SN and ESAL for the RS Aggregate at the Different Cases	3-54
Table 3-18	Comparison of SN and ESAL for the Sawyer Aggregate at the Different Cases	3-55
Table 4-1	The Optimum Moisture Content (w_{opt})-Maximum Dry Density (γ_{dmax}) of Stabilized Meridian Aggregate and Curing Period for M_R Test	4-27
Table 4-1a	Range of RM Values (MPa) of the Stabilized Meridian Aggregate	4-27
Table 4-2	Material Parameters k_1 and k_2 of the Raw and Stabilized Aggregates	4-28
Table 4-3	Unconfined Compressive Strength and the Elastic Modulus of the Stabilized Aggregates	4-29
Table 4-4	Layer Coefficients (a_2) for Raw Meridian 1 Aggregates and Richard Spur Aggregates	4-30
Table 4-5	Layer Coefficients (a_2) for 28-day Cured CFA Stabilized Meridian Aggregate	4-31
Table 4-6	Layer Coefficients (a_2) for 90-day Cured CFA Stabilized Meridian Aggregate	4-32
Table 4-7	Layer Coefficients (a_2) for 28-day Cured FBA Stabilized Meridian Aggregate	4-33
Table 4-8	Layer Coefficients (a_2) for 90-day Cured FBA Stabilized Meridian Aggregate	4-34
Table 4-9	Layer Coefficients (a_2) of the Raw and CKD Stabilized Meridian Aggregate	4-35
Table 4-10	Layer Coefficients (a_2) of the 15% CKD Stabilized Meridian Aggregate Cured for Different Periods	4-36

Table 4-11 Comparison of SN and ESAL of the Raw and Stabilized Aggregate Bases..... 4-37

Table 5-1 Minerals Identified by X-ray Diffraction Analysis..... 5-4

LIST OF FIGURES

Figure 2-1 Map of Oklahoma Showing the Location of the Aggregate Sources 2-10

Figure 2-2 Grain Size Distribution of the Three Aggregates and the ODOT Specified Gradations 2-11

Figure 3-1 Equipment Used for the Preparation of M_R Testing Specimen 3-56

Figure 3-2 Overall Setup of the M_R Testing Equipment 3-57

Figure 3-3 Haversine, Triangular, and Rectangular Waveforms Used 3-58

Figure 3-4 Mean M_R Values from Different Loading Waveforms (RS Aggregate) 3-59

Figure 3-5 Mean M_R Values from the T 292-91I and T 294-94 Methods (RS Aggregate) 3-59

Figure 3-6 Mean M_R Values of the RS Aggregate at Different Gradations 3-60

Figure 3-7 Mean M_R Values of the Sawyer Aggregate at Different Gradations. 3-60

Figure 3-8 Mean M_R Values of the RS Aggregate at Different Moisture Contents 3-61

Figure 3-9 Mean M_R Values of the Sawyer Aggregate at Different Moisture Contents 3-61

Figure 3-10 Pore Pressure Measured in Undrained I and II M_R Tests (RS Aggregate) 3-62

Figure 3-11 Pore Pressure Measured in the Undrained I and II M_R Tests (Sawyer Aggregate) 3-62

Figure 3-12 Mean M_R Values of the RS Aggregate from the Drained and Undrained Tests 3-63

Figure 3-13 Mean M_R Values of the Sawyer Aggregate from the Drained and Undrained Tests 3-63

Figure 3-14 Variation of k_1 Values with the No. 200 (0.075 mm) Percent Passing 3-64

Figure 3-15 Variation of k_2 Values with the No. 200 (0.075 mm) Percent Passing 3-64

Figure 3-16 Variation of k_1 Values with Moisture Content 3-65

Figure 3-17 Variation of k_2 Values with Moisture Content 3-65

Figure 3-18 Variation of k_1 Values with Drainage Condition 3-66

Figure 3-19 Variation of k_2 Values with Drainage Condition 3-66

Figure 3-20 Experimental and the Multiple Model Predicted M_R Values of the RS Aggregate 3-67

Figure 3-21 Experimental and the Multiple Model Predicted M_R Values of the Sawyer Aggregate 3-68

Figure 3-22 Pavement Configuration Used for the ELBK Calculation 3-69

Figure 4-1 Mean M_R Values of Raw and 7-day Cured CFA Stabilized Aggregate 4-38

Figure 4-2 Mean M_R Values of Raw and 28-day Cured CFA Stabilized Aggregate 4-38

Figure 4-3 Mean M_R Values of Raw and 90-day Cured CFA Stabilized Aggregate 4-39

Figure 4-4 Mean M_R Values of Raw and 7-day Cured FBA Stabilized Aggregate 4-39

Figure 4-5 Mean M_R Values of Raw and 28-day Cured FBA Stabilized Aggregate 4-40

Figure 4-6 Mean M_R Values of Raw and 90-day Cured FBA Stabilized Aggregate 4-40

Figure 4-7 Mean M_R Values of Raw and 7-day Cured CKD Stabilized Aggregate 4-41

Figure 4-8 Mean M_R Values of Raw and 15-day Cured CKD Stabilized Aggregate 4-41

Figure 4-9 Relationship Between Resilient Modulus and Amount of CFA 4-42

Figure 4-10 Relationship between Resilient Modulus and Curing Period for 10% CFA-Stabilized Aggregate 4-43

Figure 4-11 Relationship between Resilient Modulus and Amount of FBA 4-44

Figure 4-12 Relationship between Resilient Modulus and Curing Period for 10% FBA-Stabilized Aggregate 4-45

Figure 4-13 Relationship Between Resilient Modulus and Amount of CKD 4-46

Figure 4-14 Relationship between Resilient Modulus and Curing Period for 15% CKD-Stabilized Aggregate 4-47

Figure 4-15 Relationship between Increase in Resilient Modulus and Bulk Stress for 28-day Cured Aggregate Stabilized with Different Agents (15%) 4-48

Figure 4-16 Layer Coefficient Versus Thickness of Base Layer for Different Stabilizing Agents 4-49

Figure 5-1 (a) X-Ray Diffractogram of the Raw Meridian Aggregate 5-5

Figure 5-1 (b) X-Ray Diffractogram of the 28-day Cured Aggregate Stabilized with 10% FBA 5-6

Figure 5-2 Micrograph of the Raw Meridian Aggregate..... 5-7

Figure 5-3 Micrographs of the 28-day Cured Aggregate Stabilized with 10% FBA 5-8

SUMMARY

A comprehensive study involving laboratory testing of resilient moduli (M_R) of aggregate materials, determination of layer coefficients, and their application in AASHTO flexible pavement design was conducted. Three coarse aggregates, namely, Richard Spur (RS), Sawyer, and Meridian, that are commonly used as subbase/base of roadway pavements in Oklahoma were selected. Based on the Los Angeles abrasion (LA) values, the RS (LA = 24) and the Sawyer (LA = 28) aggregates are considered good quality aggregates, whereas the Meridian (LA = 38) is considered a marginal aggregate. A series of laboratory tests on the RS and the Sawyer aggregates was conducted to investigate the effect of testing procedure, gradation, moisture content, and drainage condition on the M_R values. For the marginal (Meridian) aggregate, the effect of stabilization on the M_R values was investigated by mixing raw aggregate with three different industrial by-products (Class C fly ash, Fluidized bed ash, and Cement-kiln-dust). The variations of M_R values due to these effects were examined and the material parameters k_1 and k_2 required by the AASHTO design equation were evaluated.

To ensure the same gradation among the three aggregate types, the median gradation of Type A aggregate was selected so as to investigate the effects of testing procedure, moisture content, drainage condition, and stabilization on the M_R values. However, to investigate the effect of gradation on the M_R values, three gradations, namely, the coarser limit, the median, and the finer limit were selected. Additionally, three different moisture contents, namely, optimum moisture content (OMC), 2% below and 2% above the OMC, were selected to examine the effect of moisture content on the M_R values. Two types of undrained M_R tests, undrained I and undrained II, were

conducted in order to simulate the different situations induced by traffic in the field.

A series of M_R tests was performed on stabilized Meridian aggregate specimens to evaluate the effect of type and amount of stabilizing agent and curing time on the M_R values. Three different mix proportions with varying amount of stabilizing agents (5%, 10%, and 15% of the dry weight of the raw aggregate) and three different curing periods, 7-day, 28-day, and 90-day, were used.

Scanning electron microscopy (SEM) and X-ray diffraction (XRD) analyses were conducted on the raw and stabilized Meridian aggregate to qualitatively identify the hydration products and the change in the microstructure of the matrix of the stabilized aggregate and to help interpret the results of the M_R and the unconfined compression tests.

The AASHTO flexible pavement design methodology uses layer coefficients to relate the structural design of the pavement with its performance. Layer coefficient values (a_2) for the base course layer were determined for each combination of three different M_R values of asphalt concrete (AC) layer, three different AC layer thicknesses, and four different base layer thicknesses. A finite element software, MICH-PAVE, was used to calculate the Equivalent Layer Bulk Stress (ELBK). The layer coefficients were determined from the ELBK for each of the above combinations. Furthermore, the effects of gradation, moisture content, drainage condition, and different stabilizing agents on layer coefficients were investigated. Finally, the regression equations for predicting the layer coefficients of base layers were developed for the selected aggregates for practical applications in pavement design and their applications illustrated through design examples.

CHAPTER 1

INTRODUCTION

1.1 PROBLEM STATEMENT

The worsening conditions of roadway pavements have caused a lot of public and legislative concern. Many of the existing roadways were designed using conventional design methods that were available some 25 to 30 years ago. Among other reasons, the ever increasing volume and weight of vehicular and truck traffic as well as extra heavy farm machinery are believed to have contributed to the premature failure of roadway pavements. The maintenance costs of roadway pavements have increased in recent years. In order to improve service quality and life, some improvement in pavement design and maintenance practice is necessary. The 1993 "AASHTO Guide for Design of Pavement Structure" (AASHTO 1993) recognized this need and recommended the use of Resilient Modulus (M_R) instead of the subgrade support values. Subsequently, the Oklahoma Department of Transportation (ODOT) adopted these recommendations. M_R is the property of pavement materials (e.g., soil, aggregate, asphalt mixes, etc.) that reflects their response to a simulated repetitive traffic load.

While the AASHTO recommendations address the importance of material property, they do not adequately address issues such as state standards, acceptability criteria, and construction practice. Moreover, the standards for M_R testing have been revised in recent years. In 1992, AASHTO adopted a new testing method T 294-92I (AASHTO 1992) in accordance with the Strategic Highway Research Program (SHRP) recommendations. The M_R testing procedure in this method is significantly different from

that recommended previously by AASHTO, i.e., the T 274-82 (AASHTO 1982) and T 292-91I (AASHTO 1991) methods. In 1994, AASHTO proposed the standard testing procedure T 294-94 (AASHTO 1994a) which is the same as the interim test procedure T 294-92I, except for the units used. The testing procedures T 292-91I and T 294-92I are the two new versions provided by AASHTO in order to overcome the deficiencies in the T 274-82 method. However, there are a lot of differences between the two procedures in terms of loading duration, number of loading cycles, loading waveform, applied stress sequence, and location of LVDTs. The different testing procedures are expected to affect the measured M_R values (Mohammad et al. 1994), and hence, result in the difference in pavement design.

As a general rule, void ratio has a significant influence on the stiffness characteristics of granular materials (Spangler and Handy 1973). In practical applications, open or coarse aggregates are frequently used in constructing a drainage layer in order to efficiently drain water out of the pavement. Also, aggregates with dissimilar grain size distribution may be used in base/subbase layers to meet various needs of the pavement structure. On the other hand, if the gradation used in the field does not satisfy the gradation requirement established by specifications, certain level of tolerances should be considered in the design to account for such effects. In this study, the gradation variation within the specified range of Type A aggregate (ODOT 1996) was selected and the influence of the gradation variation on the M_R values is investigated.

Drainage of water from pavements has always been an important consideration in pavement design. However, as indicated by the AASHTO design guide (AASHTO 1993), current design methods often result in base courses that do not drain well. The excess

pore water pressure generated, combined with increased traffic volumes and loads, often leads to early distress in the pavement structure. In the AASHTO pavement design procedure (AASHTO 1993), drainage is treated by considering the effect of water on the properties of the pavement layers and their consequences to the structural capacity of a pavement. However, in real design practice, it is still unclear as to how to select the material properties (M_R) during the wetting phase of the pavement under different drainage conditions. It has been pointed out in the design guide that additional work is needed to document the actual effect of drainage on pavement life. Therefore, properly characterizing the material properties during the wetting phase is an extremely important factor in pavement design practice. To this end, the present study addresses the influence of drainage condition on the M_R values of raw aggregates.

The 1993 AASHTO design procedure requires only a single M_R value for each flexible layer to determine the layer coefficient used in the evaluation of structural number (SN) of the entire pavement system (AASHTO 1993). However, the M_R value depends on the state of stress at a specific point in the pavement layer induced by the gravity and traffic loads. Moreover, the M_R values determined from laboratory testing are usually represented as a function of bulk stress rather than a single M_R (Laguros et al. 1993; Zaman et al. 1995). Therefore, when using the AASHTO design guidelines, it becomes imperative to determine only one stress state which will lead to the determination of a single M_R value to be used in the design. However, variations in stresses within base/subbase layers depend on several factors including the thickness and modulus of elasticity of each pavement layer (Chen et al. 1994). This type of variation in material response was not considered in the earlier AASHTO Design Guide

(AASHTO 1972). Also, and unfortunately, the recent AASHTO Guide (AASHTO 1993) does not provide any methodology as to how to consider this M_R - thickness - stress relationship in pavement design.

The research work conducted previously in the School of Civil Engineering and Environmental Science (CEES) at the University of Oklahoma (OU) focused on the effect of aggregate sources on the M_R values and their relationship with other index properties (Laguros et al. 1993; Chen 1994). However, due to limited duration and scope, the previous study did not address the effect of stabilization with industrial by-products such as fly ash (FA), Fluidized bed ash (FBA), and Cement-kiln-dust (CKD) on the M_R values. Although this type of stabilization is frequently used in pavement construction projects in Oklahoma, no systematic study has been conducted in the past on M_R values of raw and stabilized marginal aggregates. The marginal aggregate is defined here as the aggregate that is not considered suitable for use as a base material because the relatively high LA values. As such, their impact on roadway performance is not known. In this study, an attempt is made to compare the structural contributions of a marginal aggregate (Meridian) relative to two good quality aggregates (RS and Sawyer) in terms of their M_R values and the associated layer coefficients.

1.2 OBJECTIVES AND TASKS

This project was pursued with two major objectives in view: (i) determine the resilient moduli and layer coefficients of some commonly encountered aggregate base/subbase materials so that they can be used in the mechanistic design of flexible pavement in accordance with the AASHTO design guidelines; and (ii)

demonstrate if the properties of a marginal aggregate can be improved by chemical stabilization such that it becomes a useful material for a roadway base/subbase. To achieve these objectives, an extensive laboratory testing program was undertaken in which the M_R values of selected raw and stabilized aggregates were evaluated including the effects of some important factors on the M_R values and the layer coefficients. The specific tasks of this study are enumerated below:

1. Determine the resilient moduli of two good quality aggregates by using the AASHTO testing procedure T294-94 and compare the M_R values with those obtained from the T292-91I method. The following four sub-tasks embodied in this task:
    (a) Investigate the reliability and confidence level of the M_R values.
    (b) Investigate the effects of moisture content and gradation on the M_R values.
    (c) Investigate the effects of drainage conditions on the M_R values.
    (d) Investigate the effect of testing procedures (T 292-91I and T 294-94) on the M_R values.
2. Determine the resilient moduli of a marginal aggregate (Meridian) by using the AASHTO T294-94 method, and compare the M_R values with those of the two good quality aggregates (RS and Sawyer).
3. Investigate the effect of stabilization on the M_R values for the marginal aggregate, and selectively perform XRD and SEM analyses.
4. Evaluate layer coefficients, which are required parameters in the design of flexible pavement using the AASHTO guidelines, for all three aggregates. Evaluate the effects of gradation, moisture content, drainage condition, and stabilization on the layer coefficients.

1.3 FORMAT OF THE REPORT

The detailed results from this study are presented in three separate volumes: Volume II (Richard Spur and Sawyer Aggregates) by Tian et al. (1998); Volume III (Meridian Aggregate Stabilized with Fly Ash and Fluidized Bed Ash) by Pandey et al. (1998); and Volume IV (Meridian Aggregate Stabilized with Cement-Kiln-Dust) by Zhu et al. (1998). This report, which is designated as Volume I, is only a comprehensive summary of the results and it consists of six chapters as outlined below.

Following the problem statement and objectives of the study discussed in Chapter 1, Chapter 2 provides a brief discussion on the sources and the fundamental properties of the materials used in the study. Results for the two good quality aggregates (RS and Sawyer) are discussed in Chapter 3, along with the effects of gradation, moisture content, and drainage conditions on the M_R values, unconfined compressive strength (UC), cohesion (C), friction angle (ϕ), and layer coefficient of the raw aggregates. Chapter 4 includes the results from testing the marginal aggregate (Meridian) including the effect of stabilization on the M_R, unconfined compression strength (UC), elastic modulus (EM), and layer coefficients. The effect of the type and amount of stabilizing agent, and curing time is also discussed in this chapter. The microanalyses, including the X-ray diffraction (XRD) and the Scanning electron microscopy (SEM) aimed at revealing the mechanisms of stabilization, are presented in Chapter 5. In Chapter 6, the conclusions of the study are presented, along with the recommendations for further research. This report (Volume I) is prepared as a short report; as such, many figures and tables could not be included herein and only representative results are presented without loss of significant scope of the study.

CHAPTER 2

MATERIALS USED IN THE STUDY AND THEIR FUNDAMENTAL PROPERTIES

2.1 INTRODUCTION

This chapter describes the characteristics and origin of the materials used in this study: three coarse aggregates, namely, Meridian, Richard Spur, and Sawyer, and three types of stabilizing agents, namely, Class C fly ash (CFA), Fluidized bed ash (FBA), and Cement-kiln-dust (CKD). Some fundamental physical properties of these aggregates, such as, the grain size distribution, moisture-density relationship, Los Angeles abrasion, and specific gravity are briefly discussed in this chapter.

2.2 GRANULAR BASE AGGREGATES

Meridian, Richard Spur (RS), and Sawyer aggregates are commonly used in Oklahoma for the construction of pavement bases. These aggregates were selected for this study in cooperation with the Oklahoma Department of Transportation (ODOT). The Meridian aggregate (limestone) was sampled from a quarry at Willis in Marshall County, at two different times, first in April, 1995 and then in March, 1996. The aggregate sampled in 1995 is referred here as Meridian 1 which was used in the fly ash stabilization, while the one sampled in 1996 is referred as Meridian 2 and was used for CKD stabilization.

The RS aggregate (limestone) was sampled from a quarry at Richard Spur in Comanche County, and the Sawyer aggregate (sandstone) was sampled at Sawyer in Choctaw County. The locations of the three quarries are shown in Figure 2-1.

The Meridian aggregate is quarried from the Goodland limestone (Gould 1930). This limestone is pure, semi-crystalline, massive, and white, and is approximately 25 feet (7.5 m) in thickness. Generally, this kind of limestone is moderately hard.

The RS limestones crop out in a series of small hills in southwestern Oklahoma appropriately called the "Limestone Hills" (Rowland 1972); these rocks belong to the Arbuckle Group of Cambrian-Ordovician age, comprising limestones and dolomites primarily of the Kindblade and West Spring Creek formations. This group rock has an overall homogeneity of character, consisting of thin beds of brittle, well indurated limestone and dolostone. The RS limestones can be characterized generally as interbedded, mud-supported and grain-supported rocks with zones containing chert, quartz sand, and silt; hence it is a hard and durable aggregate material. Most of this stone has been used as concrete aggregate and road-base material.

The Sawyer sandstones belong to the Wildhorse Mountain formation of the Jackfork group (Huffman et al. 1975). It presents a light brown to light purple color and stratifies in beds up to 30 cm. It is a quartzitic sandstone and generally is a hard and durable aggregate material.

All aggregates were transported and brought to the laboratory in 20 kg bags, and a total of 80 bags were sampled for each type of aggregate.

2.3 FUNDAMENTAL MATERIAL PROPERTIES

2.3.1 Grain Size Distribution

After the raw aggregates were brought to the laboratory, they were dried in an oven for 24 hours at a temperature of 110 degrees. Then, the grain size distribution test

was performed using a mechanical sieve shaker in accordance with the AASHTO T 27-93 method (AASHTO 1993a). In Figure 2-2, the field gradations for the three aggregates are compared with the gradation limits or band specified by the Oklahoma Standard Specifications for Highway Construction (ODOT 1996) for Type A aggregate.

It is observed that the field gradations for all three aggregates fall within the band of the ODOT 1996 specifications. To investigate the effect of gradation on resilient moduli and layer coefficients, three different gradations were selected. The selected gradations include: the coarser limit (the lower limit of the ODOT gradation band), the median (the median points of the ODOT gradation band), and the finer limit (the upper limit of the ODOT gradation band). Only the RS and the Sawyer aggregates were included in this investigation. On the other hand, to ensure uniformity among the three aggregate types, the median gradation was selected to investigate the effect of stabilization on the properties of the marginal Meridian aggregate.

2.3.2 Moisture-Density Relationship

Moisture-density tests were conducted according to the AASHTO T180-93 method (AASHTO 1993b). The method is designed for determining the relationship between the moisture content and the dry density of aggregates. For the Meridian aggregate, samples were prepared according to the ODOT median gradation, but for the RS and the Sawyer aggregates, samples were prepared following three different gradations: median, coarser limit, and finer limit of the ODOT specifications. The optimum moisture content (OMC), and the maximum dry density (MDD) values for each case are presented in Table 2-1.

In view of Table 2-1, the Meridian 1 and Meridian 2 aggregates have similar OMC and MDD values. However, both aggregates have higher OMC and lower MDD values than those of the RS and the Sawyer aggregates. For the RS and the Sawyer aggregates, the median gradation produced a higher MDD than the coarser limit and the finer limit gradations. This is because the median gradation is well graded and hence produces denser (i.e. less void ratio) specimens than other gradation. It was also observed that the RS aggregate has a higher MDD and a lower OMC than those of the Sawyer aggregate for all of the three gradations selected. For example, the median gradation yielded the MDD of 23.3 kN/m^3 for the RS aggregate and 21.9 kN/m^3 for the Sawyer aggregate. The OMC, however, is 4.6% and 6.0% for the RS and the Sawyer aggregates, respectively. It was also found that the finer limit gradation yielded the highest OMC among the three gradations for the RS and the Sawyer aggregates; one of the possible reasons for this observation is that a larger amount of fines contained in the specimen with the finer limit gradation can absorb more water than specimens with other gradations.

2.3.3 Los Angles Abrasion

The Los Angeles (LA) abrasion test is a measure of degradation of mineral aggregates of standard gradation resulting from a combination of actions including abrasion or attrition, impact, and grinding in a rotating steel drum containing steel spheres or balls. This test is widely used as an indicator of the relative quality or acceptability of aggregates for pavement construction from various sources having similar mineral compositions. The test was conducted according to the AASHTO T 96-94 method

(AASHTO 1994b). Five replicate tests were performed for the Meridian aggregate. Based on the results, it was considered adequate to conduct only four replicate tests instead of five. Hence, only four replicate tests were performed for each of the RS and the Sawyer aggregates.

The data indicate that the LA abrasion value (percent loss) of the Meridian 1 aggregate is from 36 to 40.68 and with a mean value of 37.7 (Pandey et al. 1998), while for the Meridian 2 aggregate the corresponding mean value is 33.26 (Zhu et al. 1998). The limiting LA abrasion value for a good quality aggregate according to the ODOT specifications (ODOT 1996) is 40, above which the aggregate is not considered suitable for use as a base material. It is observed that the LA abrasion value of Meridian 1 is slightly higher than that of Meridian 2, but in view of the ODOT limiting value and relative to the RS and the Sawyer aggregates, both samples approach the category of marginal aggregates. On the other hand, the LA abrasion values of the RS and the Sawyer aggregates range from 23.54 to 24.19 and 27.69 to 29.09 with mean values of 24 and 28, respectively (Tian et al. 1998), which are significantly lower than 40. Therefore, both the RS and the Sawyer aggregates are considered good quality aggregates. Also, the LA values indicate that the RS aggregate is more resistant than both the Sawyer and the Meridian aggregates.

2.3.4 Specific Gravity

Specific gravity (SG) is an important property that is generally used in the calculation of volume occupied by an aggregate in various mixtures. Bulk specific gravity is also used in the computation of voids in an aggregate and in the determination of

moisture (degree of saturation) in a given aggregate mixture. The specific gravity tests were conducted according to the AASHTO T 84-94 method (AASHTO 1994c). For each of the RS and the Sawyer aggregates at the median gradation, four specific gravity tests were conducted (Tian et al. 1998). The SG values of the RS aggregate range from 2.69 to 2.72 with a mean value of 2.7, and the values of the Sawyer aggregate range from 2.54 to 2.56 with a mean value of 2.55.

2.4 STABILIZING AGENTS

Three stabilizing agents, Class C fly ash (CFA), Fluidized bed ash (FBA) and Cement-kiln-dust (CKD) were used in this study. The sources, and physical and chemical properties of these agents are summarized below.

2.4.1 Class C Fly Ash

The Class C fly ash (CFA) used was obtained from Oologah, Oklahoma. The CFA was produced in a coal-fired electric utility plant. The CFA was brought in air tight plastic containers to the laboratory in order to avoid exposure to the atmosphere during transport and storage. The specific gravity of CFA is 2.69, and the average grain size ranges from 0.005 mm to 0.2 mm (Laguros and Zenieris 1987). The chemical characteristics of CFA are presented in Table 2-2.

2.4.2 Fluidized Bed Ash

The Fluidized bed ash (FBA) used was produced by AES Shady Point Operations in Panama, LeFlore County, Oklahoma. Brazil Creek Minerals, Inc., Fort Smith,

Arkansas, supplied the FBA and it was brought to the laboratory in air tight plastic containers in order to avoid any contact with air and moisture during transport and storage. The FBA has a specific gravity of 2.87 and a grain size distribution of 0.005 mm to 2.36 mm. The chemical characteristics of the FBA are also presented in Table 2-2.

2.4.3 Cement-Kiln-Dust

The Cement-kiln-dust (CKD) used was provided by Blue Circle Cement, Inc., located in Tulsa, Oklahoma. The Tulsa plant utilizes two giant rotary kilns of 129.5 m (425 feet) long and 3.657 m (12 feet) in diameter. The CKD is a very fine granular material which is similar in appearance to that of cement and is collected from the exhaust gases of the cement kilns using bag houses. It is an odorless gray powder with a specific gravity of 2.74 and solubility in water of 0.1 to 0.5%. The chemical composition of the CKD is listed in Table 2-2.

From Table 2-2, one can see that CKD has the highest loss on ignition (LOI) value among the three stabilizers due to high content of $CaCO_3$ (64% in CKD and 41% in FBA). The content of free lime (CaO) which is considered beneficial to pozzolanic stabilization is much higher in FBA (18.2%) than in CKD (2% to 3%). Also, one can note that the sum of SiO_2 +Al_2O_3 +Fe_2O_3, which is an influencing factor in the effectiveness of stabilization, is high in CFA, followed by FBA and CKD in that order. The differences in chemical compounds among the stabilizers usually bring about different stabilization effects which will be described in Chapter 4.

Table 2-1 The Optimum Moisture Content (OMC), Maximum Dry Density (MDD) of Raw and Stabilized Aggregates.

Sample Type	Optimum Moisture Content (%)	Maximum Dry Density (kN/m^3)
Meridian 1	7.3	20.9
Meridian 2	7.5	20.9
Meridian 1 + 5% CFA	7.5	20.8
Meridian 1 + 10% CFA	7.7	20.8
Meridian 1 + 15% CFA	8.0	20.5
Meridian 1 + 5% FBA	8.5	20.5
Meridian 1 + 10% FBA	9.0	20.2
Meridian 1 + 15% FBA	9.3	20.0
Meridian 2 + 5% CKD	7.9	20.8
Meridian 2 + 10% CKD	8.3	20.6
Meridian 2 + 15% CKD	8.8	20.3
RS of Median Gradation	4.6	23.3
RS of Finer Limit	5.3	22.8
RS of Coarser Limit	5.5	22.3
Sawyer of Median Grad.	6.0	21.9
Sawyer of Finer Limit	6.3	21.5
Sawyer of Coarser Limit	5.0	21.5

Table 2-2 Chemical Composition of Stabilizing Agents Used

Chemical Compounds	Amount, %		
	CFA	FBA	CKD
Silica (SiO_2)	-	16.94	13.82
Aluminum oxide(Al_2O_3)	-	8.92	3.85
Iron oxide (Fe_2O_3)	-	9.40	1.56
$SiO_2 + Al_2O_3 + Fe_2O_3$	62.08	35.26	19.23
Calcium oxide (CaO)	26.53	41.25	44.07
Magnesium oxide (MgO)	5.44	2.66	1.46
Sulphur oxide (SO_3)	2.00	19.31	2.49
Sodium oxide (Na_2O)	-	-	0.34
Potassium oxide (K_2O)	-	-	1.54
Calcium Carbonate ($CaCO_3$)	-	41.00	64.22
Free lime (CaO)	-	18.20	2 - 3
Loss on ignition (LOI)	0.23	5.34	29.38

Data Source: CFA from Oologah, Oklahoma (Laguros and Zenieris, 1987).
FBA from Brazil Creek Minerals, Inc., Forth Smith, Arkansas, 1991.
CKD from Blue Circle Cement, Inc., 1997.

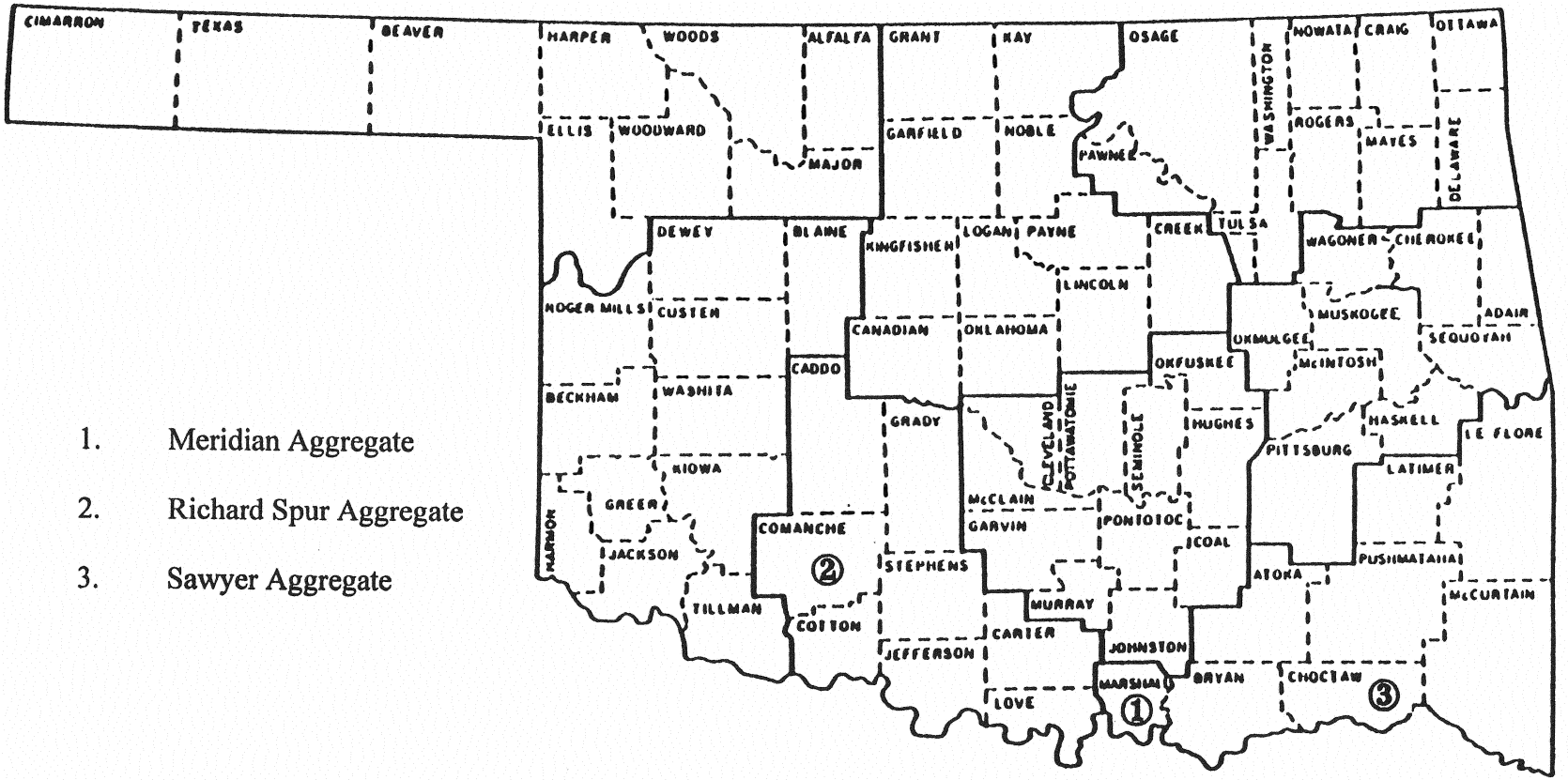

1. Meridian Aggregate
2. Richard Spur Aggregate
3. Sawyer Aggregate

Figure 2-1 Map of Oklahoma Showing the Location of the Aggregate Sources

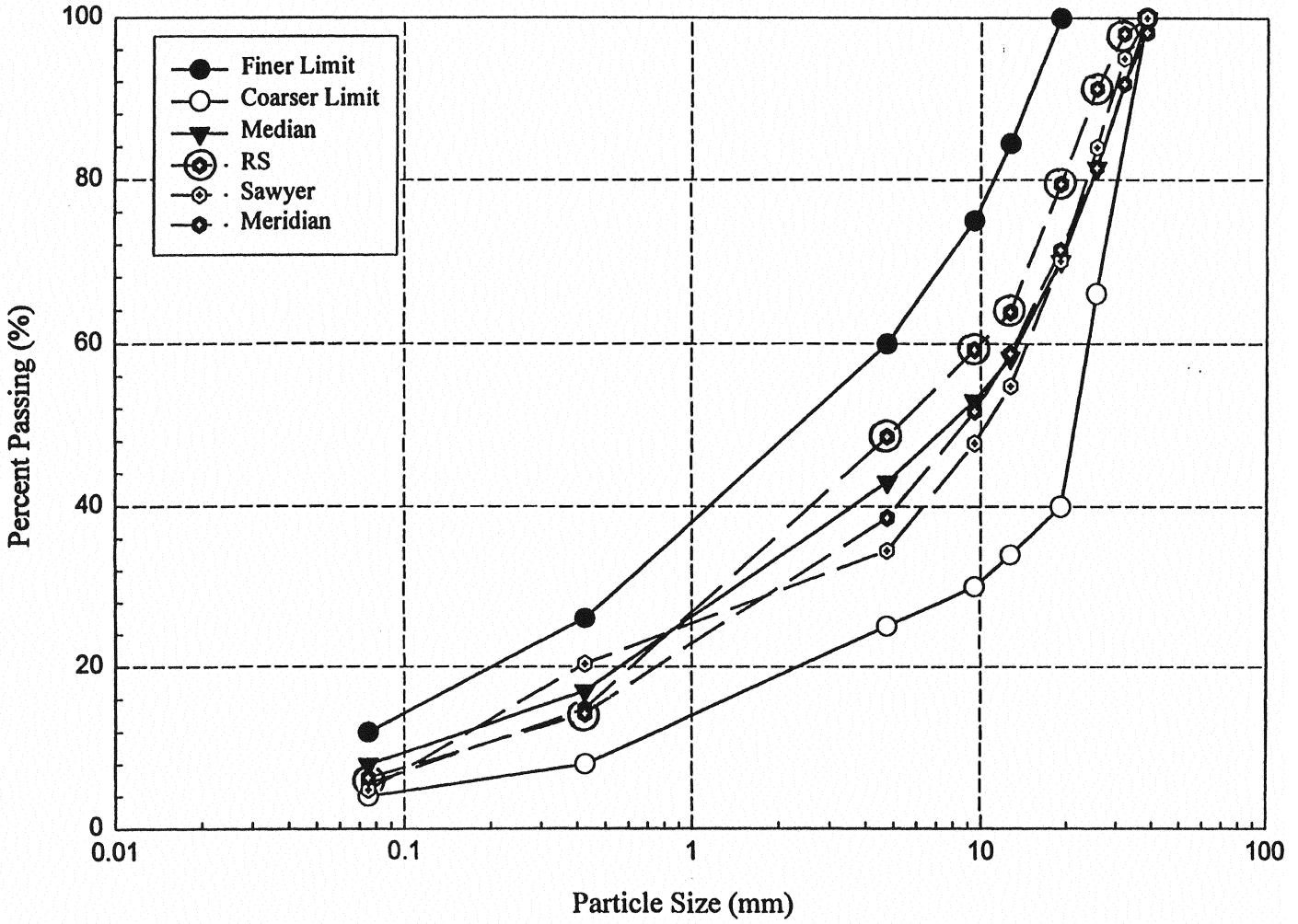

Figure 2-2 Grain Size Distribution of the Three Aggregates and the ODOT Specified Gradations

CHAPTER 3

RESILIENT MODULI AND LAYER COEFFICIENTS OF RS AND SAWYER AGGREGATES

3.1 INTRODUCTION

The resilient moduli for the RS and the Sawyer aggregate obtained from the laboratory testing is presented in this chapter. The influence of testing procedure, gradation, moisture content, and drainage condition on the M_R values is discussed. Also, the variability of the experimental results and its significance are analyzed. The material model parameters, k_1 and k_2 of the k-θ model (for prediction of M_R), are determined and the effects of gradation, moisture content, and drainage condition on these values are examined. Further, multiple linear regression models relating M_R with some of the conventional properties and important influencing factors are established for both aggregates. Finally, the layer coefficients that are used in the AASHTO flexible pavement design are evaluated, and the effects of gradation, moisture content, and drainage condition on the layer coefficients and on the pavement performance are demonstrated by using several design examples.

3.2 PREPARATION OF TEST SPECIMEN

A vibratory compaction method has been recommended by the AASHTO T 294-94 for granular type soils and aggregates (AASHTO 1994a). The desirability of this method is that it prevents the breakage of particles during sample preparation. The AASHTO T 294-94 method suggests using the OMC and MDD for a given aggregate type in accordance with the AASHTO T 180-93 (AASHTO 1993b), and using the OMC

and at least 95% of MDD for specimen preparation. Experimental investigation conducted in the present study indicates that the vibratory compaction method yields the dry density values having a range of 93-97% of the maximum dry density produced by the T 180-93 method.

Steel split molds having 152 mm diameter, 305 mm height, and 6 mm thickness were used to prepare the test specimens. The mold was fitted with a hose connected to the vacuum pump so that vacuum could be applied to the space between the membrane and the inner surface of the mold. The vacuum helps fit the membrane tightly against the inner surface of the mold during specimen compaction. A vibrating table was used for compacting the specimen. Figure 3-1 shows a photographic view of the split mold and the vibrating table used. The vibrating table consists of 760 mm x 760 mm square and 6 mm thick steel plate resting on four 38 mm x 38 mm x 6 mm steel angle legs. The split mold mounted with membrane was bolted tightly on top of the vibrating table. The aggregates were mixed at optimum moisture content and compacted in ten equal layers in the molds. The vibration of the table was controlled by a controller with a maximum speed of 3600 vibrations per minute. For each of the first 8 layers, 30 seconds vibration was applied and for the last 2 layers 4 minutes vibration was applied in order to obtain a uniform compaction along the length of the specimens. A steel tamping rod was used to tamp the aggregate during compaction along with the vibration to aid in the compaction.

The procedure described above was used to prepare the M_R test specimens. A total of six replicate specimens were prepared for the drained tests and four replicate specimens were prepared for the undrained tests.

3.3 TESTING PROCEDURE AND EQUIPMENT

For granular aggregate materials, the AASHTO suggests using the T 294-94 method to conduct M_R tests. The deviator stress, confining pressure, loading sequence, and the number of loading cycles specified in this method are presented in Table 3-1.

The M_R testing equipment setup consists of: (a) a loading device controlled by an MTS repeated load actuator, (b) a load frame, (c) a triaxial chamber, (d) a chamber pressure gauge, (e) a chamber pressure regulator, (f) an MTS 458.20 Microconsole and Microprofiler, (g) a personal computer for data acquisition, (h) a load cell , (i) two LVDTs, and (j) a numerical gauge to measure pore pressure. The overall setup of the M_R testing equipment is shown in Figure 3-2.

The M_R specimens were brought to the loading frame with minimum disturbance and were extracted from the split molds on the base of the loading frame. Then, a new membrane was mounted on the specimen to ensure proper sealing. The new membrane was needed because the membrane used during compaction was usually found punctured. The specimen was mounted in the triaxial chamber and porous stones were placed at both ends. The chamber was then subjected to the desired confining pressure. Air was used as the confining medium (cell fluid) instead of water because the load cell was located in the triaxial chamber and air pressure is easy to operate and available in most laboratories. The air pressure inside the chamber was precisely controlled by an air pressure gauge that was installed on the triaxial cell. A 270-kg load cell mounted inside the triaxial chamber was used to monitor the applied deviator load. Two external LVDTs were clamped onto the deviator rod and mounted on the top of the triaxial chamber to measure the deformation of the specimen as shown in Figure 3-2. The main advantage of this system is that the

load cell is housed within the triaxial cell to allow in-vessel load measurement and to overcome the detrimental effects of friction caused by the push rod.

After the specimen was subjected to the desired confining pressure, the M_R test was started with the help of the MTS testing system (Figure 3-2). The MTS Microconsole and Microprofiler provide an excellent facility to apply various types of cyclic loading in an efficient and accurate manner. The Microprofiler (a digital function generator) was programmed to conduct a test under the desired cyclic loading. The Microconsole was used to operate the MTS repeated load actuator.

A Gateway 2000, 486 DX2 personal computer with a 50 MHZ microprocessor and a data acquisition board DT 2801 (Data Translation, Inc.) was used for data collection (Figure 3-2). The load cell and the LVDTs were connected to the computer for acquiring the stress-strain data. Thus, the test data were electronically collected and stored by the computer during the test. The AASHTO T 294-94 testing procedure requires the specimen to be subjected to a haversine waveform having a 0.1 second loading period followed by a 0.9 second relaxation period. This requirement calls for a data acquisition system that can acquire and store a sufficient number of data points during the one second loading cycle. The data acquisition system used in this test can collect more than 200 data points per second; this rate is suitable for executing the T 294-94 testing method.

The drainage lines were kept open for most of the M_R tests except for studying the effect of drainage condition on the M_R values. For the undrained M_R tests, two undrained testing methods were used to approximately simulate the drainage conditions in the field. In the first method (undrained I), the pore pressure was allowed to dissipate at the end of

each deviator stress application; this method enables the measurement of the amount of pore pressure increase for each deviator stress cycle. In terms of field situation, it assumes that the traffic is halted over a period of time so that the pore pressure can dissipate before another cycle of traffic transverses the pavement. In the second method (undrained II), the pore pressure was allowed to build up during the entire testing period and its accumulated effect was measured. In terms of real application, this can simulate a continuous traffic flow situation.

It should be mentioned that following the M_R tests, the material properties including cohesion (C), friction angle (ϕ), and unconfined compressive strength (U_C) were evaluated and the test results are presented in Table 3-2.

3.4 PRESENTATION AND DISCUSSION OF TEST RESULTS

3.4.1 Effect of Testing Procedure

Historically, AASHTO has proposed several testing methods for the determination of M_R in the laboratory, namely, AASHTO T 274-82, T 292-91I, T 294-92I, and T 294-94. The basic differences among these methods are presented in Table 3-1.

The testing procedures T 292-91I and T 294-94 (T 294-92I) provided by AASHTO were intended to overcome the deficiencies in its early procedure T 274-82 (Pezo et al. 1992). However, major differences between these two methods (Table 3-3) raised a question: "What is the influence of these differences on M_R values, and hence, the difference in pavement design?"

The RS aggregate was selected to demonstrate the effect of testing procedures on the M_R values. The ODOT median gradation (Figure 2-1) and the corresponding optimum moisture content (OMC = 4.6%) were used in the preparation of test specimens. Two sets of M_R tests were conducted using the AASHTO T 292-91I and T 294-94 procedures, respectively. The major influences on M_R values due to the two different testing procedures are discussed below.

Sample Conditioning

In order to minimize the effects of initially imperfect contact between the end platens and the test specimen, the sample conditioning stage is applied before M_R testing in both testing procedures. This stage can also be viewed as a way to simulate the real situation of the pavement base in service. The sample conditioning stages for the T 292-91I and T 294-94 differ only in the magnitude of the confining pressure σ_c applied. In the T 292-91I method, the σ_c is 138 kPa, and in the T 294-94 method, the σ_c is 103 kPa. However, the same magnitude of cyclic loading (deviator stress σ_d = 103 kPa) and the same number of loading cycles (1000) are used in both testing methods. Due to the small difference in sample conditioning stage between the two testing methods, it is expected that this difference cannot have any significant effect on the M_R test results.

Stress Sequence

The M_R values of aggregate materials can be influenced by various factors among which the applied confining pressure is considered a very important factor (Rada and Witczak 1981). Thus, in order to adequately characterize such materials, it is desirable to

conduct the M_R tests under a wide range of confining pressures expected within the pavement base and subbase layers. The AASHTO T 292-91I and T 294-94 (T 294-92I) methods use a variety of constant confining pressures and cyclic deviator stresses. However, the sequences of the applied pressures and stresses are completely different. The T 292-91I starts with a higher confining pressure and deviator stress and ends with a lower confining pressure and deviator stress. On the other hand, the T 294-94 uses a reverse sequence which starts with a lower confining pressure and deviator stress and ends with a higher confining pressure and deviator stress (Table 3-3). Zaman et al. (1994) investigated these two stress sequences by using the rectangular waveform, in which two sets of M_R tests were conducted under identical conditions, except for the stress application sequence. Their test results indicate that the stress sequence used in the T 294-94 method yielded higher M_R values (15-34% higher) than those produced by the stress sequence used in the T 292-91I method. This variation was attributed to the cyclic stress having a stiffening effect on the specimen structure because the stress application sequence goes from a lower to a higher level in the T 294-94 testing method.

Number of Loading Cycles

To determine the number of loading cycles necessary to reach a stable permanent deformation, the T 292-91I method suggests comparing the recoverable axial deformation at the twentieth and the fiftieth cycles. If the difference is greater than 5%, an additional 50 cycles are necessary at that stress state. On the other hand, the T 294-94 method suggests comparing the recoverable axial deformation at the seventieth and the hundredth cycles to check if the difference is less than 5%. Both testing methods require to report

the mean M_R value from the last five cycles. It has been reported by Khedr (1985) that the response of granular materials is fairly steady and stable after approximately 100 cycles of constant cyclic loading because the rate of permanent strain accumulation decreases logarithmically with the number of load cycles. The number of loading cycles required by the T 292-91I and the T 294-94 methods in the conditioning stage is the same (1000); however, it is different in the M_R testing stages (50 and 100, respectively). In the T 292-91I method, the waveform is rectangular and has a 0.6 second loading duration and a 1.2 second rest period. However, in the T 294-94 method, the waveform is haversine and has a 0.1 second loading duration and a 0.9 second rest period (Figure 3-3). The recoverable axial deformations at the twentieth and the fiftieth cycles for the T 292-91I method and at the seventieth and the hundredth cycles for the T 294-94 method were calculated for the last applied deviator stresses, respectively, and the results are reported in Table 3-4. It can be observed that the recoverable axial deformations measured from the T 292-91I method are very stable and the difference of the recoverable axial deformation at the twentieth and the fiftieth cycles is less than 5%. However, in the T 294-94 method, the loading duration and rest period are shorter than those in the T 292-91I method. Therefore, when using the T 294-94 method to conduct a M_R test, a larger number of load cycles are required to reach the stable permanent deformation. It can be observed from Table 3-4 that the difference of the recoverable axial deformation at the seventieth and the hundredth cycles ranges from 0 to 2.1% in the T 294-94 method which is less than 5%. Hence, it can be concluded that 50 and 100 loading cycles are adequate for the testing methods T 292-91I and T 294-94, respectively, to reach the stable permanent deformation.

Loading Waveform

According to the AASHTO T 292-91I either a triangular or a rectangular waveform can be used in M_R testing of subgrade soils and base/subbase materials to simulate traffic loading. However, the T 294-94 method recommends that a haversine waveform with a 0.1 second loading, followed by a 0.9 second rest period, be used in M_R testing for both soil and granular materials. A fixed loading duration of between 0.1 and 1.0 second and a fixed cycle duration of between 1.0 and 3.0 seconds are specified by the T 292-91I method. Further, for a granular specimen, a minimum of 0.9 second relaxation between the end and the beginning of consecutive load repetitions is required in the T 292-91I method. The same loading magnitudes were used for all three waveforms.

In order to compare the effect of different loading waveforms, three sets of M_R tests with rectangular, triangular, and haversine waveforms were conducted by using the T 294-94 procedure. The three different waveforms used in this series of tests are shown schematically in Figure 3-3. In order to render the test results comparable, the areas under the rectangular and the triangular loading forms are kept nearly the same. In these tests only the waveforms were varied, while all other factors were kept the same. The mean M_R values from each waveform are plotted in Figure 3-4, wherein it is observed that the haversine waveform produced substantially higher M_R values (nearly 80% higher), overall, than the triangular and the rectangular waveforms. However, the M_R values are nearly equal for the triangular and the rectangular waveforms. One of the reasons for this difference could be that in the case of the triangular and the rectangular waveforms the longer loading period is likely to produce more viscoelastic deformation, and hence more elastic strains, compared to the elastic strains produced by the haversine waveform

having a short loading duration. Therefore, it can be advanced that M_R values decrease with increased loading duration. Of course, other factors such as different loading frequencies and rest periods used in these waveforms may have also contributed to these differences in the M_R values. Nonetheless, these results demonstrate the importance of the loading waveform on the M_R values.

General Comparison

In order to generally compare the effect of testing procedure on M_R values, the mean M_R values obtained from the T 292-91I and T 294-94 methods are grouped in Figure 3-5. It can be observed that the M_R values from the T 294-94 method are 32 to 122% higher than the corresponding values from the T 292-91I method. Some of the potential reasons, as mentioned above, are: (i) the stress sequence used in the T 294-94 method has a stiffening effect on the specimen; (ii) the haversine waveform used in the T 294-94 method has a shorter loading duration that produced less viscoelastic strain than the strain produced by the rectangular waveform used in the T 292-91I method.

From Table 3-2, it can be observed that there are some discernible changes in the static material properties which were measured after M_R testing. For cohesion (C), the specimens subjected to the T 294-94 M_R testing present higher values than the specimens subjected to the T 292-91I M_R testing. On the other hand, the friction angle (ϕ) and the unconfined compressive strength (U_C) present lower values for the specimens which were subjected to the T 294-94 M_R testing. For example, the C value of 120.6 kPa obtained after the T 294-94 M_R testing is higher than the C value of 68.9 kPa obtained after the T 292-91I M_R testing. On the other hand, the U_C value of 299 kPa obtained after the T 294-

94 M_R testing is less than the U_C value of 348 kPa obtained after the T 292-91I M_R testing. The corresponding measured ϕ values are 50.1° and 58.2° after the M_R tests. One of the possible reasons for the increase in U_C and ϕ values is as follows. It has been observed that the T 292-91I method yielded lower M_R values than the T 294-94 method which means higher elastic strains were produced in the specimen by the T 292-91I method. As noted by Huang (1993), generally, plastic strains are proportional to elastic strains in paving materials including an aggregate base. Accordingly, a higher permanent deformation is expected to be induced in a specimen due to the T 292-91I method than by the T 294-94 method. As a result, the void ratio of the specimen would become smaller, making the specimen more compact and stronger and thereby resulting in higher U_C and ϕ values when such tests are conducted following the M_R testing using the T 292-91I method.

3.4.2 Effect of Gradation

Three gradations of the RS and the Sawyer aggregates were selected to evaluate the effect of gradation on M_R. The three gradations, which are presented in Figure 2-1, are the median, finer limit, and coarser limit gradations of the ODOT gradation band (ODOT 1996). The mean M_R values from each gradation type are presented graphically in Figures 3-6 and 3-7 for the RS and the Sawyer aggregates, respectively.

In view of Figure 3-6, the median gradation of the RS aggregate produced substantially higher M_R values (41 to 129% higher) than the finer limit gradation but only slightly higher values (nearly 0 to 26% higher) than the coarser limit gradation. However, in Figure 3-7, the coarser limit gradation of the Sawyer aggregate produced the highest

M_R values (nearly 10 to 36% higher than the finer limit and the median gradations), and the M_R values of the median and the finer limit gradations are nearly in the same range. In comparing the data in these two figures, it becomes evident that the finer limit gradation in both cases gives lower M_R values than those of the coarser limit gradation. This difference is more obvious for the RS aggregate than the Sawyer aggregate. The reasons for this difference between the finer and the coarser limit gradations may be: (1) the drainage rate of the finer limit aggregates is slower than that of the coarser limit aggregates; (2) the finer limit aggregates lack larger irregular particles (maximum size 1.27 cm) to provide a strong interlock between particles; (3) the large top size particles (themselves) in the coarser limit aggregates can provide a strong aggregate structure.

In documenting the effect of gradation on M_R values, similar results were reported by other studies. For example, Kamal et al. (1993) reported that the M_R value increased as the gradation changed from the finer to the coarser end of the gradation envelope. By comparing the resilient behavior of an uncrushed base material with a crushed base material, Johnson and Hicks (1987) reported that the uncrushed base course performed better than the crushed base course. The uncrushed base is superior because of larger maximum particle size and greater maximum density. Barksdale and Itani (1989) studied the M_R values of granitic gneiss, and it was found that the coarse gradation of this material consistently resulted in higher M_R values than those of the medium and fine gradations.

Extending the findings in this study into pavement design, it is safe to state that the pavement designed by using the median gradation of the RS aggregate, or the coarser limit gradation of the Sawyer aggregate, which yielded the highest M_R values, would

require less thickness for a given level of performance. However, the coarser limit gradation of the RS aggregate produced the M_R values which are closer to those of the median gradation. Considering the factor that the coarser limit aggregate provides faster drainage, it can be expected that coarser limit aggregates are less likely to induce or permit damage in pavements under saturated condition and hence, lead to more durable pavements. Johnson and Hicks (1987) once reported that the future performance of a roadway with equal thicknesses of asphalt indicates that a pavement over an uncrushed base would have a 54% longer life than a pavement over a crushed base.

The findings in this study may have significant consequences in terms of field applications because aggregate particles may break down during the compaction process producing more fines than accounted for in specifications. It is generally agreed that having a certain amount of fines is beneficial, but any excess amount would lead to a reduced strength (M_R values), and hence, reduced pavement performance. Monitoring of aggregate break down during construction and development of appropriate specifications will be necessary to help avoid any detrimental effect, particularly when aggregates with lower LA abrasion values are involved in pavement construction.

It can be observed from Table 3-2 that, as the amount of fines (percent passing No. 200 (0.075 mm) sieve) increased from 4 to 12% between the coarser limit and the finer limit gradations, the cohesion (C) increases from 83.4 to 134.4 kPa and 34.5 to 75.8 kPa, however, the friction angle (ϕ) decreases from 52.9° to 46.9° and 58.4° to 51.2° for the RS and the Sawyer aggregates, respectively. This is consistent with the general principles of soil mechanics, because the fine particles are the primary contributing factor to cohesion, and the coarser particles are the major contributing factor to internal friction.

This finding also has significance in terms of practical application, since the amount of fines can increase significantly resulting from the rolling compaction during a pavement construction.

3.4.3 Effect of Moisture Content

An attempt was made to investigate the effect of moisture content on M_R by considering three different moisture contents: the OMC, 2% above, and 2% below the OMC. Median gradation was used in this phase of the study. The mean M_R values were calculated for each moisture content and are plotted in Figures 3-8 and 3-9 for the RS and the Sawyer aggregates, respectively. Following the M_R tests, the material properties including cohesion (C), friction angle (ϕ), and unconfined compressive strength (U_C) were also evaluated and the results are presented in Table 3-2.

In view of Figures 3-8 and 3-9, it can be observed that an increase in moisture content leads to a decrease in M_R values for both aggregates. This finding for aggregate materials is consistent with the observations by Rada and Witczak (1981) and by Thompson (1989) who demonstrated that relatively small changes in the water content can result in substantial differences in the M_R values. For example, Thompson (1989) indicated that increased moisture contents (above optimum) tend to decrease M_R values. Moisture sensitivity will vary depending on specific gradations and the amount and nature of the fines. Lary and Mahoney (1984) developed moisture sensitivity data for several granular base materials sampled from a number of typical roads and indicated that for an initial modulus of 138 MPa, an 1% increase in moisture content would induce M_R decrease from about 4.1 to 11 MPa. One of the possible reasons for this trend could be

the matric suction present in an unsaturated specimen. When the moisture content increases, the matric suction decreases, which reduced the strength of the specimen. According to Spangler and Handy (1973), the capillary water in soil pores sets up compressive stresses for the soil skeleton which are directed inward and contribute to the strength and stability of soils. However, the capillary-induced strength is temporary and may disappear entirely if the soils become saturated, since saturation eliminates the capillary menisci.

It can also be observed (Figures 3-8 and 3-9) that the variation in the M_R values between 2% below the OMC and the OMC is nearly -13 to 27% (RS aggregate) and 11 to 37% (Sawyer aggregate), while the variation between the OMC and 2% above the OMC is more than 25 to 80% (RS aggregate) and 18 to 71% (Sawyer aggregate). Obviously, when the moisture content is greater than the OMC, the increasing moisture content has a greater influence on the decreasing of M_R values. The reason could be that the specimen compacted at 2% above the OMC produces a smaller dry density than that at the OMC; also the specimen has less suction at the higher moisture content. Both factors are detrimental in terms of the strength in the specimen. However, at 2% below the OMC, the specimen has a higher suction that offsets the factor of the smaller dry density (because maximum dry density is achieved at the OMC); hence, a smaller variation in the M_R values. It should be noted that only a 2% increase in moisture content (above OMC) changes the degree of saturation (S_r) considerably. The S_r increases from 83 to 95% and 78 to 86% for the RS and the Sawyer aggregates, respectively. In fact, Haynes and Yoder (1963) conducted cyclic triaxial tests on gravel and crushed stone and indicated that there was a critical degree of saturation near 80 to 85%. Above this critical degree of

saturation, the M_R decreases rapidly as the degree of saturation increases. Below the critical point, the degree of saturation has little influence on the M_R values. In the present study, 2% above the OMC gave the initial degree of saturation of 95% and 86% for the RS and the Sawyer aggregates, respectively. Although this moisture content did not cause a complete saturation of the specimen, the decreasing of M_R values is obvious. Therefore, it can be concluded that the M_R values are likely to decrease significantly when specimens reach the state of saturation or near saturation. Of course, while other variables such as the void ratio (the amount of fines) and drainage during the tests are important factors to consider, these results clearly demonstrate the importance of the influence of moisture content on the M_R values.

The results obtained from the present study are helpful in understanding the behavior of pavement base materials under different moisture conditions. When the drainage of a pavement base does not function properly or during an excessive rainfall, the moisture in the pavement base may increase and could possibly reach saturation; this is possibly the worst scenario with respect to the pavement performance. On the other hand, when the base of a pavement goes through a dry season, the pavement is expected to exhibit good performance due to the relatively higher M_R values. For example, in discussing the effect of seasonal variations of M_R values on the pavement performance, Elliott and Thornton (1988) utilize the concept of relative damage in a pavement design example. They developed a procedure for calculating the "effective roadbed soil resilient modulus" which is primarily based on data (deflection, etc.) obtained from flexible pavements in the vicinity of the AASHO Road Test (Ottawa, Illinois, 1962). Except for January and February, the M_R values of pavement subgrade are of the order of 69 MPa

(10 ksi) and the relative damage of the order of 0.060. For January M_R is 207 MPa (30 ksi) and the relative damage of the pavement was 0.005, while for February M_R is 38 MPa (5.5 ksi) and the relative damage was 0.25. The reason is that the subgrade will be frozen resulting in the lowest moisture content in January, hence, the highest M_R values (207 MPa). However, February is assumed to be a period of thawing, resulting in the highest moisture content in subgrade, hence the lowest M_R values (38 MPa).

In reference to the data in Table 3-2, as the moisture changed, for both aggregates, regardless of which side of the OMC, the cohesion (C) decreases compared to the case of OMC. However, the friction angle (ϕ) increases as the moisture increases. This could be partly attributed to the fines being lost during the sample preparation process. As the specimen compacted at 2% above the OMC, the excess water was pumped out from the top and bottom sides of the specimen that carried away fines from the specimen. As the fines reduced in a specimen, the cohesion decreases, and at the same time the specimen has a coarser gradation which results in a higher friction angle.

3.4.4 Effect of Drainage Condition

The effect of drainage condition on M_R was investigated for the RS and the Sawyer aggregates. The ODOT median gradation and the OMC were selected for specimen preparation in this case. The OMC for the RS aggregate is 4.6%, representing a degree of saturation (S_r) of about 83%. However, for the Sawyer aggregate, a degree of saturation of 78% was attained at the OMC of 6.0%. Therefore, it was decided to soak these specimens in a water tank for one week, and thus increase the average degree of

saturation to about 91%. The effects of pore pressure and drainage condition on the M_R values are discussed below.

Pore Pressure Generation

An attempt was made to measure the excess pore pressure build-up in the specimens during the M_R testing under the undrained condition. The average measured pore pressure values are plotted in Figures 3-10 and 3-11 for the RS and the Sawyer aggregates, respectively. It is observed that as the stress level (bulk stress) increases, the pore pressure also increases. Since the pore pressure was allowed to accumulate in the undrained II test, but not in the undrained I test, it produced higher excess pore pressures in the former, as expected. The pore pressure increases from the undrained II to the undrained I tests are substantial, 146% (average) for the RS aggregate and 162% (average) for the Sawyer aggregate.

In terms of practical consequences, the generation of pore pressure in the pavement base layers could be one of the major causes for the rapid deterioration of pavement structure. An increase in pore pressure reduces the strength and the stiffness of the underlying granular layers, causing an increased surface deflection and eventually a reduction of pavement service life. Also, the dissipation of pore pressure with the escape of water from the matric is conducive to decrease in void ratio and subsequent settlement of the granular layers, causing an additional loss of pavement support and increased surface cracking.

Drainage Condition

The mean M_R values for the drained and the undrained conditions are presented in Figures 3-12 and 3-13 for the RS and the Sawyer aggregates, respectively. These figures depict the drained M_R values being significantly higher than the corresponding undrained values. For example, the M_R values from the drained tests are 34 to 88% higher than those obtained from the undrained I tests and 53 to 124% higher than those obtained from the undrained II tests for the RS aggregate. For the Sawyer aggregates, the M_R values from the drained tests are 25 to 53% higher than those obtained from the undrained I tests and 28 to 58% higher than those obtained from the undrained II tests. This is so possibly because: (1) the pore pressure was generated in the undrained tests; an increase in pore pressure reduces the effective stress which translates to a reduction in the strength and stiffness of a material; (2) the water was allowed to drain out in the drained tests and the moisture contents of the specimens reduced during the drained testing, and consequently, the dry densities of the specimens increased. Generally, a decrease in moisture content and an increase in dry density lead to an increase in the material strength, and hence, the increased M_R values. Extending this finding to pavement design, it can be postulated that constructing a permeable base, maintaining the drainage efficiency, and reducing moisture in pavement base are important factors in ascertaining pavement quality and extended service life.

Very few researchers have examined the influence of drainage conditions on the M_R values of aggregate materials. Hicks (1970) performed an experiment under undrained conditions and pore pressures were measured throughout the tests. As the number of cyclic loads increased, pore water pressure developed and weakened the

specimen. Hicks (1970) and Das (1990) stated that the undrained conditions probably do not occur in a (granular) pavement base layer, but it indicates the propensity of a reduction in the modulus when the pavement is near saturated.

3.4.5 Variability of Experimental Results

The extent to which the M_R values obtained from replicate specimens differ from each other is an important factor in determining the reliability of the M_R values. The variations in the individual M_R values are measured by standard deviation (SD). The higher the magnitude of the SD, the larger the variation of M_R values. For a good set of tests, it is desirable that the individual M_R values not differ from the mean by any significant amount. In other words, it is desirable and important to have a SD of smaller magnitude with respect to the mean value. The extent to which the individual values fall within a certain range or interval (confidence interval) depends on the number of observations (number of replicate specimens tested), the confidence coefficient desired, and the SD of the observations (Mendenhall and Sincich 1992). In this study, since the number of observations and the SD are known, the confidence coefficient, is determined as:

$$Z_{\alpha/2} = \frac{e\sqrt{n}}{s} \qquad (3\text{-}1)$$

where e is the error in estimation, s is the SD, n is the number of observations, and $Z_{\alpha/2}$ is the upper $\alpha/2$ critical value for the standard normal distribution.

In order to evaluate the confidence level of the M_R values and hence the test data obtained from the present study, the M_R values of the RS aggregate at 2% below the

OMC are selected for this purpose. This set of data has the maximum sample standard deviations. Based on the general experience of geotechnical testing, a 15% relative error was selected in the analysis. In other words, the goal here is to determine the confidence level in the measured M_R values such that all the test results are within 15% (i.e., 15% below or above) of the mean M_R values. Based on Eq. (3-1), the confidence levels were calculated for all of the M_R values and are presented in Table 3-5. The mean confidence level for this case is about 90%, which means 90% of the obtained M_R values fall within the range of 15% below or above the mean M_R values. As mentioned previously, this is the worst case, and all other cases would have higher confidence levels since the measured SD values for these cases are lower than those used in this analysis. For example, the confidence levels of the M_R values from the Sawyer aggregate at the finer limit gradation and OMC were calculated and presented in Table 3-6. Overall, this set of data has the minimum sample standard deviations and the mean confidence level for this case is 98%, which means 98% of the individual M_R values fall within the range of 15% below or above the mean M_R values.

For the measured M_R values, the relative error can be represented by the SD/mean M_R values at different bulk stresses. For the M_R values of the RS aggregate at 2% below the OMC, the average relative error for this case is 22.7% (Table 3-5). As mentioned above, this is the worst case, and all other cases would have lower relative errors. For example, the average relative error of the M_R values for the Sawyer aggregate at the finer limit gradation and OMC is 11.5% (Table 3-6). The maximum 22.7% relative error obtained in the present study, generally, can be accepted in geotechnical testing. Actual error in most cases, however, is much smaller than these maximum error values.

3.5 STATISTICAL CORRELATIONS

3.5.1 Determination of Material Model Parameters

According to the AASHTO testing method T 294-94, the M_R values for granular materials can be conveniently reported by using the k-θ model,

$$M_R = k_1 \theta^{k_2} \tag{3-2}$$

where k_1 and k_2 are regression coefficients, and θ is the bulk stress ($\sigma_1 + \sigma_2 + \sigma_3$). In the present study, regression analyses were performed to evaluate the k_1 and k_2 values for the different testing cases. The parameters k_1 and k_2 thus obtained for all the cases are presented in Table 3-7 for the RS and the Sawyer aggregates and so are the standard deviations (SD) and the coefficient of determination (R^2). In view of Table 3-7, as M_R values changed due to different influencing factors, the k_1 values also vary significantly; however, the variation in k_2 is relatively insignificant. The k_1 and k_2 values in Table 3-7 conform the observations made by Rada and Witczak (1981) where six different granular materials were investigated.

It should be noted that the k-θ model in Eq. (3-2) did not yield high R^2 values in the regression analyses for some cases. For example, in the cases having the finer limit gradation and 2% below the OMC for the RS aggregate, the R^2 values are found to be 0.6585 and 0.6628, respectively. For the Sawyer aggregate, the R^2 values are 0.6698 and 0.6673, respectively, for the cases having 2% below the OMC and the undrained I.

Figures 3-14 and 3-15 show the variation of k_1 and k_2 as a function of gradation factor defined as percent passing No. 200 sieve (0.075 mm). It can be observed that the RS aggregate produced higher k_1 value than that of the Sawyer aggregate. As the percentage of fines increases, the k_1 values decrease. However, there is no clear trend for

the k_2 values. All k_2 values are located near the $k_2 = 0.5$ line as the percentage of fines increases. For both of the aggregates investigated in this study, the coarser limit gradation yielded the highest k_1 values, and the finer limit gradation yielded the lowest k_1 values.

Figures 3-16 and 3-17 show the variation of k_1 and k_2 as a function of the moisture content. It can be observed that as the moisture increases, the k_1 decreases, and the k_2 increases but insignificantly. It is interesting to note that both aggregates exhibit a similar trend line for k_1 and k_2. Hence, it may be postulated that this relationship is independent of the aggregate type. If so, it has significance in terms of practical application, because the k_1 and k_2 values for other moisture contents can be obtained by interpolation.

Figures 3-18 and 3-19 show the variation of k_1 and k_2 as a function of the drainage condition. As the M_R values decrease due to the change in drainage condition, for the RS aggregate, the k_1 value decreases from 10633 to 6538 kPa and the k_2 value decreases from 0.5403 to 0.4718. For the Sawyer aggregate, the corresponding decrease in k_1 is 7098 to 4818 kPa, while the k_2 values remain nearly unchanged at 0.5. Obviously, drainage condition has a significant effect on the k_1 values.

It is believed that the k_1 and k_2 values obtained in the present study can be used in the AASHTO pavement design equation when the pavement bases are constructed with the aggregates used in this study.

3.5.2 Multiple Linear Regression Model

Overview of M_R Correlation Model

The AASHTO Guide for Design of Pavement Structure (AASHTO 1993) suggests the use of resilient modulus to characterize the base material or subgrade soil.

However, due to the complexity involved and the need for specialized equipment for M_R testing, it is desirable to explore approximate methods estimating of M_R values. Statistical correlations between M_R and engineering index properties are often found to be useful in practical applications since the basic engineering index properties are relatively easy and inexpensive to evaluate. Previous research indicated that the M_R values are neither intimately related to the plasticity index (PI) of the granular materials nor to the conventional soil classification system used (Rada and Witczak 1981; Zaman et al. 1994). California Bearing Ratio (CBR) is widely used as an indicator of the strength characteristics of subgrade soils and aggregates in pavement design. However, due to the differences in the laboratory testing conditions, it was found that CBR values usually do not correlate well with the M_R values (Rada and Witczak 1981; Chen 1994). Pandey et al. (1998) attempted to correlate M_R with unconfined compressive strength (U_C) and elastic modulus (EM) of a raw and stabilized marginal aggregate, called Meridian aggregate. It was found that the M_R values cannot be correlated with the U_C and the EM values, for both raw and stabilized aggregates, with a reasonable degree of accuracy. Chen (1994) developed a correlation between the M_R and the cohesion and friction angle; it was found that this correlation provided a better prediction of M_R values for aggregate materials than that with CBR. A possible explanation is that deformation characteristics for the conventional triaxial compression test and M_R test are more similar than those between the M_R and the CBR tests (Chen 1994).

From the experimental results presented in Section 3.4, it is evident that the stress state has the most significant influence on the M_R values. Gradation and moisture content also significantly influence the M_R values of aggregates (Figures 3-6 and 3-8). It has been

observed that the cohesion, friction angle, and unconfined compressive strength of the aggregates are mainly dominated by the gradation and the moisture contents (Table 3-2). Therefore, an attempt is made here to develop a regression model in which M_R is correlated with the stress state, static material properties, gradation, and moisture content.

Evaluation of Model Variables

Based on the discussion above, the possible influencing factors on the M_R values could be listed as: bulk stress (θ), deviator stress (σ_d), moisture content (MC), gradation (percent passing No. 200 sieve), cohesion (C), friction angle (ϕ), and unconfined compressive strength (U_C). The percent of fines passing No. 200 (0.075mm) sieve is used here to represent the gradation factor. It should be noted that some of these factors may not be independent and some factors may not have a significant influence on the M_R values. In order to obtain the most significant factors to correlate M_R values, the Least Square (LS) method was used to evaluate these factors in the light of their importance on the M_R values.

The elastic modulus (EM) was not incorporated in the regression analysis partly because of the sensitivity in determining the EM values based on the initial slope of the stress-strain curves. A better approach to determine EM would be to conduct tests with unloading-reloading cycles, but it was not pursed in this study.

Table 3-8 shows all the possible models with associated R^2 values. Here no parameters are estimated. It is observed that bulk stress (θ) gives the best one variable model with R^2 values of 0.4617 and 0.6672 for the RS and the Sawyer aggregates, respectively. The cohesion (C), friction angle (ϕ), and the unconfined compressive

strength (U_C) have very small direct influence on the M_R values. So the two variable models are evaluated based on the combination of variables of θ, σ_d, MC, and No. 200. It was found that the best two variable model is the θ and MC model; R^2 values of 0.6162 and 0.8542 were obtained for the RS and the Sawyer aggregates, respectively. Furthermore, the three variable models were evaluated based on adding one variable (σ_d or No. 200) in the θ, MC model. It was found that adding the No. 200 variable in the θ, MC model becomes more critical than adding the σ_d variable for the RS aggregate in terms of the increased R^2 value. For the RS aggregate, the R^2 value increased from 0.6162 to 0.7534 due to adding the No. 200 variable. However, for the Sawyer aggregate, the R^2 value only slightly increases from 0.8542 to 0.8544 due to adding the No. 200 variable. Further, adding the σ_d, C, ϕ, and U_C variables did not increase the R^2 value compared with the θ, MC, and No. 200 model for both aggregates. Therefore, the three variables (θ, MC, and No. 200) are considered to be the most significant influencing factors as such they were used in establishing the multiple linear regression model.

Determination of Model Parameters

Multiple regression analysis can be either linear or nonlinear depending on the form of the unknown parameters. Usually, the functional form of the model known from physical phenomena leads to nonlinear regression analysis. In the present study, the analysis is restricted to linear regression because a prior knowledge of nonlinearity in parameters is not available. Also, in case of nonlinear regression, evaluation of model parameters is difficult because a solution may not converge if the proper form of the nonlinearity in parameters is not included (Mendenhall and Sincich 1992).

In the present study, a multiple linear regression model between the M_R and the bulk stress (θ), moisture content (MC) and aggregate gradation (No. 200) is formulated as

$$M_R / Pa = A_o + A_1*\theta / Pa + A_2*MC + A_3*No.\ 200 \quad (3\text{-}3)$$

where A_0, A_1, A_2, and A_3 are regression constants, and Pa is the atmospheric pressure (101.3 kPa). The purpose of introducing the constant pressure of Pa is to obtain the non-dimensional coefficients A_i.

A database having the M_R values for different cases was established first in order to evaluate the regression coefficients A_i for the two selected aggregates. Six duplicate M_R tests and five different factors considered in the experimental program (the median, finer limit, and coarser limit gradations, 2% below OMC, and 2% above OMC) resulted in a total of 450 M_R values. These M_R values were separated into two groups. Test 1 through Test 5 having a total of 375 M_R values were used to develop the model, and all of Test 6 having a total of 75 M_R values were used to validate the obtained models. The following numerical values of the regression constants were obtained for the RS and the Sawyer aggregates, respectively:

$A_0 = 3433$; $A_1 = 354$; $A_2 = -291$; and $A_3 = -138$ (RS aggregate).

$A_0 = 1637$; $A_1 = 250$; $A_2 = -177$; and $A_3 = -0.81$ (Sawyer aggregate).

The coefficients of determination (R^2) of the regression analyses are 0.7534 and 0.8544 for the RS and the Sawyer aggregates, respectively. A comparison between the experimental observations and the model predictions is presented in Figures 3-20 and 3-21 for the RS and the Sawyer aggregates, respectively. It can be observed that both models reasonably fit the experimental data. By comparing the multiple regression model with the k-θ model in terms of R^2 values, it can be observed that both models present the

same level of R^2 values. However, the multiple regression model has a wide range of applications since the M_R values of the two selected aggregates at different gradations and moisture contents can be predicted by using the multiple regression model, and hence it has a significance in the practical pavement design.

3.6 EVALUATION OF LAYER COEFFICIENT

3.6.1 Layer Coefficients

In the AASHTO flexible pavement design procedure, structural number (SN), which provides a link between the structural design of a pavement and its performance, is defined as a function of layer thickness, layer coefficient, and drainage coefficient as follows:

$$SN = a_1D_1m_1 + a_2D_2m_2 + a_3D_3m_3 + \ldots\ldots + a_nD_nm_n \qquad (3\text{-}4)$$

where, a_1, a_2, ..., a_n are the layer coefficients of layer 1, layer 2, ...layer n, respectively; D_1, D_2, ..., D_n represent the thicknesses of layer 1, layer 2, ... layer n, respectively; and m_1, m_2, ...m_n are the drainage coefficients of layer 1, layer 2, ..., layer n, respectively.

For a three layer pavement system shown in Figure 3-22, layer 1 corresponds to the asphalt concrete (AC) layer, layer 2 is the aggregate base layer, and layer 3 is the subgrade layer. The layer coefficients (a_i) in Eq. (3-4) express an empirical relationship between SN and thickness and represent a measure of the relative ability of a unit thickness of a given material to function as a structural component of the pavement (AASHTO 1993). Layer coefficients can be determined from test roads, as was done in the AASHTO Road Test (AASHTO 1993), or from correlations with material properties

(Van Til et al. 1972). The AASHTO design guide (AASHTO 1993) recommends that the layer coefficient be based on M_R values which are measured in the laboratory cyclic load test using the AASHTO T 294-94 method.

According to the AASHTO design guide, the relationship between the layer coefficient (a_2) of the aggregate base material and its M_R is given by the following empirical equation:

$$a_2 = 0.249 (\log M_R) - 0.977 \qquad (3\text{-}5)$$

which requires only a single M_R value for the base layer to determine the layer coefficient. However, the M_R value depends on the stress state (bulk stress) within the base layer induced from the surface load, and the variation of bulk stress within the base layer depends on the thickness and M_R value of the AC layer and the roadbed soil M_R (Huang 1993). Therefore, it becomes imperative to determine only one stress state (Equivalent Layer Bulk Stress (ELBK)) which will lead to the determination of the single M_R to be used in the design equation.

3.6.2 Determination of Equivalent Layer Bulk Stress (ELBK)

In this study, the MICH-PAVE program (Harichandran et al. 1989), which is based on the finite element analysis was used to compute the ELBK for the base layer. MICH-PAVE evaluates the ELBK in the section of the layer that lies within an assumed 2:1 load distribution zone. Thus, it is possible to adequately reflect the stress-dependent variations of M_R within the base layer. Chen (1994) compared the results from several available computer programs and concluded that MICH-PAVE is one of the most appropriate codes available for the routine structural analysis of flexible pavements.

Figure 3-22 shows the three layer flexible pavement system used for ELBK computation. The material parameters used as inputs are also shown in this figure. Bulk stresses were computed for three different thicknesses 76 mm, 152 mm, and 228 mm, and three different M_R values, 1725 MPa, 3450 MPa, and 5175 MPa of the AC layer. For each of the AC layer thickness and M_R value combination, four different base layer thicknesses, 76 mm, 152 mm, 228 mm, and 304 mm were used. The above selected AC layer thickness and M_R values as well as the base layer thickness are within the range of numbers usually encountered in practical pavement designs. The various sets of AC thicknesses and M_R values and base layer thicknesses resulting in 36 different cases with their corresponding ELBK values are presented in Table 3-9.

In view of Table 3-9, as the M_R values and the thicknesses of the AC layer increase, the ELBK shows a decreasing trend. It is consistent with the general concept that as the AC layer becomes stiffer, more energy or more loading is sustained by the AC layer. Thus, the stresses induced in the sub layers are reduced. Also, it can be observed that the thickness of base layer has a very small influence on the values of ELBK.

3.6.3 Determination of Layer Coefficients

Based on the ELBK values obtained (Table 3-9), the Equivalent Layer Resilient Modulus (ELRM), for a particular set of AC layer thickness, M_R values, and base layer thickness, was determined by the following equation,

$$ELRM = k_1 * (ELBK)^{k_2} \qquad (3\text{-}6)$$

The k_1 and k_2 values are material dependent parameters and could be determined by laboratory M_R tests. The ELRM value obtained from Eq. (3-6) is a representative M_R

for the entire base layer. Subsequently, the layer coefficients (a_2) based on the ELRM of the base layer were computed by using Eq. (3-5). The layer coefficients for the RS aggregates at the three gradations, three moisture contents and two drainage conditions are presented in Tables 3-10, 3-11, and 3-12, respectively. Similarly, the layer coefficients of the Sawyer aggregate for the corresponding cases are presented in Tables 3-13, 3-14, and 3-15.

As indicated in Eq. (3-5), the larger the M_R values, the larger the layer coefficients. So the median gradation (Table 3-10) and the coarser limit gradation (Table 3-13) yield the highest layer coefficients for the RS and the Sawyer aggregates, respectively.

Similarly, the 2% below the optimum moisture (Tables 3-11 and 3-14) yields the highest layer coefficients for both aggregates. Also, the layer coefficients for the drained conditions are significantly higher than those under the undrained conditions for both aggregates (Tables 3-12 and 3-15). Layer coefficients were reduced about 50% when the drainage condition changed from drained to undrained.

In view of Tables 3-10 though 3-15, some cases yield small negative layer coefficient values. The layer coefficients that have a negative value do not have any practical significance and therefore, should be considered as values approaching zero. The layer coefficient is a measure of the relative ability of the material to function as a structural component of the pavement (AASHTO 1993). Hence, layer coefficients having values approaching zero or below zero essentially mean that the material is of insignificant structural support compared to the other materials used in the pavement system. In contrast, the layer coefficients of the RS aggregate are higher than those of the

Sawyer aggregate for corresponding cases; hence, the RS aggregate is likely to be more suitable for use as base course than the Sawyer aggregate.

Also, it should be noted that all the layer coefficients obtained above correspond to certain gradation and moisture content. In a practical design, if the material gradation and moisture content used are different than those studied in this research, the layer coefficients for these cases can be obtained using an interpolation. In this study, a multiple linear regression analysis was attempted in order to facilitate the application of the layer coefficients for other moisture contents and gradations.

A number of possible variables such as the thickness of AC layer (D_{ac}), thickness of base layer (D_{bs}), modulus of AC layer (E_{ac}), moisture content (MC), and the gradation effect (No.200) were evaluated based on their influence on M_R values by using the Least Square (LS) method (Tian et al. 1998). Table 3-16 shows all the possible models for the RS and the Sawyer aggregates with the associated R^2 values. It was observed that the D_{ac} gives the best one variable model with R^2 values of 0.5044 and 0.5339 for both aggregates. The D_{bs} has very little direct influence on the a_2 values. So the two variable models were evaluated based on the combination of variables of D_{ac}, E_{ac}, MC, and No. 200. It was found that the best two variable model is the D_{ac} and MC model; for this model, R^2 values of 0.7211 and 0.8904 were obtained for the RS and the Sawyer aggregates, respectively. Furthermore, the three variable models were evaluated based on adding one variable (E_{ac} or No. 200) in the D_{ac}, MC model. It was found that adding the No. 200 variable in the D_{ac}, MC model is more significant than adding the E_{ac} variable in terms of increasing the R^2 value for the RS aggregate. The R^2 value increased from 0.7211 to 0.8676 due to adding the No. 200 variable. However, for the Sawyer aggregate,

adding the E_{ac} variable is more effective than adding the No.200 variable as measured by the increase in the R^2 value. The R^2 value increased from 0.8904 to 0.9485 due to adding the E_{ac} variable. The next consideration is the four variable model, it was found that either adding the E_{ac} variable or the No. 200 variable in the corresponding best three variable models increases the R^2 values from 0.8676 to 0.9226 and 0.9485 to 0.9510 for the RS and the Sawyer aggregates, respectively. Additionally, adding the variable of D_{bs} did not increase the R^2 value from the best four variable models for both aggregates. Therefore, the four variables of D_{ac}, MC, No. 200, and E_{ac} were used next to develop the regression model for estimating the layer coefficient (a_2). The following regression equations were obtained based on the a_2 values obtained the RS and the Sawyer aggregates:

i. Layer coefficient a_2 for the RS aggregate:

$$a_2 = 0.5546 - 0.4579*10^{-3}*D_{ac} - 0.0146*MC - 0.6062*10^{-2}*\text{No. } 200 - 0.0476*\log E_{ac} \qquad (R^2 = 0.9226) \qquad (3\text{-}7)$$

ii. Layer coefficient a_2 for the Sawyer aggregate:

$$a_2 = 0.5274 - 0.4872*10^{-3}*D_{ac} - 0.0179*MC - 0.8613*10^{-3}*\text{No. } 200 - 0.0506*\log E_{ac} \qquad (R^2 = 0.9510) \qquad (3\text{-}8)$$

in which: D_{ac} (mm) = thickness of AC layer, E_{ac} (kPa) = M_R of AC layer, MC (%) = moisture content, and No. 200 (%) = percent of fines passing the No. 200 (0.075mm) sieve.

3.7 Design of AASHTO Flexible Pavements

The layer coefficients determined above can be used in the flexible pavement design according to the AASHTO design guide (AASHTO 1993). The RS and the Sawyer aggregates at different conditions were used as the base layer and the relative performance of the entire pavement system can be evaluated by comparison of SN (Structure Number) and the corresponding ESAL (Equivalent Single Axle Load). In the present design, the SN and ESAL were computed for an overall standard deviation (S_0) of 0.35, initial serviceability index (P_i) of 4.2, and the terminal serviceability index (P_t) of 2.5. These values of S_0, P_i, and P_t correspond to the values observed at the AASHO Road Test (AASHTO 1993). Based on the AASHTO recommendation, a reliability level of 90% was selected as an input parameter in this study.

For the RS aggregate, Case 3, Case 6, Case 9, and Case 12 (Table 3-9) were selected for the comparison of SN and ESAL. The thickness and the M_R value of the AC layer are 228 mm (9 in) and 1725 MPa (250 ksi), respectively, and the road bed soil M_R is 51.75 MPa (7.5 ksi). Only the thickness of base layer changes among these cases. The SN and ESAL were computed using the AASHTO Flexible Pavement Design Computer Software (AASHTO 1986), and the results obtained are presented in Table 3-17.

Design ESAL of 1,000,000 is recommended by the Asphalt Institute (AI) for urban minor arterial and light industrial streets (AI 1991b). In view of Table 3-17, as the thickness of the base layer increased to 228 mm (9 in), if the median and the coarser limit gradations for the RS aggregate are used as the base layer, the ESALs (1,220,600 for the median gradation, 1,076,300 for the coarser limit gradation) can satisfy the AI requirement. Similarly, as the thickness of the base layer increased to 304 mm (12 in), if

the median and the coarser limit gradations for the RS aggregate are used as the base layer, the ESALs (1,642,400 for the median gradation, 1,405,700 for the coarser limit gradation) can satisfy the AI requirement. However, the finer limit gradation cannot yield the required design ESAL for all of the thicknesses of base layer considered. On the other hand, as moisture varies within ±2% of the OMC, the material presents a very good performance when its moisture reaches the 2% below the OMC. For example, the 1,381,300 and 1,913,300 ESALs are obtained for 228 mm (9 in) and 304 mm (12 in) base layer, respectively. However, as the moisture increased to 2% above the OMC, only 519,800 and 530,500 ESALs are obtained for the corresponding thicknesses of base layers. From this example, one conclusion can be made that the service life of a pavement will reduce significantly if the pavement designed on the basis of MDD which coincides with the OMC; but the actual moisture remains above the OMC due to frequent rainfall or some other reasons.

Similar observations can be made when the undrained condition is present in the field. For example, the ESALs of 1,220,600 and 1,642,400 are obtained for 228 mm (9 in) and 304 mm (12 in) thick drained base layers. However, the ESAL value reduces to only 519,800 if the drainage condition is changed to undrained. Hence, half of the service life or two-thirds of the service life will be lost for the pavement designed based on the assumption that the drained conditions are in control whereas the undrained conditions are operative in the field.

In practice, if the moisture content of aggregate base is different from the study cases given here. For example, if the moisture content is 1% below or 1% above the OMC, the layer coefficients predicted by Eqs. (3-7) and (3-8) can be used in the design.

The following design examples based on the Sawyer aggregate show such an application. Assume that the coarser limit gradation for the Sawyer aggregate at the OMC, 1% below, and 1% above the OMC is used as a base layer. The corresponding thicknesses of the base layer are 76 mm, 152 mm, 228 mm, and 304 mm. The thickness of the AC layer and its M_R value are assumed to be 178 mm and 3450 MPa, respectively. Based on these parameters, the layer coefficients for each base layer were predicted by using Eq. (3-8). Furthermore, the SN and the ESAL of the pavements for different bases were computed and the results obtained are presented in Table 3-18.

In view of Table 3-18, the Sawyer aggregate at 1% below the OMC gave the highest design ESAL. As the base thickness increases from 76 mm to 304 mm, the corresponding ESAL increased from 1,024,700 to 1,767,300. At the OMC, the 76 mm thick base produced a design ESAL of only 815,400 that does not satisfy the AI requirement. However, as the thickness of the base layer increases to 152 mm, a design ESAL of 1,017,200 was obtained. For the Sawyer aggregate at 1% above the OMC, none of these bases could produce a desired design ESAL.

Since the RS aggregate generally gave higher layer coefficients than those of the Sawyer aggregate (Tables 3-10 to 3-15), it is interesting to compare the design results between the RS and the Sawyer aggregates. It is expected that for the same design ESAL, the RS aggregate would require less base thickness than the Sawyer aggregate. For example, the RS aggregate in Case 6, which has 152 mm (6 in) base and 230 mm AC layers, produced a design ESAL of 1,057,000 when the moisture is 2% below the OMC. It was found that for the same thickness of AC layer and base moisture content, it requires a 457 mm (18 in) thick base for the Sawyer aggregate to produce the same

design ESAL. Therefore, it can be concluded that using the RS aggregate as a base layer is more efficient than the Sawyer aggregate as a pavement component.

Table 3-1 Comparison of Different AASHTO Resilient Modulus Testing Procedures

	AASHTO T 274-82			AASHTO T 292-91I			AASHTO T 294-92I and T 294-94		
	σc (kPa)	σd (kPa)	No. of Cycles	σc (kPa)	σd (kPa)	No. of Cycles	σc (kPa)	σd (kPa)	No. of Cycles
Sample conditioning	34	34	200						
	34	69	200						
	69	69	200						
	69	103	200						
	103	103	200						
	103	138	200	138	103	1000	103	103	1000
Test	138	7	200	138	69	50	21	21	100
	138	14	200	138	138	50	21	41	100
	138	34	200	138	207	50	21	62	100
	138	69	200	138	276	50	34	34	100
	138	103	200	103	69	50	34	69	100
	138	138	200	103	138	50	34	103	100
	103	7	200	103	207	50	69	69	100
	103	14	200	103	276	50	69	138	100
	103	34	200	69	34	50	69	207	100
	103	69	200	69	69	50	103	69	100
	103	103	200	69	138	50	103	103	100
	103	138	200	69	207	50	103	207	100
	69	7	200	34	34	50	138	103	100
	69	14	200	34	69	50	138	138	100
	69	34	200	34	103	50	138	276	100
	69	69	200	21	34	50			
	69	103	200	21	48	50			
	34	7	200	21	62	50			
	34	14	200						
	34	34	200						
	34	69	200						
	34	103	200						
	7	7	200						
	7	14	200						
	7	34	200						
	7	52	200						
	7	69	200						

Table 3-2 Unconfined Compressive Strength (U_c), Cohesion (C), and Friction Angle (ϕ) Measured for the RS and the Sawyer Aggregates

	RS			Sawyer		
	U_c (kPa)	C (kPa)	ϕ °	U_c (kPa)	C (kPa)	ϕ °
T 292-91I	347.9	68.9	58.2			
T 294-94	299.0	120.6	50.1	416.7	68.9	55.4
Coarser Limit	120.6	83.4	52.9	177.9	34.5	58.4
Finer Limit	295.6	134.4	46.9	283.6	75.8	51.2
2% below OMC	226.7	82.7	46.7	255.8	65.5	53.7
2% above OMC	150.9	44.8	55.5	214.0	51.7	56.8
Undrained I	267.6	62.0	55.0	257.1	48.2	57.5
Undrained II	316.6	68.9	54.7	302.8	55.1	56.9
Raw Sample				262.2	68.9	50.8

Table 3-3 Salient Features of AASHTO T 292-91I and T 294-94 Testing Procedures

	AASHTO T 292-91I	AASHTO T 294-92I and AASHTO T 294-94
Sample conditioning	Confining Pressure: 138 kPa Deviatoric Stress: 103 kPa	Confining Pressure: 103 kPa Deviatoric Stress: 103 kPa
Stress Sequence	From a higher confining pressure and deviatoric stress to a lower confining pressure and deviatoric stress	Opposite to T 292-91I
Number of loading cycles	Conditioning: 1000 RM testing: 50	Conditioning: 1000 RM testing: 100
Stress pulse	Haversine, Triangular, Rectangular	Haversine
LVDT Location	Internal, at 1/3 to 1/4 of the specimen; or external, at the top of the specimen	External, at the top of the specimen
Compaction Method	Vibration	Vibration
Bulk Stress	From 97 to 690 kPa	From 83 to 690 kPa

Table 3-4 Measured Recoverable Deformations from the T 292-91I and T 294-94 Testing Methods

Testing Method	Recoverable Deformation ($1x10^{-3}$ in)	Test 1	Test 2	Test 3	Test 4	Test 5	Test 6
T 292-91I	Δ1 (at the 20th cycle)	7.8	8.8	6.8	7.8	8.8	8.8
	Δ2 (at the 50th cycle)	7.8	8.8	6.8	7.8	8.8	8.8
	(Δ2-Δ1)/Δ2 (%)	0.0	0.0	0.0	0.0	0.0	0.0
T 294-94	Δ1 (at the 70th cycle)	9.8	7.8	9.8	7.8	8.8	10.8
	Δ2 (at the 100th cycle)	9.6	7.8	9.6	7.8	8.8	10.6
	(Δ2-Δ1)/Δ2 (%)	2.1	0.0	2.1	0.0	0.0	1.9

1 in = 25.4 mm

Table 3-5 Confidence Level Calculated from the Measured M_R Values (RS Aggregate at Median Gradation and 2% below OMC)

Bulk Stress (kPa)	M_R (MPa)	SD (MPa)	EE (MPa)	Sample Number	$Z_{\alpha/2}$	Confidence Level (%)	Relative Error (%)
84	102.6	37.3	15.39	6	1.011	68.8	36.4
104	139.4	30.1	20.91	6	1.702	91.0	21.6
125	188.7	50.5	28.31	6	1.373	83.0	26.8
136	209.4	66.3	31.41	6	1.662	90.4	31.7
171	200.7	48.4	30.11	6	1.524	87.2	24.1
205	232.3	40.0	34.85	6	2.134	96.6	17.2
276	260.2	59.0	39.03	6	1.620	89.4	22.7
345	312.2	58.9	46.83	6	1.948	94.8	18.9
414	303.4	46.3	45.51	6	2.408	98.4	15.3
378	271.2	80.3	40.68	6	1.241	78.6	29.6
412	321.8	69.7	48.27	6	1.696	91.0	21.7
516	352.3	53.9	52.85	6	2.402	98.4	15.3
517	339.8	81.5	50.97	6	1.532	87.4	24.0
552	380.8	74.5	57.12	6	1.878	94.0	19.6
690	396	62.3	59.40	6	2.335	98.0	15.7

Average Confidence Level = 90%
Average Relative Error = 22.7%

Table 3-6 Confidence Level Calculated from the Measured M_R Values (Sawyer Aggregate at Finer Limit Gradation and OMC)

Bulk Stress (kPa)	M_R (MPa)	SD (MPa)	EE (MPa)	Sample Number	$Z_{\alpha/2}$	Confidence Level (%)	Relative Error (%)
84	51.7	17.7	7.76	6	0.142	71.6	34.2
104	75.3	9.3	11.30	6	0.001	99.8	12.4
125	79.4	9.6	11.91	6	0.000	100.0	12.1
136	104.9	20.8	15.74	6	0.032	93.6	19.8
171	99.2	9.8	14.88	6	0.000	100.0	9.9
205	106.1	8.7	15.92	6	0.000	100.0	8.2
276	141.7	19.7	21.26	6	0.004	99.2	13.9
345	145.6	14.1	21.84	6	0.000	100.0	9.7
414	151.2	10.1	22.68	6	0.000	100.0	6.7
378	163.2	9.1	24.48	6	0.000	100.0	5.6
412	160.0	9.3	24.00	6	0.000	100.0	5.8
516	181.1	13.5	27.17	6	0.000	100.0	7.5
517	188.2	19.5	28.23	6	0.000	100.0	10.4
552	191.8	19.5	28.77	6	0.000	100.0	10.2
690	213.0	12.4	31.95	6	0.000	100.0	5.8

Average Confidence Level = 98%
Average Relative Error = 11.5%

Table 3-7 Material Parameters k_1 and k_2 of the RS and the Sawyer Aggregates

Material Type	Case	k_1 (kPa)	SD (kPa)	k_2	SD	R^2
RS	Median	10633	2191	0.5403	0.0344	0.8139
	Coarser Limit	11037	2746	0.5213	0.0415	0.7351
	Finer Limit	8710	2171	0.4603	0.0418	0.6585
	2% below OMC	14306	4181	0.5091	0.0489	0.6628
	2% above OMC	5909	1278	0.5893	0.0359	0.8317
	Undrained I	9198	3422	0.4718	0.0624	0.6271
	Undrained II	6539	1738	0.5247	0.0444	0.8034
Sawyer	Median	7098	930	0.5162	0.0219	0.9061
	Coarser Limit	8110	1550	0.5235	0.0319	0.8272
	Finer Limit	5554	852	0.5610	0.0255	0.8996
	2% below OMC	11063	2860	0.4728	0.0434	0.6698
	2% above OMC	2815	606	0.6281	0.0357	0.8518
	Undrained I	4846	1516	0.5092	0.0532	0.6673
	Undrained II	4819	1181	0.5166	0.0409	0.7712

Table 3-8 Measure of Fit for Multiple M_R Models with Different Variables

Number in Model	Variables	R^2 (RS)	R^2 (Sawyer)
1	No.200	0.1233	0.0185
1	MC	0.1545	0.1870
1	σ_d	0.3065	0.4551
1	θ	0.4617	0.6672
2	MC, No.200	0.2917	0.1870
2	σ_d, No.200	0.4298	0.4736
2	σ_d, MC	0.4610	0.6421
2	θ, σ_d	0.4623	0.6674
2	θ, No.200	0.5850	0.6857
2	θ, MC	0.6162	0.8542
3	θ, σ_d, No.200	0.5856	0.6860
3	σ_d, MC, No.200	0.5981	0.6421
3	θ, MC, σ_d	0.6168	0.8542
3	θ, MC, No.200	0.7534	0.8544
4	θ, MC, No.200, σ_d	0.7539	0.8544
5	θ, MC, No.200, σ_d, C	0.7555	0.8568

Table 3-9 The Various Combinations of AC layer Thickness (D_{ac}), AC Layer M_R (E_{ac}), Base Layer Thickness (D_2), and the Corresponding Case Numbers and ELBK

E_{ac}	Base Thickness	D_{ac}, mm (in)								
		76 (3)			152 (6)			228 (9)		
kPa	D_2	Case	ELBK		Case	ELBK		Case	ELBK	
(psi)	mm (in)	No.	psi	kPa	No.	psi	kPa	No.	psi	kPa
1725000	76 (3)	Case 1	27.62	190.59	Case 2	12.60	86.92	Case 3	7.83	54.00
(250000)	152 (6)	Case 4	28.92	199.52	Case 5	12.60	86.92	Case 6	7.59	52.37
	228 (9)	Case 7	30.08	207.53	Case 8	13.00	89.71	Case 9	7.00	48.29
	304 (12)	Case 10	26.27	181.26	Case 11	11.98	82.66	Case 12	7.20	49.69
3450000	76 (3)	Case 13	21.70	149.73	Case 14	9.17	63.26	Case 15	5.88	40.56
(500000)	152 (6)	Case 16	21.73	149.95	Case 17	9.26	63.88	Case 18	5.93	40.95
	228 (9)	Case 19	22.53	155.45	Case 20	8.86	61.11	Case 21	6.19	42.69
	304 (12)	Case 22	20.42	140.87	Case 23	8.22	56.69	Case 24	6.44	44.40
5175000	76 (3)	Case 25	17.35	119.68	Case 26	7.52	51.88	Case 27	5.37	37.02
(750000)	152 (6)	Case 28	18.33	126.49	Case 29	7.33	50.55	Case 30	5.64	38.91
	228 (9)	Case 31	19.31	133.22	Case 32	7.27	50.17	Case 33	5.89	40.62
	304 (12)	Case 34	17.93	123.68	Case 35	7.43	51.24	Case 36	6.11	42.18

Table 3-10 Layer Coefficients (a_2) of the RS Aggregate at Different Gradations

E_{ac}	Base Thickness	Median Gradation			Finer LimitGradation			Coarser LimitGradation		
	D_2	D_{ac} (mm)			D_{ac} (mm)			D_{ac} (mm)		
		76	152	228	76	152	228	76	152	228
(kPa)	(mm)	a_2	a_2	a_2	a_2	a_2	a_2	a_2	a_2	a_2
1725000	76	0.1256	0.0824	0.0562	0.0619	0.0278	0.0071	0.1185	0.0750	0.0486
	152	0.1281	0.0824	0.0545	0.0639	0.0278	0.0058	0.1211	0.0750	0.0469
	228	0.1303	0.0841	0.0500	0.0656	0.0292	0.0022	0.1233	0.0767	0.0424
	304	0.1228	0.0796	0.0516	0.0597	0.0256	0.0035	0.1158	0.0722	0.0440
3450000	76	0.1123	0.0649	0.0404	0.0514	0.0140	-0.0053	0.1052	0.0574	0.0327
	152	0.1124	0.0654	0.0410	0.0515	0.0144	-0.0049	0.1052	0.0579	0.0332
	228	0.1144	0.0630	0.0433	0.0530	0.0125	-0.0031	0.1072	0.0554	0.0355
	304	0.1089	0.0589	0.0454	0.0488	0.0092	-0.0014	0.1018	0.0513	0.0377
5175000	76	0.1000	0.0540	0.0354	0.0417	0.0054	-0.0093	0.0927	0.0464	0.0276
	152	0.1030	0.0526	0.0382	0.0441	0.0042	-0.0071	0.0958	0.0449	0.0304
	228	0.1059	0.0521	0.0405	0.0463	0.0039	-0.0053	0.0987	0.0445	0.0328
	304	0.1018	0.0533	0.0426	0.0431	0.0048	-0.0036	0.0946	0.0457	0.0349

Table 3-11 Layer Coefficients (a_2) of the RS Aggregate at Different Moisture Contents

E_{ac}	Base Thickness	Optimum Moisture			2% below Optimum			2% above Optimum		
	D_2	D_{ac} (mm)			D_{ac} (mm)			D_{ac} (mm)		
		76	152	228	76	152	228	76	152	228
(kPa)	(mm)	a_2	a_2	a_2	a_2	a_2	a_2	a_2	a_2	a_2
1725000	76	0.1256	0.0824	0.0562	0.1382	0.0919	0.0639	0.0885	0.0373	0.0063
	152	0.1281	0.0824	0.0545	0.1409	0.0919	0.0621	0.0915	0.0373	0.0043
	228	0.1303	0.0841	0.0500	0.1432	0.0938	0.0573	0.0941	0.0394	-0.0010
	304	0.1228	0.0796	0.0516	0.1352	0.0890	0.0590	0.0853	0.0340	0.0008
3450000	76	0.1123	0.0649	0.0404	0.1240	0.0732	0.0470	0.0728	0.0166	-0.0124
	152	0.1124	0.0654	0.0410	0.1241	0.0738	0.0476	0.0729	0.0172	-0.0118
	228	0.1144	0.0630	0.0433	0.1262	0.0712	0.0501	0.0752	0.0143	-0.0091
	304	0.1089	0.0589	0.0454	0.1204	0.0668	0.0524	0.0688	0.0094	-0.0065
5175000	76	0.1000	0.0540	0.0354	0.1108	0.0615	0.0417	0.0582	0.0036	-0.0184
	152	0.1030	0.0526	0.0382	0.1140	0.0600	0.0446	0.0618	0.0019	-0.0151
	228	0.1059	0.0521	0.0405	0.1171	0.0596	0.0471	0.0652	0.0015	-0.0123
	304	0.1018	0.0533	0.0426	0.1127	0.0608	0.0494	0.0603	0.0028	-0.0099

Table 3-12 Layer Coefficients (a_2) of the RS Aggregate at Different Drainage Conditions

E_{ac}	Base Thickness	Drained			Undrained I			Undrained II		
	D_2	D_{ac} (mm)			D_{ac} (mm)			D_{ac} (mm)		
		76	152	228	76	152	228	76	152	228
(kPa)	(mm)	a_2	a_2	a_2	a_2	a_2	a_2	a_2	a_2	a_2
1725000	76	0.1256	0.0824	0.0562	0.0680	0.0264	0.0013	0.0628	0.0179	-0.0093
	152	0.1281	0.0824	0.0545	0.0704	0.0264	-0.0004	0.0654	0.0179	-0.0111
	228	0.1303	0.0841	0.0500	0.0725	0.0281	-0.0046	0.0676	0.0197	-0.0157
	304	0.1228	0.0796	0.0516	0.0653	0.0238	-0.0031	0.0599	0.0150	-0.0141
3450000	76	0.1123	0.0649	0.0404	0.0552	0.0096	-0.0139	0.0490	-0.0003	-0.0257
	152	0.1124	0.0654	0.0410	0.0553	0.0102	-0.0134	0.0491	0.0003	-0.0251
	228	0.1144	0.0630	0.0433	0.0572	0.0078	-0.0112	0.0511	-0.0022	-0.0228
	304	0.1089	0.0589	0.0454	0.0520	0.0038	-0.0091	0.0455	-0.0065	-0.0205
5175000	76	0.1000	0.0540	0.0354	0.0434	-0.0009	-0.0187	0.0362	-0.0116	-0.0309
	152	0.1030	0.0526	0.0382	0.0463	-0.0022	-0.0161	0.0393	-0.0131	-0.0281
	228	0.1059	0.0521	0.0405	0.0490	-0.0026	-0.0138	0.0423	-0.0135	-0.0256
	304	0.1018	0.0533	0.0426	0.0451	-0.0015	-0.0118	0.0381	-0.0123	-0.0234

Table 3-13 Layer Coefficients (a_2) of the Sawyer Aggregate at Different Gradations

E_{ac}	Base Thickness	Median Gradation			Finer LimitGradation			Coarser LimitGradation		
	D_2	D_{ac} (mm)			D_{ac} (mm)			D_{ac} (mm)		
		76	152	228	76	152	228	76	152	228
(kPa)	(mm)	a_2	a_2	a_2	a_2	a_2	a_2	a_2	a_2	a_2
1725000	76	0.0647	0.0208	-0.0058	0.0631	0.0131	-0.0171	0.0865	0.0423	0.0156
	152	0.0672	0.0208	-0.0075	0.0660	0.0131	-0.0191	0.0891	0.0423	0.0138
	228	0.0694	0.0226	-0.0120	0.0685	0.0152	-0.0242	0.0913	0.0441	0.0093
	304	0.0619	0.0180	-0.0104	0.0599	0.0099	-0.0224	0.0837	0.0395	0.0109
3450000	76	0.0512	0.0031	-0.0218	0.0477	-0.0071	-0.0353	0.0729	0.0245	-0.0005
	152	0.0513	0.0036	-0.0212	0.0478	-0.0064	-0.0347	0.0730	0.0250	0.0000
	228	0.0533	0.0011	-0.0189	0.0501	-0.0093	-0.0321	0.0750	0.0225	0.0023
	304	0.0478	-0.0031	-0.0167	0.0439	-0.0140	-0.0296	0.0695	0.0183	0.0046
5175000	76	0.0387	-0.0080	-0.0269	0.0335	-0.0197	-0.0411	0.0603	0.0133	-0.0057
	152	0.0418	-0.0095	-0.0241	0.0370	-0.0213	-0.0380	0.0635	0.0119	-0.0029
	228	0.0447	-0.0099	-0.0217	0.0403	-0.0218	-0.0352	0.0664	0.0114	-0.0004
	304	0.0405	-0.0087	-0.0196	0.0356	-0.0205	-0.0328	0.0622	0.0126	0.0017

Table 3-14 Layer Coefficients (a_2) of the Sawyer Aggregate at Different Moisture Contents

E_{ac}	Base Thickness	Optimum Moisture			2% below Optimum			2% above Optimum		
	D_2	D_{ac} (mm)			D_{ac} (mm)			D_{ac} (mm)		
		76	152	228	76	152	228	76	152	228
(kPa)	(mm)	a_2	a_2	a_2	a_2	a_2	a_2	a_2	a_2	a_2
1725000	76	0.0647	0.0208	-0.0058	0.0894	0.0474	0.0220	0.0311	-0.0213	-0.0530
	152	0.0672	0.0208	-0.0075	0.0919	0.0474	0.0203	0.0341	-0.0213	-0.0551
	228	0.0694	0.0226	-0.0120	0.0940	0.0491	0.0160	0.0368	-0.0192	-0.0605
	304	0.0619	0.0180	-0.0104	0.0867	0.0447	0.0175	0.0277	-0.0246	-0.0586
3450000	76	0.0512	0.0031	-0.0218	0.0765	0.0304	0.0067	0.0150	-0.0425	-0.0721
	152	0.0513	0.0036	-0.0212	0.0766	0.0310	0.0072	0.0151	-0.0418	-0.0715
	228	0.0533	0.0011	-0.0189	0.0785	0.0286	0.0094	0.0175	-0.0448	-0.0687
	304	0.0478	-0.0031	-0.0167	0.0732	0.0246	0.0115	0.0109	-0.0498	-0.0661
5175000	76	0.0387	-0.0080	-0.0269	0.0645	0.0198	0.0018	0.0000	-0.0557	-0.0782
	152	0.0418	-0.0095	-0.0241	0.0675	0.0184	0.0044	0.0037	-0.0574	-0.0749
	228	0.0447	-0.0099	-0.0217	0.0703	0.0180	0.0067	0.0072	-0.0579	-0.0720
	304	0.0405	-0.0087	-0.0196	0.0663	0.0192	0.0088	0.0022	-0.0565	-0.0695

Table 3-15 Layer Coefficients (a_2) of the Sawyer Aggregate at Different Drainage Conditions

E_{ac}	Base Thickness	Drained			Undrained I			Undrained II		
	D_2	D_{ac} (mm)			D_{ac} (mm)			D_{ac} (mm)		
		76	152	228	76	152	228	76	152	228
(kPa)	(mm)	a_2	a_2	a_2	a_2	a_2	a_2	a_2	a_2	a_2
1725000	76	0.0647	0.0208	-0.0058	0.0293	-0.0152	-0.0421	0.0270	-0.0149	-0.0403
	152	0.0672	0.0208	-0.0075	0.0319	-0.0152	-0.0438	0.0295	-0.0149	-0.0420
	228	0.0694	0.0226	-0.0120	0.0341	-0.0134	-0.0484	0.0316	-0.0132	-0.0463
	304	0.0619	0.0180	-0.0104	0.0264	-0.0180	-0.0468	0.0244	-0.0176	-0.0448
3450000	76	0.0512	0.0031	-0.0218	0.0156	-0.0331	-0.0583	0.0141	-0.0319	-0.0556
	152	0.0513	0.0036	-0.0212	0.0157	-0.0326	-0.0578	0.0142	-0.0314	-0.0551
	228	0.0533	0.0011	-0.0189	0.0177	-0.0351	-0.0554	0.0162	-0.0337	-0.0529
	304	0.0478	-0.0031	-0.0167	0.0122	-0.0393	-0.0532	0.0109	-0.0377	-0.0508
5175000	76	0.0387	-0.0080	-0.0269	0.0029	-0.0444	-0.0635	0.0022	-0.0425	-0.0605
	152	0.0418	-0.0095	-0.0241	0.0061	-0.0458	-0.0606	0.0051	-0.0439	-0.0578
	228	0.0447	-0.0099	-0.0217	0.0090	-0.0463	-0.0582	0.0079	-0.0443	-0.0555
	304	0.0405	-0.0087	-0.0196	0.0048	-0.0451	-0.0561	0.0039	-0.0431	-0.0535

Table 3-16 Measure of Fit for Layer Coefficient Models with Different Variables

Number in Model	Variables	R^2 (RS)	R^2 (Sawyer)
1	log E_{ac}	0.0549	0.0581
1	No.200	0.1297	0.0532
1	MC	0.2167	0.3564
1	D_{ac}	0.5044	0.5339
2	No.200, log E_{ac}	0.1847	0.1114
2	MC, log E_{ac}	0.2717	0.4146
2	MC, No.200	0.3633	0.3589
2	D_{ac}, log E_{ac}	0.4342	0.5921
2	D_{ac}, No.200	0.6341	0.5872
2	D_{ac}, MC	0.7211	0.8904
3	MC, No.200, log E_{ac}	0.4182	0.4171
3	D_{ac}, No.200, log E_{ac}	0.6890	0.6453
3	D_{ac}, MC, log E_{ac}	0.7760	0.9485
3	D_{ac}, MC, No.200	0.8676	0.8929
4	D_{ac}, MC, No.200, log E_{ac}	0.9226	0.9510
5	D_{ac}, MC, No.200, log E_{ac}, D_{bs}	0.9226	0.9510

Table 3-17 Comparison of SN and ESAL for the RS Aggregate at the Different Cases

	Case 3		Case 6		Case 9		Case 12	
	SN	ESAL	SN	ESAL	SN	ESAL	SN	ESAL
Median	3.14	727,300	3.30	982,400	3.42	1,220,600	3.59	1,642,400
Finer	2.99	541,300	3.00	552,300	2.99	541,300	3.01	563,500
Coarser	3.12	699,700	3.25	895,600	3.35	1,076,300	3.50	1,405,700
2% below	3.16	755,700	3.34	1,057,000	3.49	1,381,300	3.68	1,913,300
2% above	2.99	541,300	3.00	552,300	2.97	519,800	2.98	530,500
Undrained I	2.97	519,800	2.97	519,800	2.97	519,800	2.97	519,800
Undrained II	2.97	519,800	2.97	519,800	2.97	519,800	2.97	519,800

Table 3-18 Comparison of SN and ESAL for the Sawyer Aggregate at the Different Cases

	D_{base} = 76 mm D_{ac} = 178 mm E_{ac} = 3450 MPa		D_{base} = 152 mm D_{ac} = 178 mm E_{ac} = 3450 MPa		D_{base} = 228 mm D_{ac} = 178 mm E_{ac} = 3450 MPa		D_{base} = 304 mm D_{ac} = 178 mm E_{ac} = 3450 MPa	
	SN	ESAL	SN	ESAL	SN	ESAL	SN	ESAL
Coarser at OMC	3.12	699,700	3.25	895,600	3.35	1,076,300	3.50	1,405,700
1% below OMC	3.16	755,700	3.34	1,057,000	3.49	1,381,300	3.68	1,913,300
1% above OMC	2.99	541,300	3.00	552,300	2.97	519,800	2.98	530,500

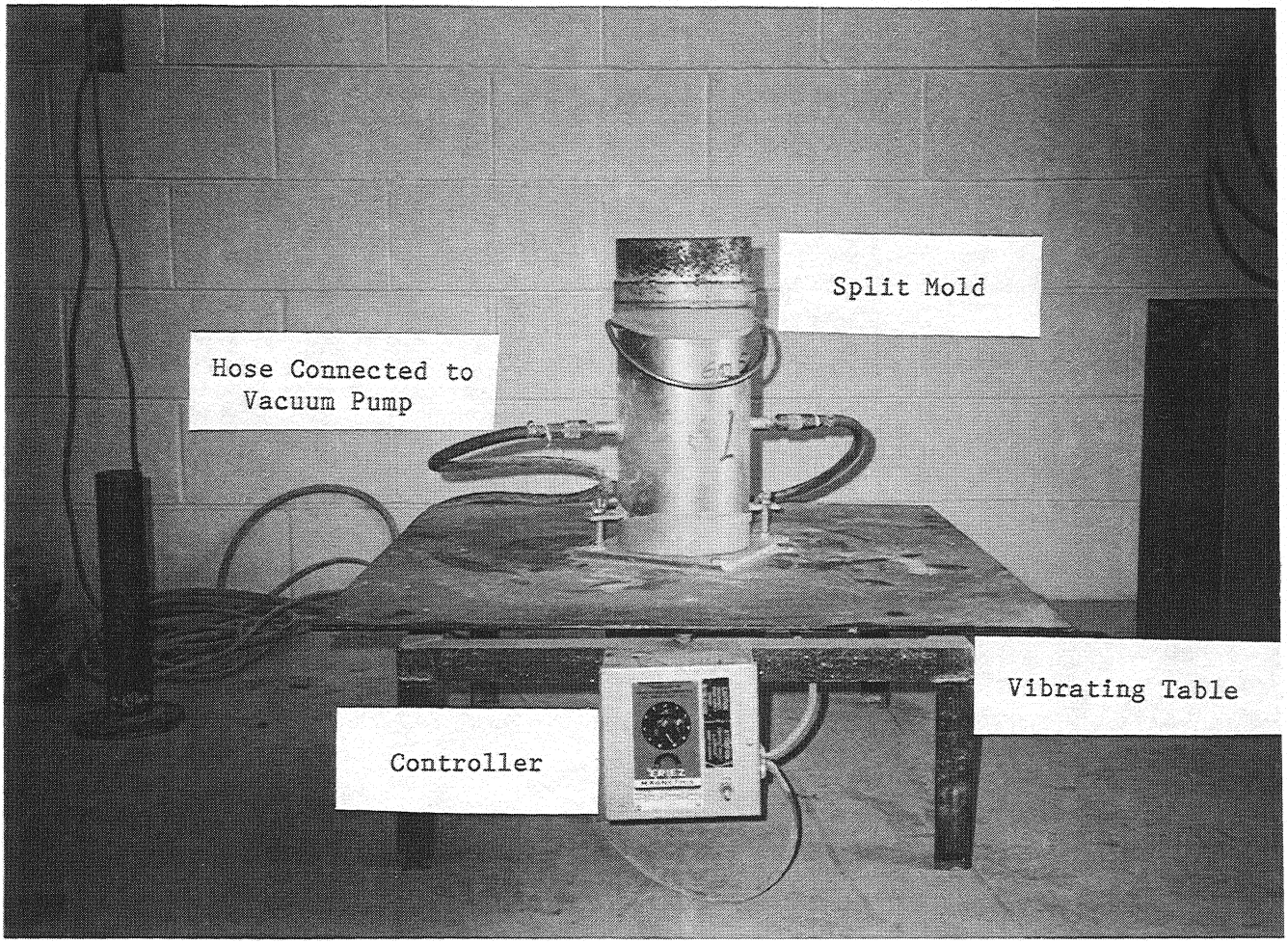

Figure 3-1 Equipment Used for the Preparation of M_R Testing Specimen

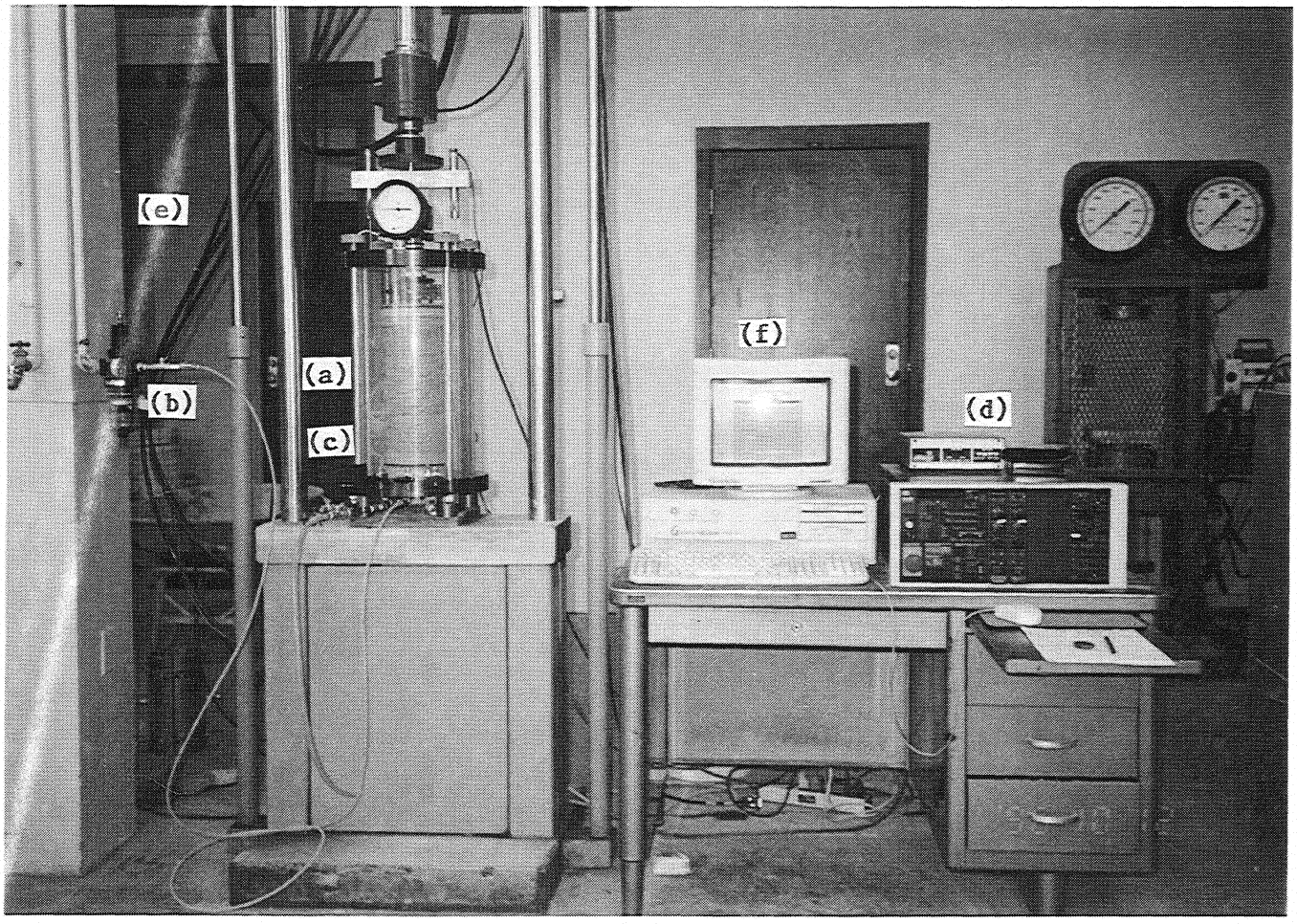

(a) Triaxial Chamber

(b) Chamber Pressure Regulator

(c) Test Specimen

(d) MTS Microconsole and Microprofile

(e) MTS Load Frame

(f) Personal Computer

Figure 3-2 Overall Setup of the M_R Testing Equipment

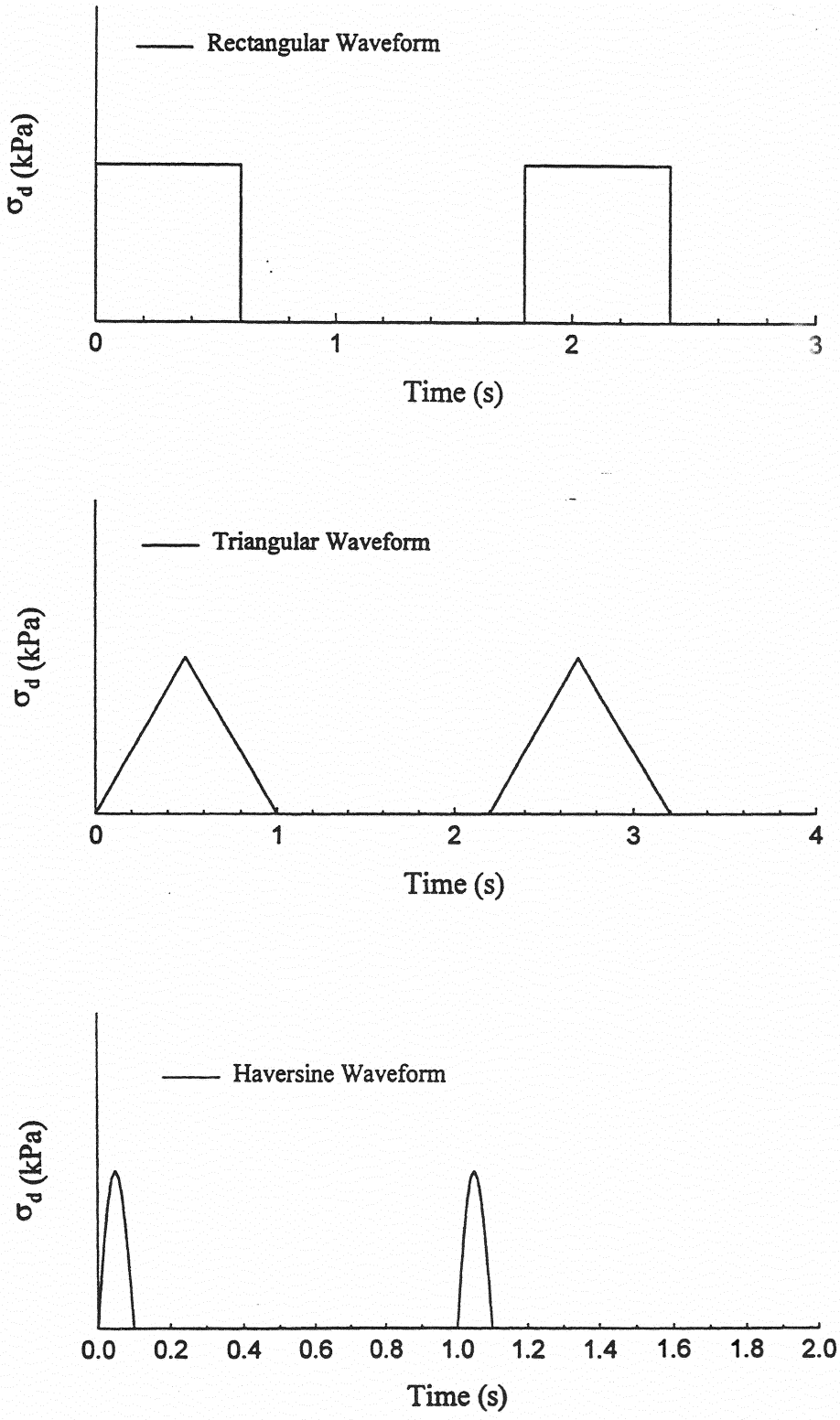

Figure 3-3 Haversine, Triangular, and Rectangular Waveforms Used

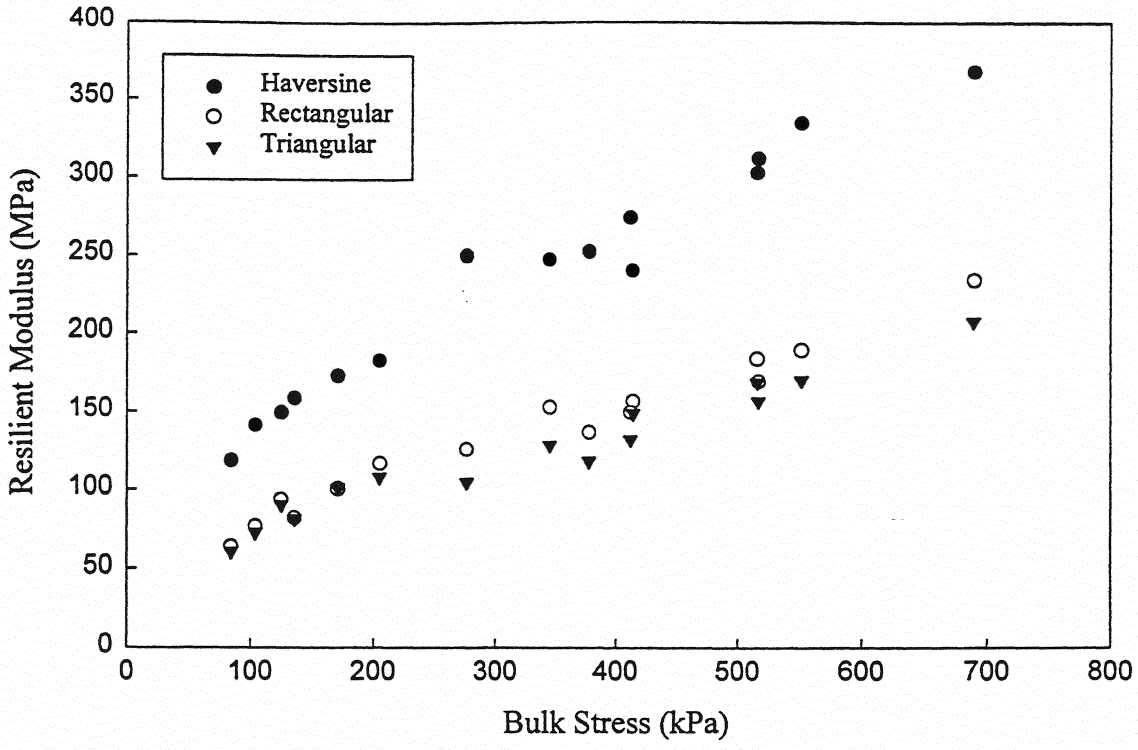

Figure 3-4 Mean M_R Values from Different Loading Waveforms (RS Aggregate)

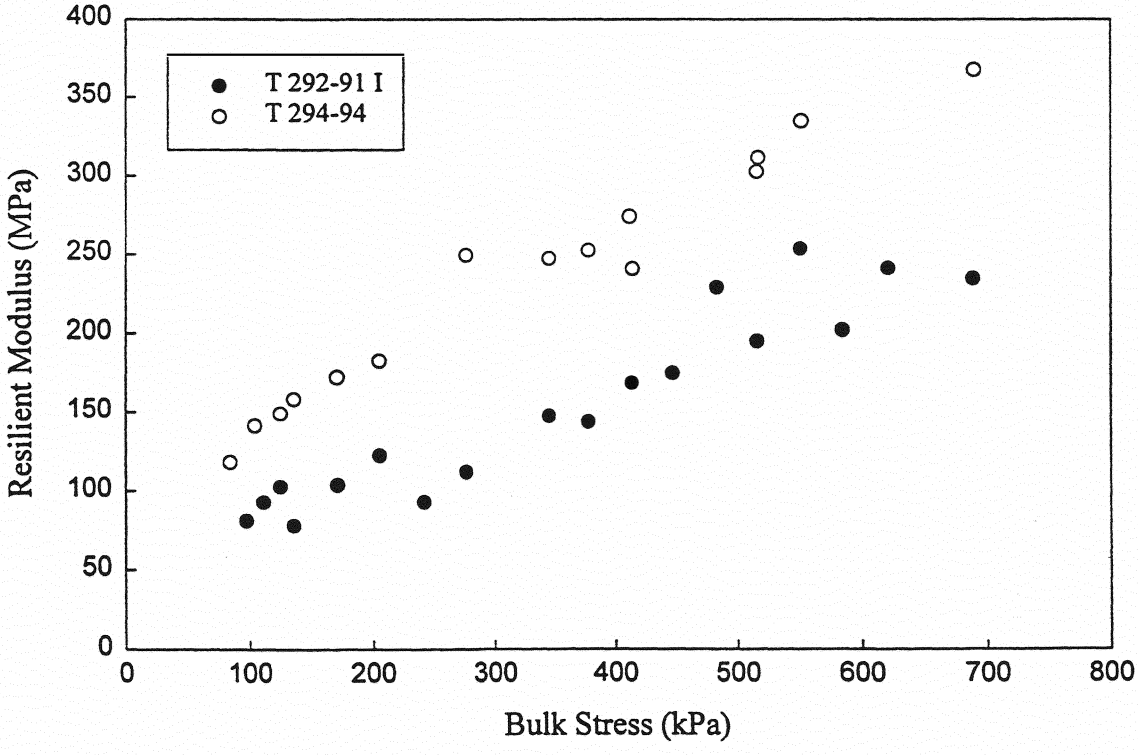

Figure 3-5 Mean M_R Values from the T 292-91I and T 294-94 Methods (RS Aggregate)

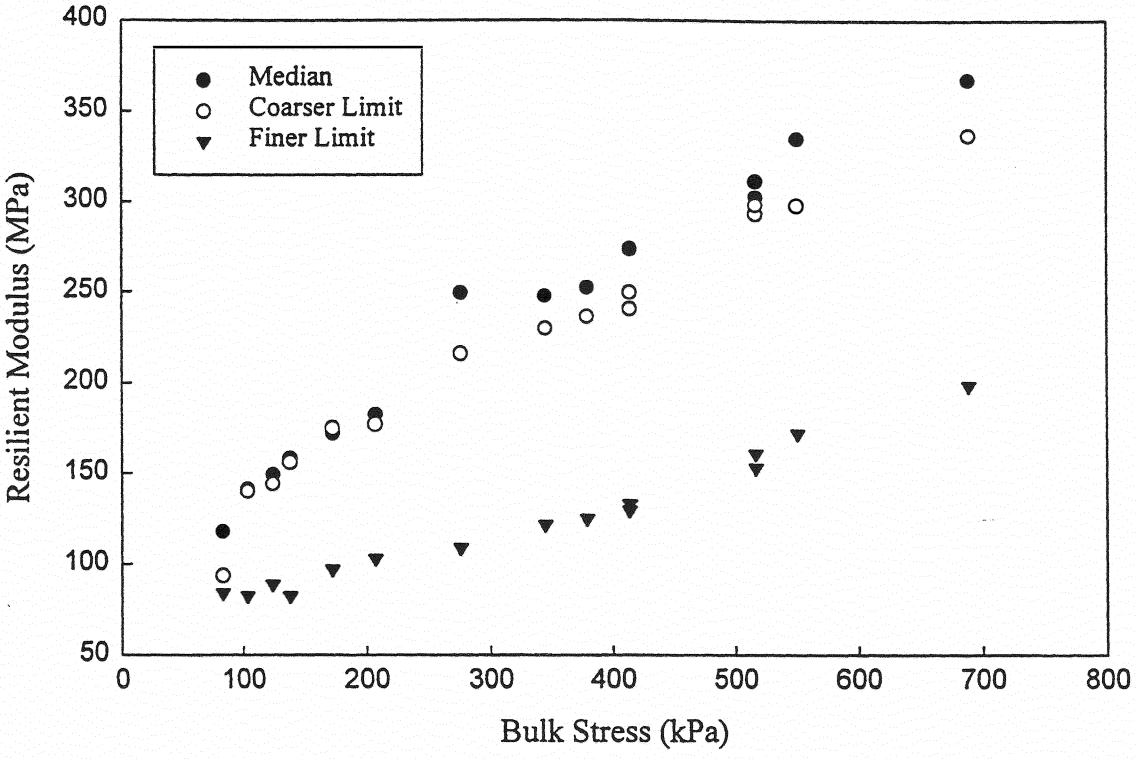

Figure 3-6 Mean M_R Values of the RS Aggregate at Different Gradations

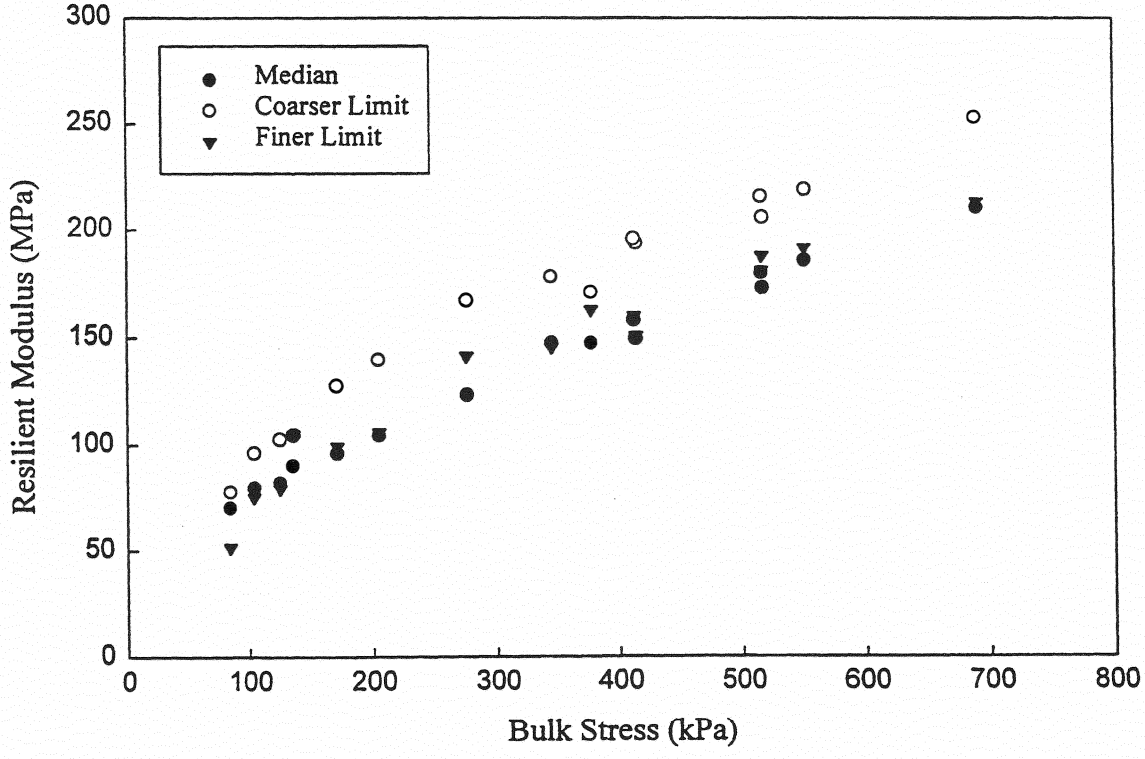

Figure 3-7 Mean M_R Values of the Sawyer Aggregate at Different Gradations

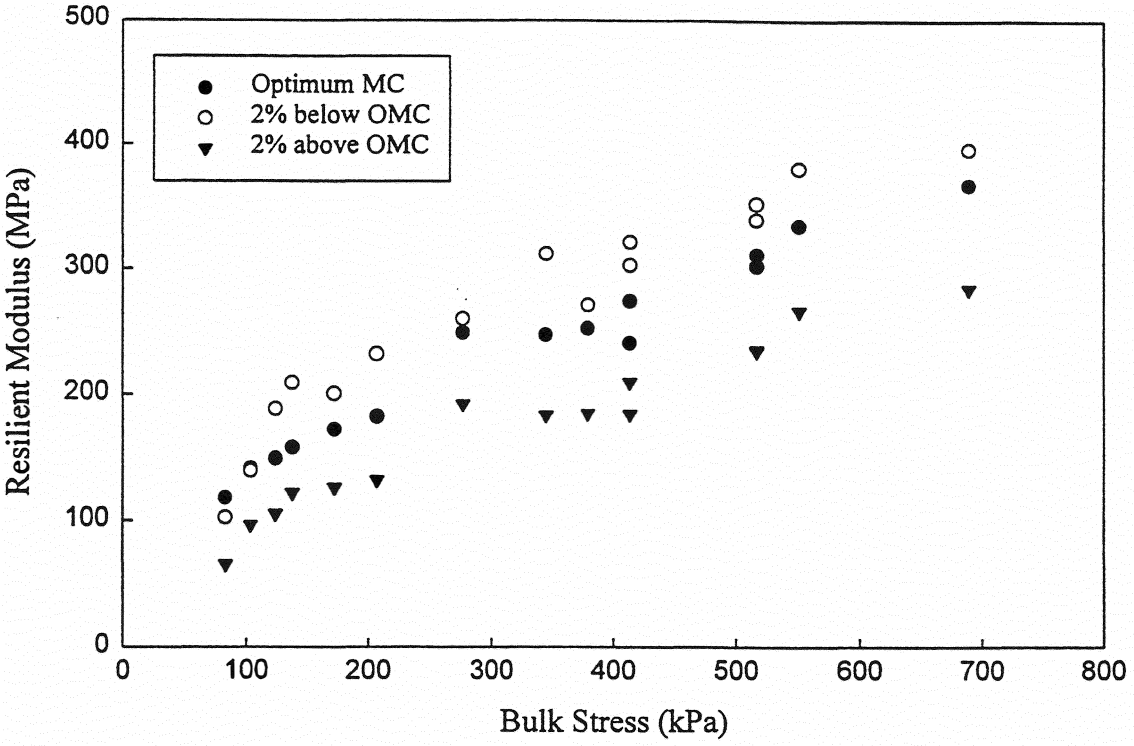

Figure 3-8 Mean M_R Values of the RS Aggregate at Different Moisture Contents

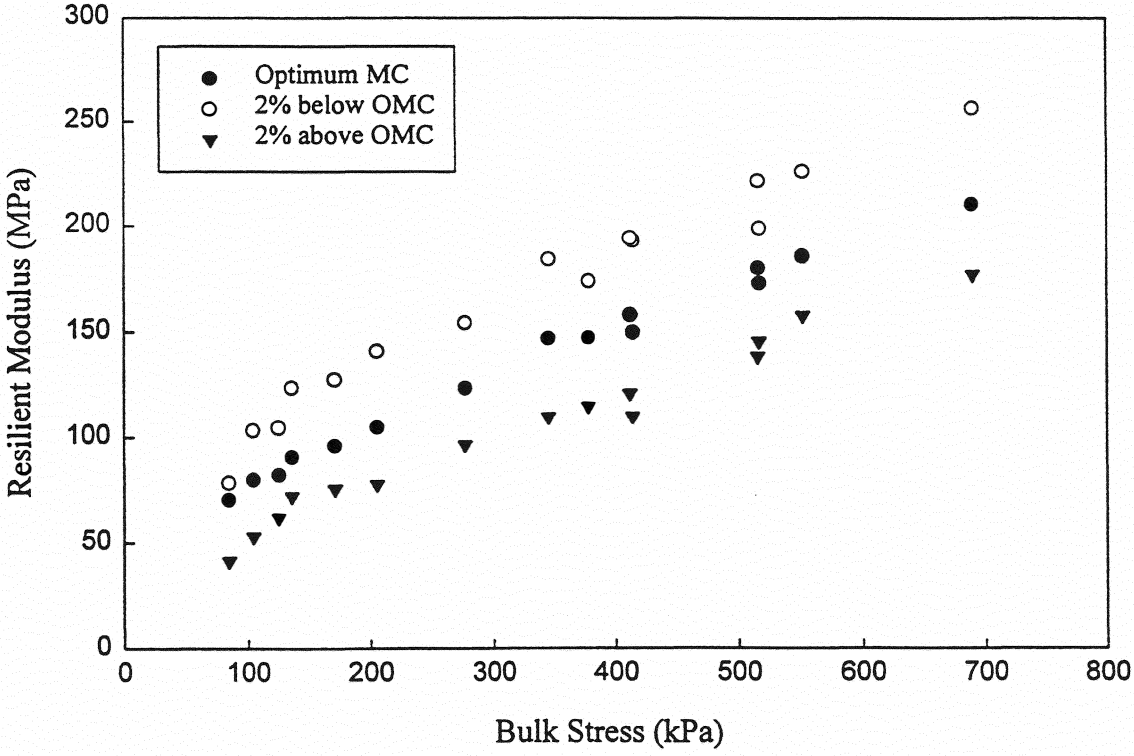

Figure 3-9 Mean M_R Values of the Sawyer Aggregate at Different Moisture Contents

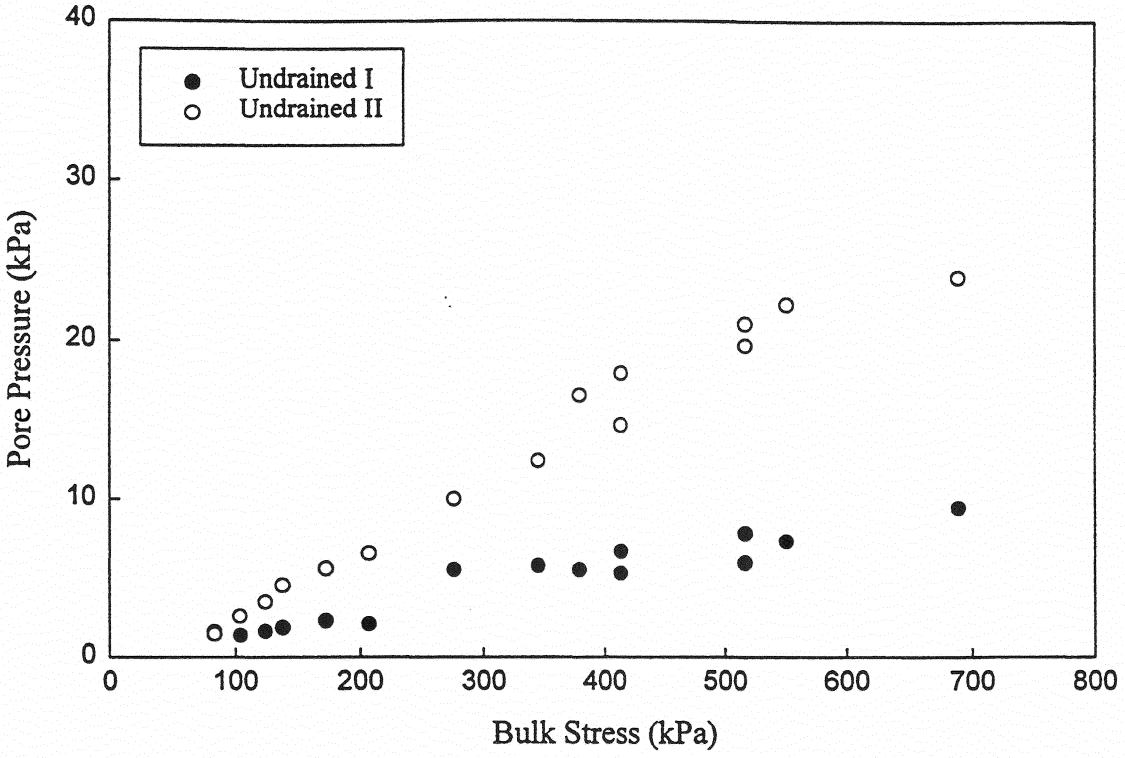

Figure 3-10 Pore Pressure Measured in Undrained I and II M_R Tests (RS Aggregate)

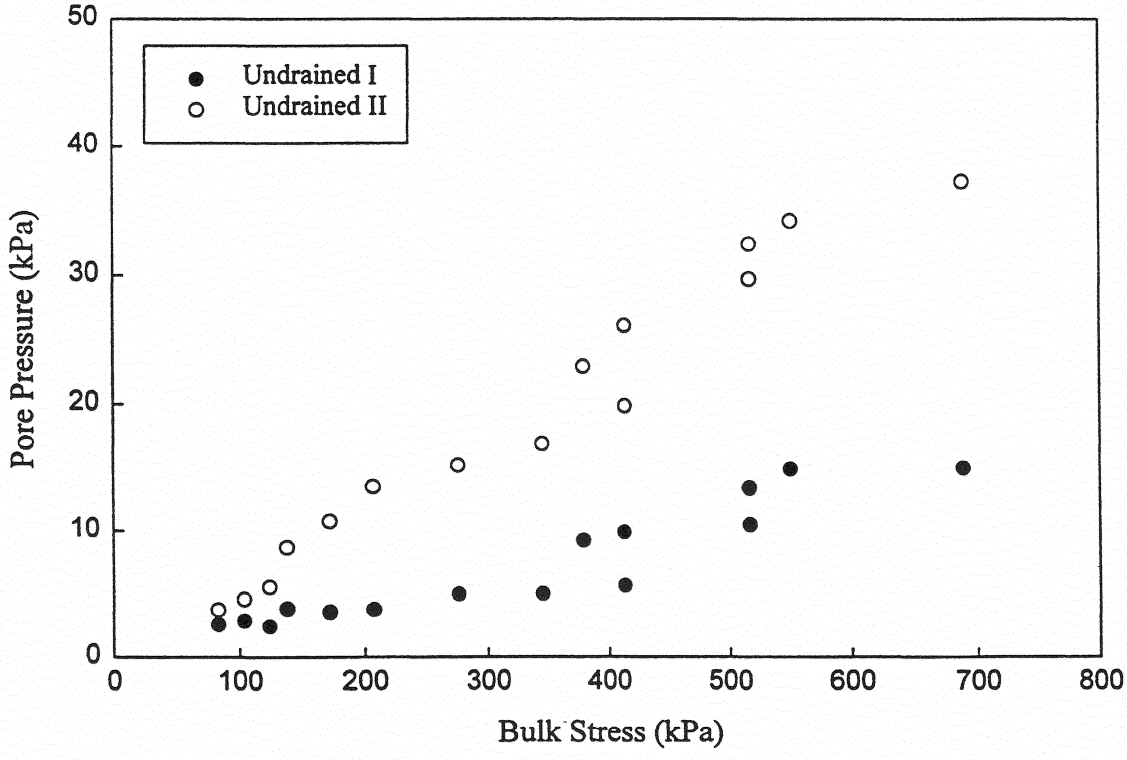

Figure 3-11 Pore Pressure Measured in Undrained I and II M_R Tests (Sawyer Aggregate)

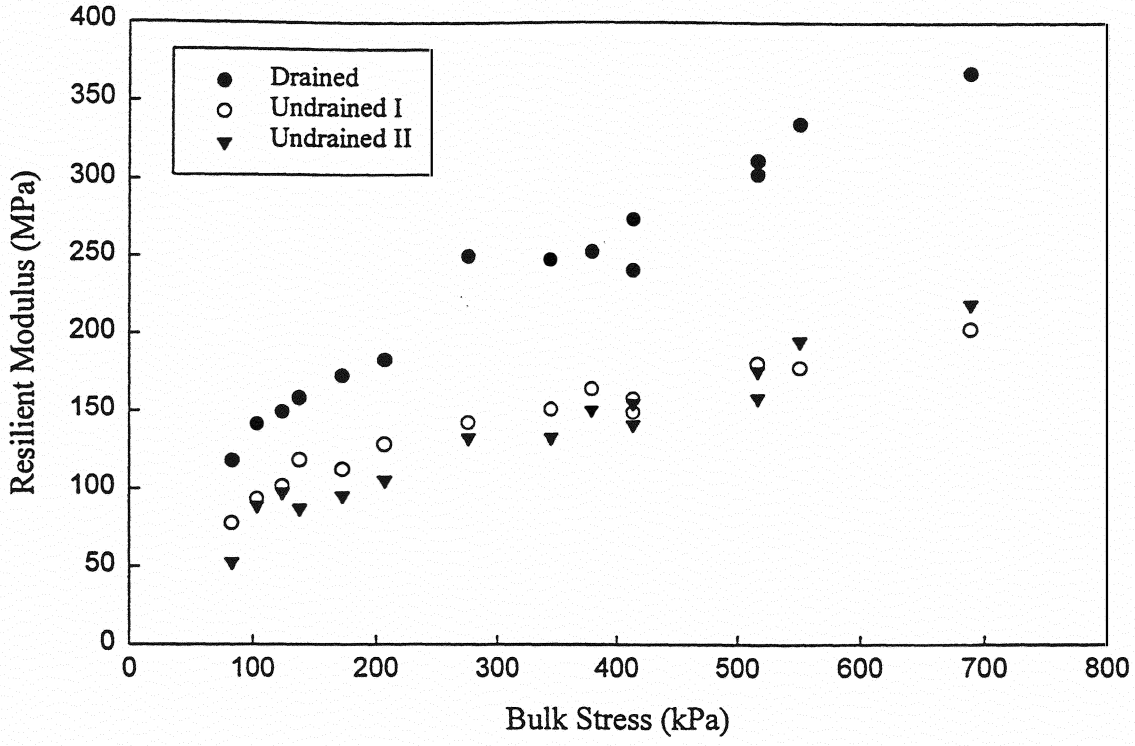

Figure 3-12 Mean M_R Values of the RS Aggregate from the Drained and Undrained Tests

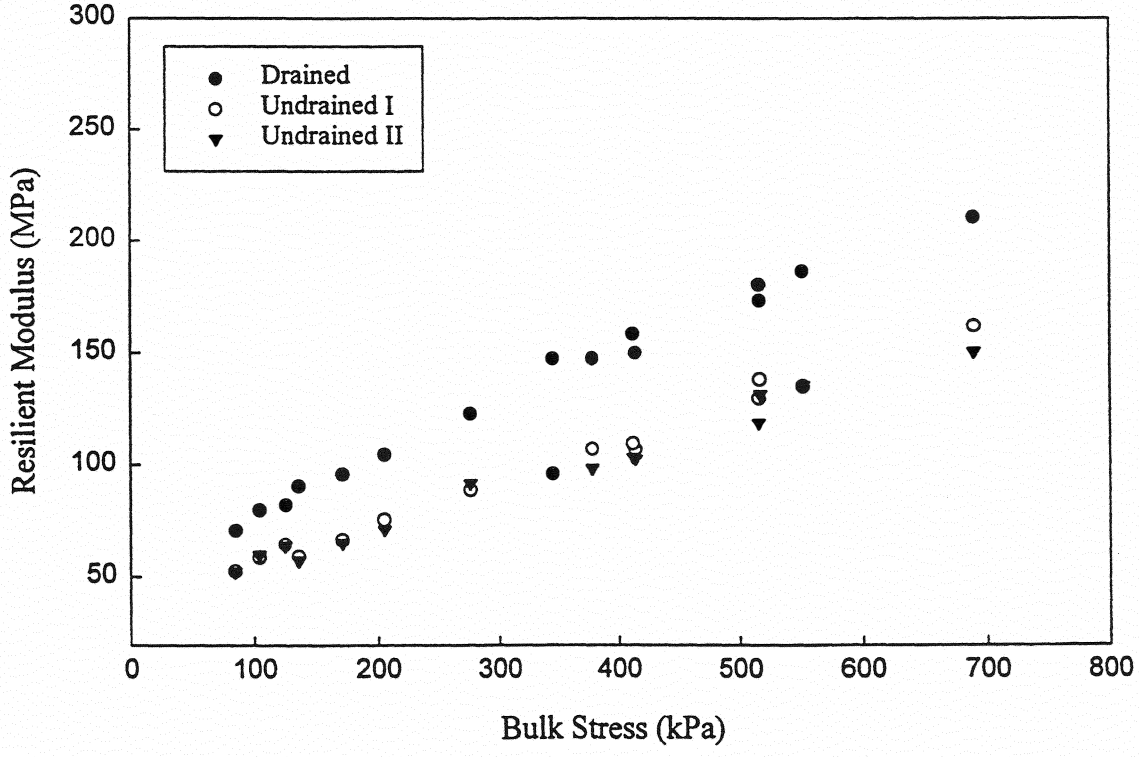

Figure 3-13 Mean M_R Values of the Sawyer Aggregate from the Drained and Undrained Tests

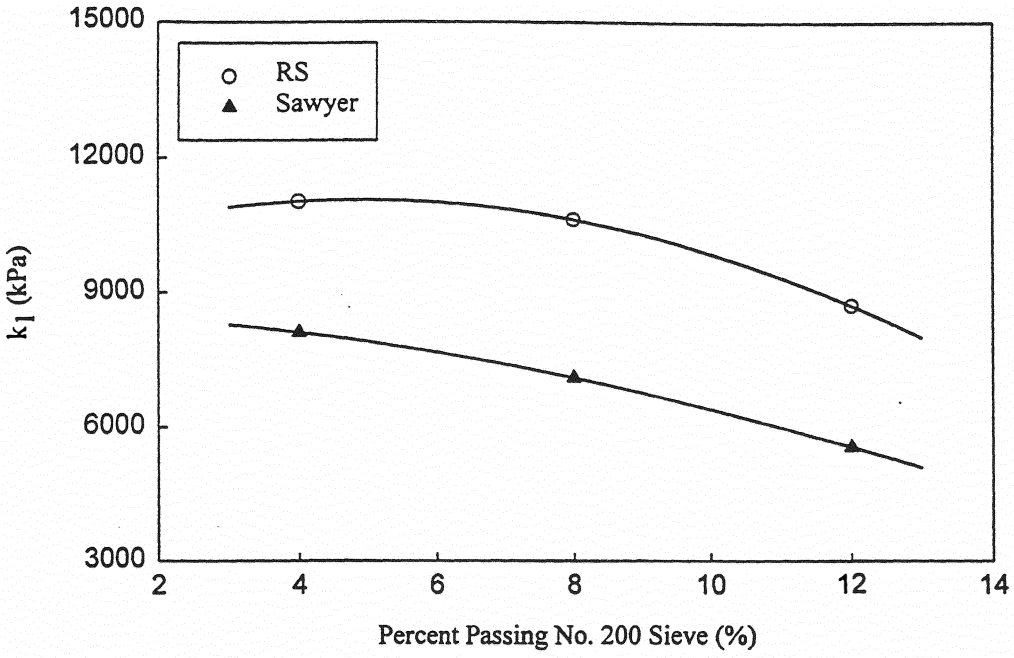

Figure 3-14 Variation of k_1 Values with the No. 200 (0.075 mm) Percent Passing

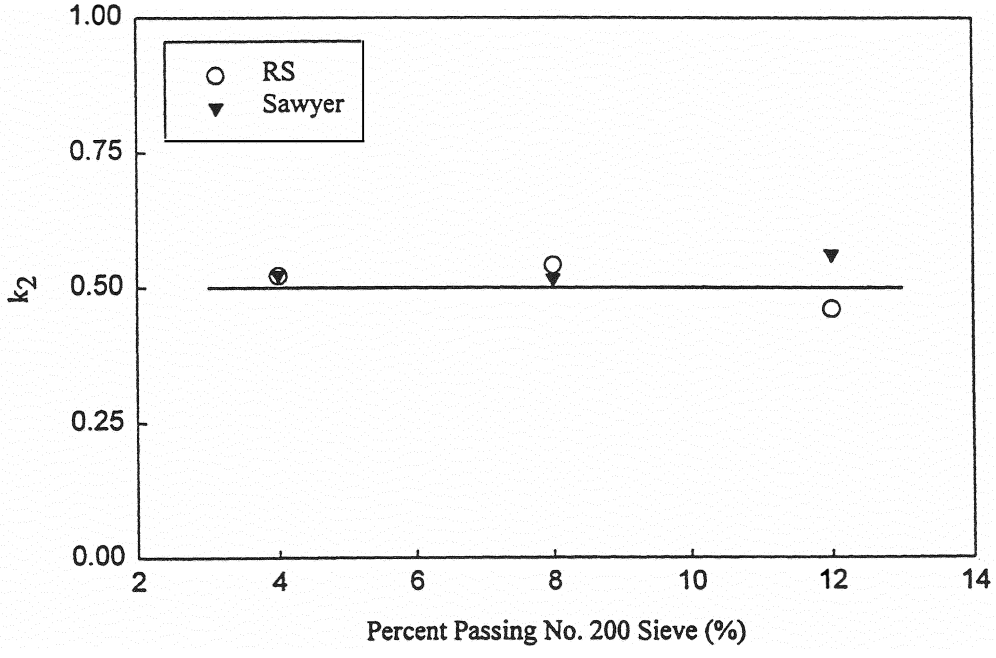

Figure 3-15 Variation of k_2 values with the No. 200 (0.075 mm) Percent Passing

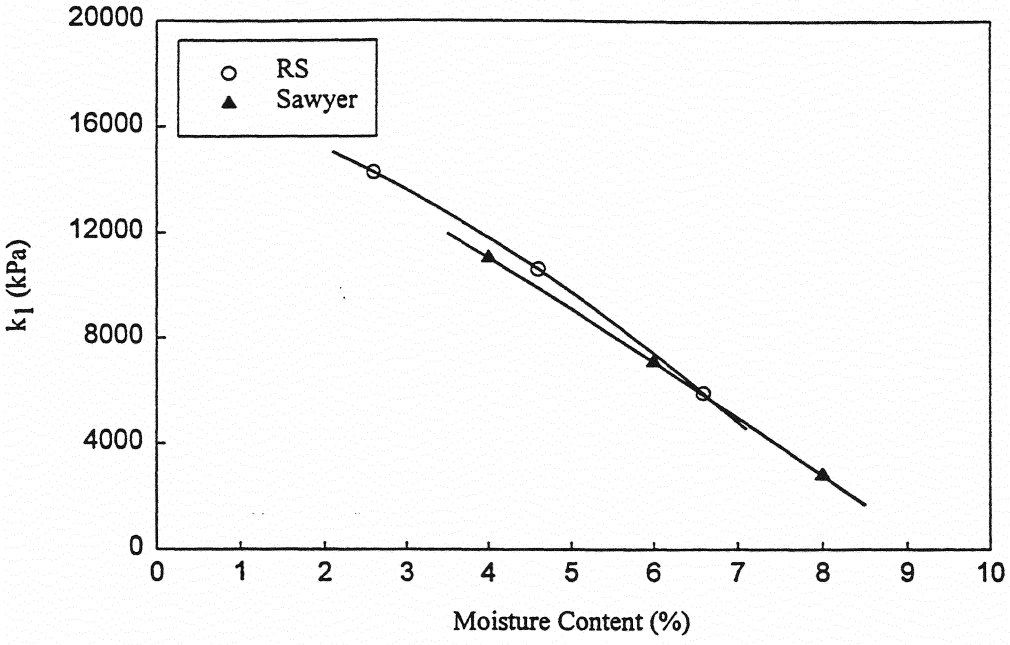

Figure 3-16 Variation of k_1 values with Moisture Content

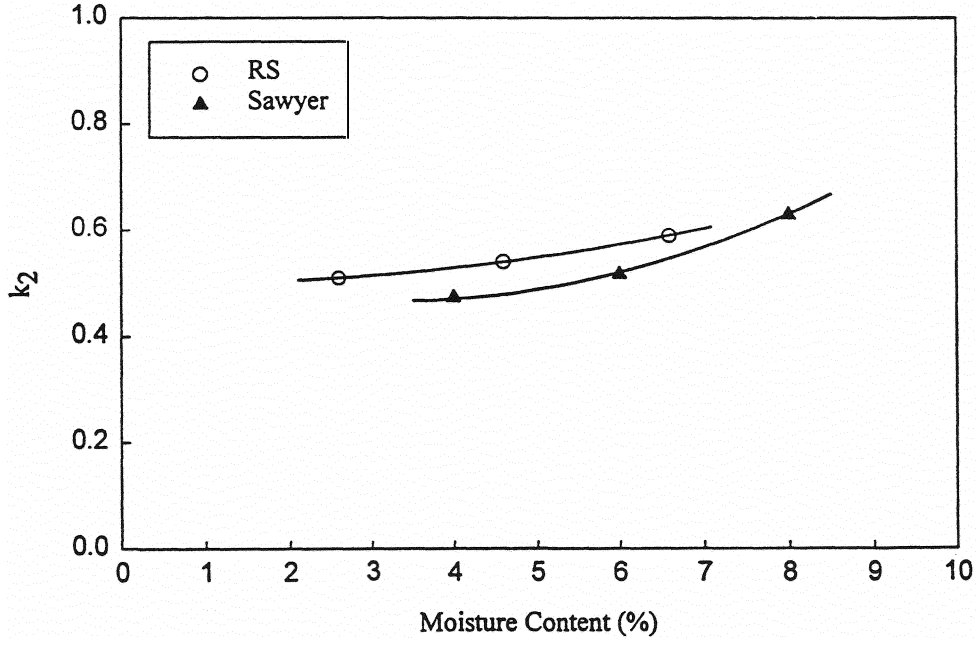

Figure 3-17 Variation of k_2 values with Moisture Content

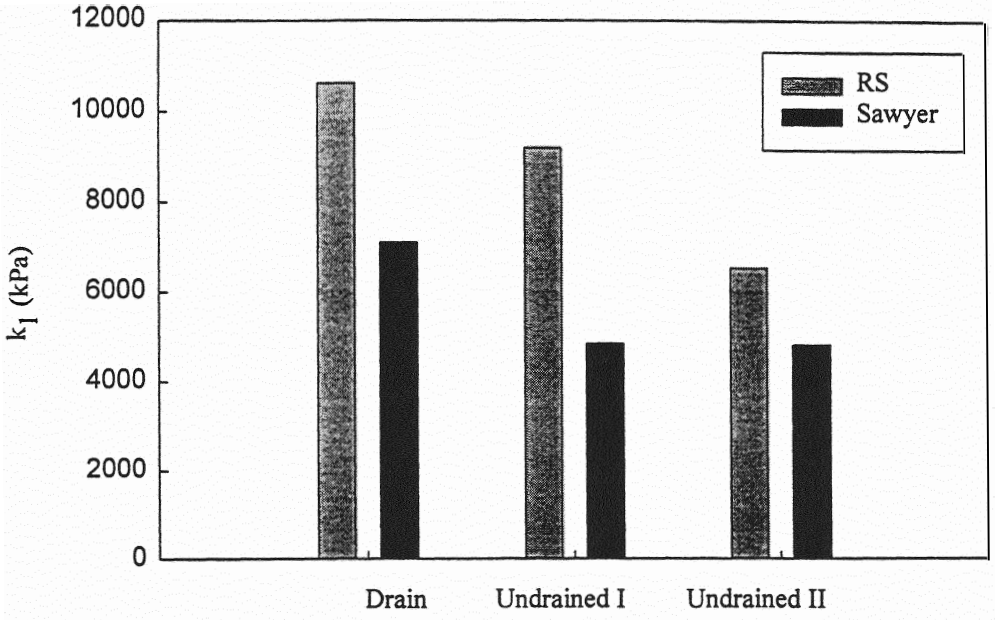

Figure 3-18 Variation of k_1 Values with Drainage Condition

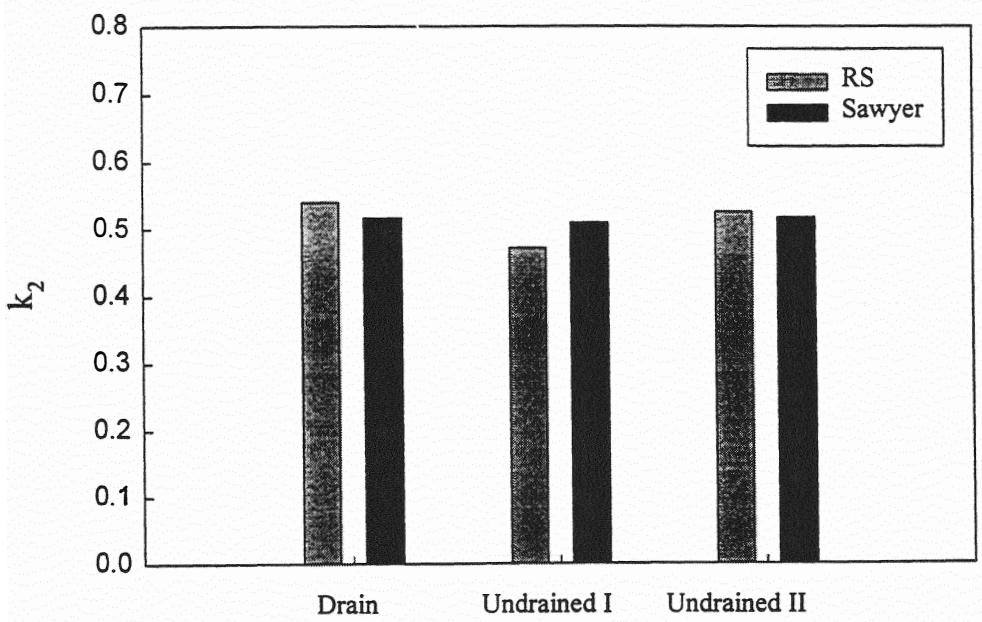

Figure 3-19 Variation of k_2 Values with Drainage Condition

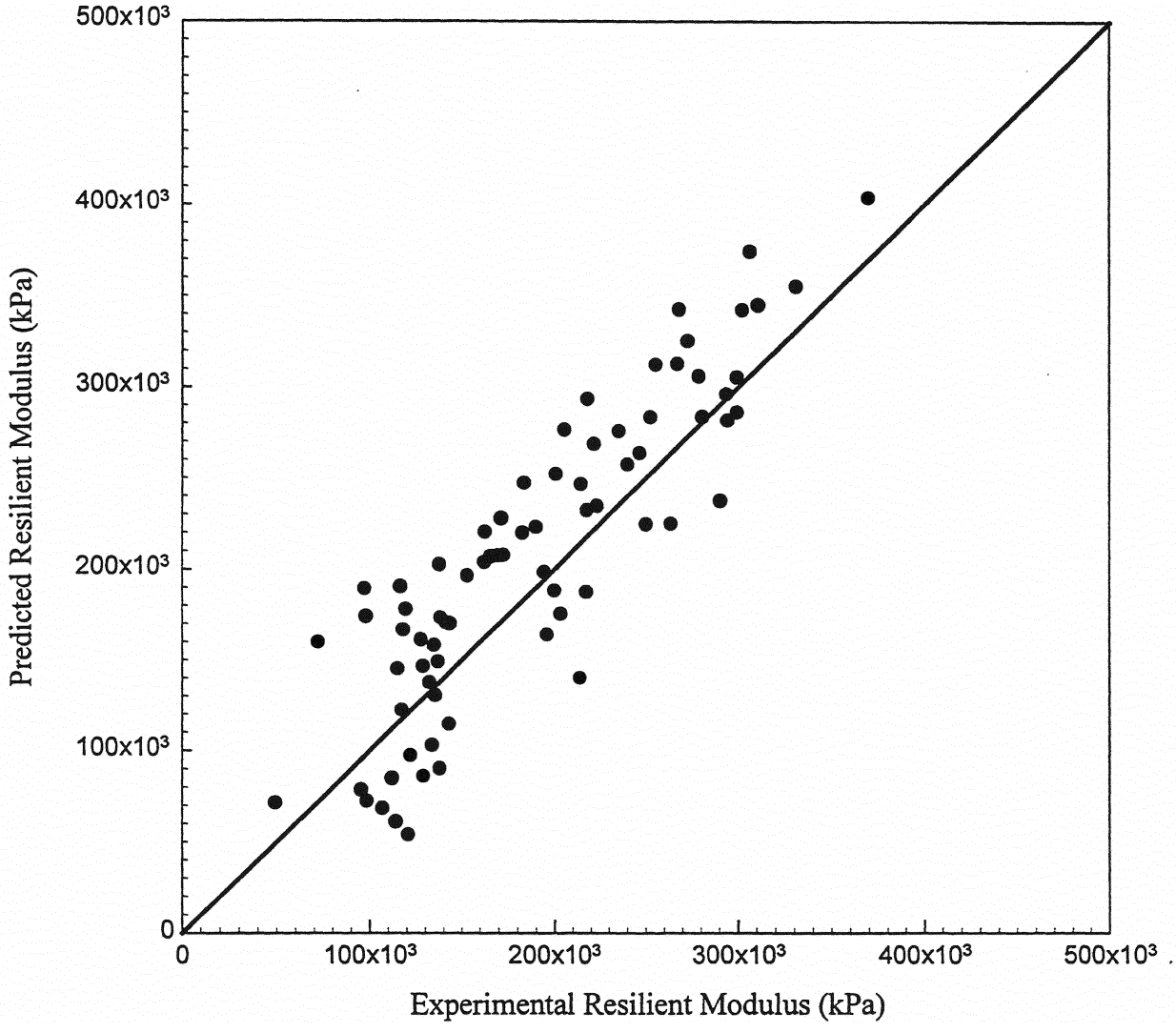

Figure 3-20 Experimental and the Multiple Model Predicted M_R Values of the RS Aggregate

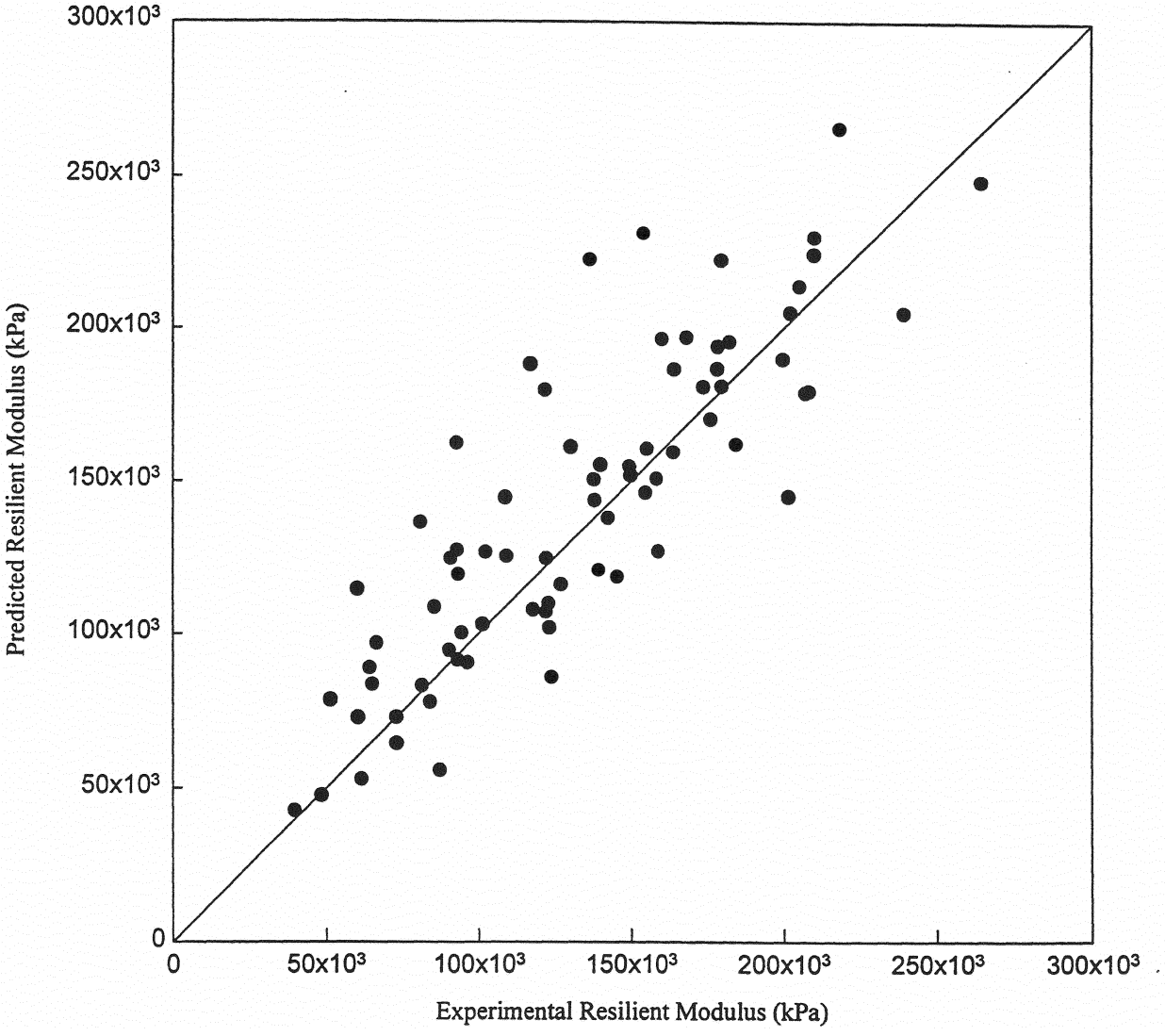

Figure 3-21 Experimental and the Multiple Model Predicted M_R Values of the Sawyer Aggregate

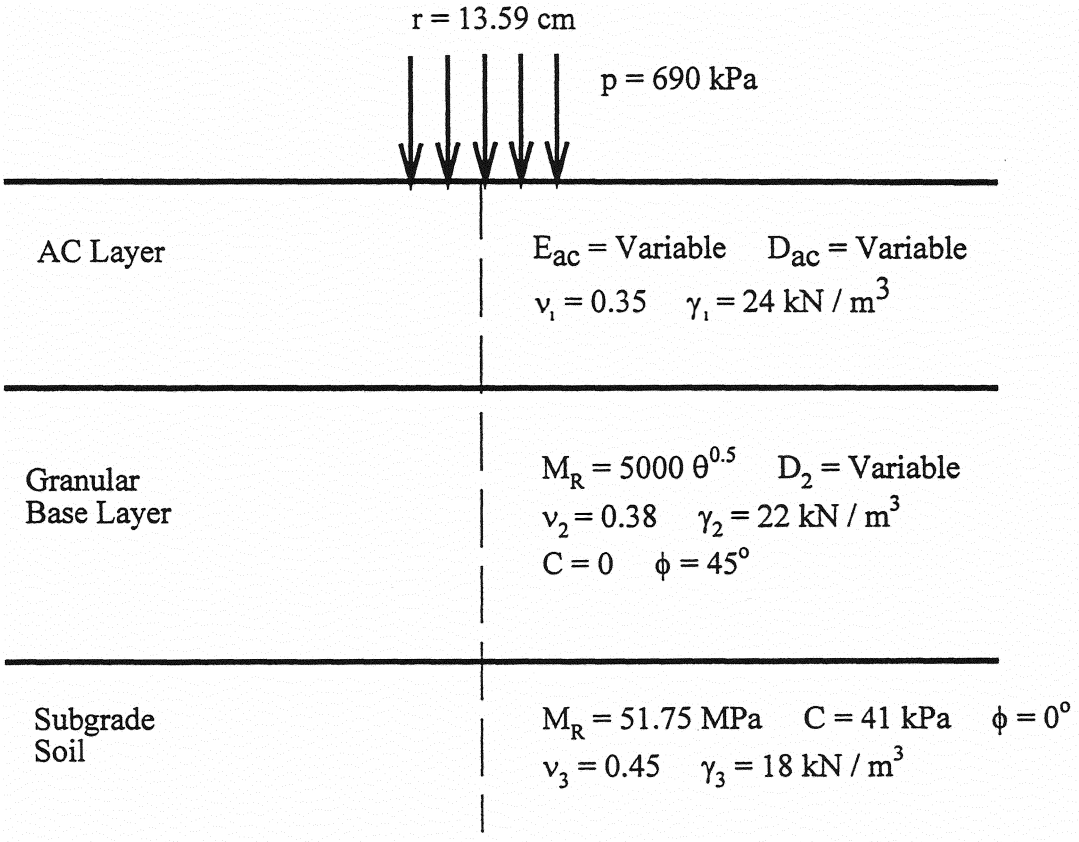

Note: E = Elastic modulus; ν = Poisson's ratio; D = Layer thickness;
C = Cohesion; ϕ = Friction angle; γ = Unit weight

Figure 3-22 Pavement Configuration Used for the ELBK Calculation

CHAPTER 4

RESILIENT MODULUS AND LAYER COEFFICIENTS OF STABILIZED AGGREGATES

4.1 INTRODUCTION

One of the main purposes of this study was to investigate the effect of stabilization of aggregates, as measured by the increase in resilient modulus values (on a marginal aggregate). The Meridian aggregate, which has a relatively high Los Angeles abrasion value (33.3 to 37.7), is selected for this purpose. One of the primary goals of this study is to determine if the properties of the aggregate can be improved by chemical stabilization to a level that they are comparable or better than those of good quality aggregates. Three different stabilizing agents, namely, Class C fly ash (CFA), Fluidized bed ash (FBA), and Cement-kiln-dust (CKD), were used as additives. Based on the laboratory test data, layer coefficients that could be used in the design of flexible pavements were evaluated. The findings are presented in this chapter.

4.2 STATE-OF-THE-ART OF STABILIZATION OF HIGHWAY BASES AND SUBBASES

As the availability of good quality natural roadway construction materials decreases, the need to utilize marginal aggregates through chemical stabilization for base and subbase construction will increase. A pozzolanic material, such as fly ash and cement-kiln-dust, is considered to have no cementitious value of its own but in the presence of moisture and air it forms compounds possessing cementitious properties. Researchers have found that fly ash and CKD can be successfully used as a subbase and base course modifier and as a full or partial replacement of Portland cement or lime

(McManis et al. 1989).

Zenieris and Laguros (1988) conducted a study in which various fine aggregate bases (FABs) and coarse aggregate bases (CABs) were stabilized with 15% to 35% of fly ash with the data showing that the unconfined compressive strength and beam strength of the aggregates improved substantially. Lee and Fishman (1992) conducted a preliminary study on the resilient characteristics of a fly ash and fine grained material (a by-product of aggregate processing) mix. The results indicated improved resilient modulus values and characteristics such that the mix was considered suitable as a roadbed material.

Usmen and Baradan (1991) conducted a study to demonstrate that both Class C and Class F fly ashes can be used with lime or cement to stabilize a pavement material without any adverse effect on the environment.

Ksaibati and Conklin (1994) concluded that cement-treated base sections containing fly ash, where fly ash has partially replaced cement, perform as well as sections without fly ash. Since fly ash is an inexpensive waste material and has been shown to enhance performance of base sections, it should be used more often in highway construction. Cross and Fager (1995), based on a study investigating the use of fly ash in cold recycled bituminous pavements, concluded that fly ash increases the strength of the mix and decreases its potential for wheel path rutting. Yi (1995) stabilized two different types of coarse aggregates with 8.5% of CFA and 8.5% of FBA individually and cured them for 3, 7, and 28 days. M_R values, using the AASHTO T 292-91I method, were found to be as high as 227% for the FBA- stabilized aggregate and 135% for the CFA-stabilized aggregate, of the M_R values of the corresponding raw (unstabilized) aggregates.

Lotfi and Witczak (1985) reported that the resilient modulus of cement-treated

dense-graded aggregate generally increases with increasing cement content. Gray et al. (1994) concluded from the post-construction monitoring of a cement and fly ash stabilized base that if the fly ash is mixed properly with a specified amount of cement and compacted to a specified density, the base is expected to perform well. Also, problems associated with surface heave and pavement cracking can be reduced by using a stabilized base. Gerrity et al. (1994) reported a similar conclusion in the case of a cement-stabilized phosphogypsum base. It was noted that if the appropriate cement content, adequate compaction, and proper drainage are ensured, the cement-stabilized phosphogypsum can be used effectively as a road base for secondary low-volume roads. Hopkins et al. (1994) found that the use of cement-treated subgrades is a valuable technique for stabilizing low bearing soil subgrades and is a good design alternative when compared with other stabilizing methods and design alternatives.

The published literature related to the soil/aggregate stabilization with CKD is relatively new and only a few publications could be traced. Baghdadi and Rahman (1990) investigated the engineering properties of CKD-stabilized dune sand which is used extensively in the construction of roadway in Saudi Arabia. It was found that the compressive strength increases with the amount of CKD and curing time. It was recommended that for a light application, 12-30% CKD is sufficient to upgrade dune sand; however, for an application of heavy loads, the content of CKD can be as high as 50%. Zaman et al. (1992) and Sayah (1993) investigated the variation in engineering properties of an expansive clay soil stabilized with varying amounts of CKD. It was observed that the maximum dry density of the soil decreased slightly with the addition of CKD, while the plasticity index (PI) was reduced and the swelling potential decreased to

an insignificant amount. The unconfined compressive strength of the stabilized soils with various amounts of CKD was about 20-30% higher than that of the raw expansive soil. Azad (1998) reported that the CKD significantly improved the strength of plastic soils, but it was not as effective as cement stabilization. Miller et al. (1997) observed that CKD is a potentially useful additive for reducing wetting-induced collapse settlements and for reducing overall compressibility of compacted shales.

The effectiveness of CKD in stabilizing marginal aggregates primarily depends upon its pozzolanic reactions accomplished with the help of calcium, silica and aluminum ions. The calcium ions are available from CaO, $CaCO_3$, and $Ca(OH)_2$ when they react with moisture. Due to low solubility of $CaCO_3$ (Boynton 1980), CKDs containing $CaCO_3$ will provide less calcium ions and take longer time to stabilize soils than CKDs containing CaO or $Ca(OH)_2$. In addition, as can be seen from Table 2-2, the amount of CaO contained in CKDs is about the same as that in fly ash. However, the latter contains less silica and aluminum than fly ash.

4.3 LABORATORY STUDY OF STABILIZED AND RAW MARGINAL AGGREGATE

A chemical stabilization involves mixing a given stabilizing agent with the aggregate and allowing the mix to cure for a prescribed period of time. Three different mix proportions, with stabilizing agents in the amount of 5%, 10% and 15% of the dry weight of the raw aggregate, were selected in preparing samples. The specimens for resilient modulus testing were prepared with a moisture content close to w_{opt} and dry density not less than 95% maximum dry density, as listed in Table 4-1. Likewise, three different curing periods (namely, 7-day, 28-day and 90-day) were selected to observe the

effect of curing time on the resilient modulus. The same sample preparation procedure (combined vibration/compaction), as described in Section 3.2 of this report for the case of good quality aggregates, was used for the stabilized aggregate, except with the addition of the stabilizing agent. The curing of stabilized samples was accomplished by placing samples, wrapped with a rubber membrane, in a humidity chamber having temperature of 71°F and relative humidity of approximately 95%. At the end of a given curing time, the M_R test was conducted following the same procedure as for the raw aggregate discussed in Section 3.2. At least five replicate M_R tests for each blend were conducted and their mean values, comprehensively given in Table 4-1a, were plotted against bulk stress, as shown in Figures 4-1 through 4-8. In general, some degree of scatter in data points is observed, the level of scatter being more visible at low stress levels. As discussed by Zhu et al. (1998), deviator stress is a more representative variable to correlate with resilient modulus than bulk stress. Also, M_R is a sensitive property because it involves the measurement of extremely small displacements, particularly at low stress levels. A discussion focusing on the stabilization effects on the strength of the raw aggregate is presented in this section. The effect of the amount of stabilizing agent and curing time on the M_R values is investigated in light of practical applications.

4.3.1 Class C Fly-Ash Stabilization

The M_R values of the 7-day cured aggregate stabilized with CFA are presented in Figure 4-1. It is observed that the M_R values are dependent upon the bulk stress. For example, at 345 kPa bulk stress, the M_R values of the Meridian aggregate stabilized with 5%, 10%, and 15% CFA are 217 MPa, 266 MPa, and 209 MPa, respectively, while at 690

kPa bulk stress, the corresponding M_R values are 264 MPa, 321 MPa, and 293 MPa. The M_R values at 690 kPa bulk stress represent 99%, 143%, and 121% increase, respectively, over the M_R values of the raw aggregate.

The M_R values of the 28-day cured aggregate are presented in Figure 4-2. The M_R values at 690 kPa bulk stress are 533 MPa, 593 MPa, and 637 MPa for aggregate stabilized with 5%, 10%, and 15% CFA. These values represent 303%, 349%, and 382% increase, respectively, over the M_R values of the raw Meridian aggregate.

To clearly observe the trend of M_R versus CFA amount and curing time, the M_R values from CFA-stabilization were plotted against the percent of CFA and curing period, as shown in Figures 4-9 and 4-10, and are discussed in following.

Effect of CFA Amount

Figure 4-9 presents a relationship between M_R values and the amount of CFA for four selected bulk stresses, i.e. 84, 414, 516 and 690 kPa, representing a wide range of values, including the smallest bulk stress (84 kPa) prescribed in the testing procedure. It is observed that the M_R values generally increase with increasing amount of CFA, when the CFA amount is within 10%. It is also observed that the increase in M_R values due to addition of CFA varies with the stress level; the increase in M_R value is more evident at a high bulk stress (say 690 kPa) than that at a low bulk stress level (say 84 kPa). When the CFA amount exceeds 10%, six out of eight curves showed tendency of M_R to slightly decrease. The observation that the M_R values decrease with CFA amount may be partly attributed to the resolution error of the data acquisition system. As discussed by Zhu et al. (1998), the relative error of the M_R values resulting from the axial strain reading system

(LVDT resolution) can be 10% to 20%. However, the results depicted in Figure 4-9 show that addition of more than 10% CFA is not beneficial to strength gain of the aggregate because the fine contents increase with the addition of CFA that reduce drainage capability and the generated excess pore water pressure would not easily dissipate. Also, addition of CFA generally results in a lower dry density. A base layer with lower density may lead to various types of distress in pavement including permanent deformation. Several researchers found that rutting of the pavement is directly related to a combination of densification and shearing in pavement layers (Monismith 1992). In view of these results and from a practical consideration, it was decided to use 10% CFA in the remaining experimental program.

Effect of Curing Time

The effect of chemical stabilization on aggregate depends on the pozzolanic reactions of the stabilizing agent with aggregate particles in the presence of moisture. These reactions are time-dependent, so are the resilient moduli of the stabilized aggregate. In civil and construction engineering applications, the 7-day strength is considered as early strength gain, and the 28-day strength is generally considered to be a standard strength, while the 90-day strength may be considered as extra strength development that would be useful for long term utilization.

The increase in M_R values with increasing curing time is a reasonable expectation in CFA-stabilization. Figure 4-10 illustrates a typical relationship between the M_R and the curing period for samples stabilized with 10% CFA. To examine the influence of bulk stress, results for the four selected bulk stresses are presented in this figure. It is observed

that the pattern for the increase in M_R value is similar for all four cases having different stress levels. There is a sharp jump in the M_R values when the curing period changes from 7 days to 28 days after which the increase in M_R is not as significant. For example, at a bulk stress of 516 kPa, the mean M_R value increases from 289 MPa to 495 MPa, an increase of 72%, for the change in the curing period from 7 days to 28 days. When cured for 90 days the M_R becomes 555 MPa, representing an increase of only 12% over the 28-day cured aggregate, which is within the range of error resulting from the resolution accuracy (Zhu et al. 1998). To further evaluate the effect of curing time on M_R, a strength gain rate, δ, is formulated and defined as follows:

$$\delta = \frac{\Delta Mr}{\Delta T} \quad (\text{MPa/Day}) \tag{4-1}$$

where:

ΔM_r = Difference in M_R value between two studied aggregates, MPa;

ΔT = Difference in number of curing days between two aggregates, days.

If the stabilized aggregate is considered with respect to the raw aggregate, the value of ΔT equals the curing time in days. If two stabilized aggregates are studied, the value of ΔT is the difference in curing time in days between the two stabilized aggregates ($\Delta T \neq 0$).

It is understandable that the value of strength gain rate δ represents the increment in strength per day for the stabilized aggregate with respect to its raw counterpart. For simplicity, the δ values are presented only for one bulk stress value, say 690 kPa, for different aggregates. For 7-day cured 10% CFA-stabilized aggregates, the strength gain rate δ_7 is 27 MPa/day with respect to the raw aggregate for the entire curing period. For the 28-day cured aggregate, the δ value with respect to the 7-day cured aggregate

$\left(\delta_{28-7} = \frac{\Delta M_{R(28-7)}}{(28-7)\text{days}}\right)$ is 13 MPa/day for an additional 21 curing days, which is of the same order of δ value as for the 7-day cured aggregate with respect to the raw aggregate. While for the 90-day cured aggregate, the strength gain rate $\delta_{90-28}\left(\frac{\Delta M_{R(90-28)}}{(90-28)\text{days}}\right)$ is only 1.4 MPa/day after the 28 days curing period, which is one order smaller than that of 28-day cured aggregate. It is clearly evident that the strength gain rate is of significance for both 7-day and 28-day cured aggregates, but after 28 days curing, the strength gain rate becomes insignificant.

From the above analyses, one is able to recognize that the resilient modulus of CFA-stabilized aggregates is a time-dependent property. This fact demonstrates that the cementitious action resulting from hydration within the aggregate matrix dominates in improving the quality of stabilized aggregate, because the longer curing time provides more opportunity for the hydration reaction between stabilizing agent and aggregate particles to occur in the presence of moisture. It should, however, be kept in mind that the curing of specimens mentioned here was achieved under room temperature at a high moisture environment (humidity-controlled) in the laboratory. These desirable conditions are difficult to maintain in a construction field. The construction cost will obviously increase with the curing time because of the long waiting period involved. An extended curing period (i.e., greater than 28 days) is neither economical nor feasible in practice. It is evident from the aforementioned discussion that 28-day cured specimens exhibited the most significant increase in M_R values and significant strength gain rate, while the curing period longer than 28 days produced relatively insignificant changes in M_R values.

Therefore, from a practical point of view, the 28-day curing period is considered adequate for CFA-stabilized aggregate base.

4.3.2 Fluidized Bed Ash (FBA) Stabilization

Addition of FBA as a stabilizing agent is expected to strengthen the aggregate in a way similar to that in CFA stabilization. For example, when cured for 7 days, the M_R test on specimens having 5%, 10% and 15% FBA gave a mean value (at bulk stress 690 kPa) of 317 MPa, 495 MPa and 541 MPa, respectively. As in the case of CFA stabilization, the M_R values increased substantially when the FBA amount was increased from 5% to 10%. When the FBA amount was increased beyond 10% to 15%, no significant changes were observed, as demonstrated in Figure 4-11. Since addition of extra FBA will increase the amount of fines in the aggregate, the reasoning of limiting the CFA amount presented above holds true in this case also. Therefore, 10% FBA is considered adequate for the Meridian aggregate from the strength gain point of view.

The FBA stabilization is also enhanced by prolonging the curing time in the same manner as in the case of CFA stabilization. Compared with the raw aggregate, the M_R values of the stabilized aggregate exhibited an increase of more than 300%, 500% and 700% for 7-day, 28-day and 90-day curing periods, respectively. As shown in Figure 4-12, the nature or pattern of relationship between the M_R and the curing periods is very similar to that of the CFA stabilization. The strength gain rate δ for the 10% FBA stabilized aggregate is 51 MPa/day for the 7-day cured aggregate with respect to the raw aggregate, and 26 MPa/day for the 28-day cured aggregate for the additional 21 days. While for the 90-day cured aggregate, the strength gain rate (δ_{90-28}) after 28 days curing

is only 1.03 MPa/day. It is apparent that the 28-day curing period is more effective in terms of strength gain and more feasible in practice than the 90-day curing period.

4.3.3 Cement-Kiln-Dust (CKD) Stabilization

The increase in M_R values due to the addition of CKD is evident from the experimental data. As shown in Figures 4-7 and 4-8, the mean M_R value of raw Meridian 2 aggregate ranges from 49 MPa to 307 MPa depending upon the bulk stress level. When 5% CKD is added to the raw aggregate, the M_R values become 65 MPa to 386 MPa depending upon the bulk stress level. This represents a ten to fifty percent increase. When 15% CKD is added, the corresponding M_R values are in the range of 81 MPa to 499 MPa, representing more than 50 percent increase compared with that of the raw aggregate.

The pattern associated with the variation of M_R with the amount of CKD is slightly different than that of fly ash (CFA and FBA) stabilization. The highest M_R values were obtained when the amount of CKD reached 15%, as shown in Figure 4-13. It is known from the moisture-density test results presented in Table 4-1 that the addition of more CKD produced lower dry densities than those having less CKD. The fact that the M_R values increase continuously with increasing CKD amount indicates that the cementitious action is enhanced by the amount of CKD. Similar to the CFA and FBA stabilization, the stress-dependent nature in M_R of the CKD-stabilized aggregate is also evident. At a low bulk stress (84 kPa) the increase in M_R due to CKD-stabilization is not as significant as in the high stress level. This is because the relative error resulting from the resolution accuracy is more significant at the low stress level than at the high stress

level (Zhu et al. 1998). Considering increase in M_R values and the ODOT gradation requirements, the recommended amount of CKD is 15% for the aggregate under study. Therefore, the rest of investigation on CKD-stabilization is based on the stabilized aggregate having 15% CKD.

The effect of curing time on M_R for the CKD-stabilized aggregate is somewhat different than that for the CFA- and FBA-stabilization. As shown in Figure 4-14, the 28-day resilient modulus values were much higher than that of the 7-day values, while the 90-day curing did not produce any significant difference in M_R values with respect to the 28-day curing. It is noted from Figure 4-14 that some M_R values for 90-day cured specimen are lower than that of 28-day cured specimens. This variation does not necessarily mean that the 90-day curing produced worse situation, rather it illustrates the fact that the changes in M_R value between 28-day and 90-day curing periods are insignificant. Various sources of errors such as rod friction, sensitivity of transducers (LVDTs), resolution of the data acquisition system and rounding of data may give rise to such level of variations in M_R values.

In terms of strength gain rate δ, the 7-day cured 15% CKD-stabilized aggregate exhibited an increase of 27 MPa per day in the M_R value with respect to the raw aggregate, at a bulk stress of 690 kPa. For 28-day curing time, the strength gain rate was 8.7 MPa/day beyond the 7-day initial curing. For 90-day curing, the strength gain rate is of insignificance for a period of curing beyond 28 days.

Since a sharp increase in M_R value was observed in the 28-day cured aggregate, compared with the 7-day cured aggregate, it is postulated that an effective curing time for

CKD-stabilization can be set at 28 days, which is the same period for CFA- and FBA-stabilization.

4.4 EFFECT OF STABILIZING AGENT TYPE

To evaluate the effect of stabilizing agent, an effort was made to compare the increase in resilient modulus values with respect to the raw aggregate, for each stabilizing agent. As discussed earlier, the patterns of variation in M_R values for CFA- and FBA-stabilized aggregates are quite similar, but are different for CKD-stabilization in terms of optimum amount and curing time. Some of the possible reasons for these differences are discussed in this section.

Difference in Increased M_R Values

A mathematical number is often the most primitive and simplest way to convey a profound scientific principle. The effectiveness of various stabilizing agents (FBA, CKD and CFA) is found by comparing the corresponding increase in M_R values for different agents. Figure 4-15 depicts the change in M_R (ΔM_R) as a function of bulk stress for all the three stabilizing agents used in this study. It is observed from Figure 4-15 that the FBA stabilization produces the highest strength gain with ΔM_R values ranging from 132 MPa to 972 MPa. The effect of CKD stabilization is the least with ΔM_R values ranging from 55 MPa to 376 MPa. The ΔM_R values for the CFA stabilization fall between those of the FBA stabilization and CKD stabilization, having values in the range of 77 MPa to 505 MPa. In all three cases, the effect of stabilization is encouraging since the ΔM_R values are

significant indicating that a marginal aggregate base can be made strong enough to behave as a good aggregate base by stabilization.

The differences in chemical composition between fly ash and CKD materials are believed to be responsible for the differences in strength gain. As shown in Table 2-2, FBA and CFA have a larger amount of oxide composition (e.g. SiO_2+Al_2O_3+Fe_2O_3) and low Loss on ignition (LOI) than CKD. In viewing the difference between CFA and FBA, one can find that the CFA has more oxide compounds than FBA, but the strength gain from CFA stabilization is smaller than FBA stabilization. The possible contributing factor for this experimental observation is that the free lime content in FBA is 18%. Since it is not known how much of the lime in CFA is available for hydration-reaction purposes, it is hypothesized that it is less than 18% and therefore CFA behaves less effectively in stabilization (Mitchell 1981). It could be also expected that the optimum amount of agent and the rate of strength gain are actually controlled by the amount of active oxide compounds contained in a stabilizing agent.

Optimum Amount of Stabilizing Agent

An optimum amount of stabilizing agent is defined as the smallest amount of stabilizing agent that would give rise to the higher increase in resilient modulus. As discussed earlier, the optimum amount of CKD (15%) is higher than CFA and FBA amount (10%) in terms of increase in M_R values. This is because a larger amount of stabilizing agent is needed for agents having lesser amount of oxide compounds than those containing more oxides.

Curing Time

Chemical reaction is a time-dependent process. The time required for accomplishing chemical reactions is expected to vary with the amount of active components. So, it is logical that the CFA having an oxide composition of 62.08% would need longer curing period than the FBA having 35.26% oxide, and the CKD would need the shortest curing time among the three stabilizing agents because it has the smallest amount of oxide (19.23%). This inference was supported by the relationship between resilient modulus and curing period for different stabilizing agents, as shown in Figures 4-10, 4-12 and 4-14. As can be seen from Figure 4-14, the CKD stabilization is actually attained within 28 days beyond which any significant strength gain is not evident. The CFA- and FBA-stabilization exhibited a continuous strength gain even when the aggregate is cured for 90 days. This inference was also confirmed by microanalysis of the stabilized aggregate with the help of SEM and XRD results, which is presented in Chapter 5.

4.5 EFFECT OF STABILIZATION ON UNCONFINED COMPRESSIVE STRENGTH AND ELASTIC MODULUS

Unconfined compressive tests were conducted on the specimens immediately following the M_R tests. The test results were used to compute the unconfined compressive strength (U_C) and elastic modulus (EM) values. The initial slope of the stress-strain curve from the test was used to determine the EM value, which imparts the EM value very sensitive because of the way it is determined. The mean U_C and EM values and their standard deviations of the various stabilized aggregates are presented in Table 4-3.

CFA Stabilization

The U_C values of the 7-day cured Meridian 1 aggregate are 631 kPa, 1221 kPa, and 1420 kPa for the samples stabilized with 5%, 10%, and 15% CFA, respectively. These values represent a 254%, 530%, and 698% increase over the mean U_C value of the raw aggregate (178 kPa), respectively. Similarly, the U_C values of the 28-day cured aggregate specimens are six to ten times greater and the U_C values of the 90-day cured aggregate specimens are seven to eleven times greater than those of the raw aggregate specimens. The EM values of the 28-day cured aggregate samples stabilized with 5%, 10%, and 15% CFA are 208 MPa, 290 MPa, and 325 MPa, respectively. These values represent a 448%, 663%, and 754% increase over the EM values of the raw aggregate (38 MPa). The nature of increase in U_C and EM values due to the CFA stabilization are found to be consistent with the changes in resilient modulus, except that a continuous substantial increase in static strength was observed when the amount of CFA and curing time continuously increased.

FBA Stabilization

The U_C values of the FBA stabilized aggregate also show a significant improvement over the U_C value of the raw aggregate. For example, the U_C values of the 28-day cured aggregate specimens are 1635 kPa, 3243 kPa, and 3881 kPa, respectively, for the aggregate stabilized with 5%, 10%, and 15% FBA. These values are 8, 17, and 20 times higher, respectively, than that of the raw aggregate. Similarly, the U_C values of the 90-day cured aggregate are 11 to 26 times greater than that of the raw aggregate. The mean EM values of the 28-day cured aggregate stabilized with 5%, 10%, and 15% FBA

represent a 850%, 1253%, and 1469% increase, respectively, over the EM values of the raw aggregate. A continuous increase in U_C and EM values with the amount of stabilizing agent and curing time was apparent in FBA and it was difficult to identify the optimum amount and most effective curing time based on the increase in static strength (U_C) and elastic modulus (EM).

CKD Stabilization

It is observed from Table 4-3 that the U_C value increases with increasing amount of CKD. For 7-day cured aggregate samples stabilized with 5% CKD, the U_C increased from 200 kPa for raw aggregate to 960 kPa, about a 380% increase. When 15% CKD is added, the corresponding U_C becomes 1566 kPa, which represents a 632% increase with respect to the raw aggregate. A trend of U_C increasing with curing time is also evident from the table. When stabilized with 15% CKD, the mean values of U_C are 1566 kPa, 2163 kPa and 2810 kPa for 7-days, 28-days and 90-days cured specimens, respectively.

The mean EM values of the 7-day cured aggregate stabilized with 5%, 10% and 15% CKD are 115 MPa, 164 MPa and 211 MPa, respectively. These values represent 260%, 413% and 559% increase over the EM values of the raw aggregate (32 MPa). The curing periods also have significant effect on the EM values. As seen from Table 4-3, the mean EM values for 7-day, 28-day and 90-day cured specimens stabilized with 15% CKD are 211 MPa, 344 MPa and 439 MPa, respectively. This represents a 63 percent increase for the 28-day cured aggregate over the 7-day cured aggregate. Similarly, a 27.6 percent increase is achieved for the 90-day cured specimens compared with the 28-day cured specimens.

The U_C and EM values of various stabilized aggregates as discussed above indicate that stabilization leads to a significant increase in both U_C and EM values. It can be concluded that the higher the ash content, and the higher the increase in the U_C and EM values and also, the longer the duration of the curing period, the higher the increase in the U_C and EM values of the stabilized aggregates. The largest increase in U_C and EM values occurs between the curing periods of 7-day and 28-day, which exhibits similar nature as observed for the case of M_R. The FBA-stabilized aggregate shows a higher degree of increase over the raw value than the CFA-stabilized aggregate. For example, for the 28-day cured aggregate, the U_C and EM values for samples stabilized with 15% FBA are 3881 kPa and 597 MPa, respectively, while, the corresponding U_C and EM values of the CFA-stabilized aggregate are 1985 kPa and 325 MPa, respectively. The CFA-stabilized aggregate shows almost equivalent increase in terms of the increased percentage over the raw aggregate, as compared with the CKD-stabilized aggregate. For example, for the 28-day cured aggregate, the U_C and EM values of 15% CKD stabilized aggregate are 2163 kPa and 344 MPa, representing a 901% and 975% increase over the raw aggregate, respectively. The corresponding U_C and EM values of the CFA stabilized aggregate are 1985 kPa and 325 MPa, representing a 1021% and 755% increase over the raw aggregate, respectively.

4.6 VARIABILITY OF STRENGTH PROPERTIES

Variability of test results (strength) associated with the replicate samples for a given aggregate type has been presented in Section 3.4.5 of Chapter 3. The general observation is that the standard deviation (SD) for M_R, U_C and EM increases with the increase in

values of these parameters. However, the relative error in terms of the ratio of the standard deviation and the average mean M_R value (SD/Mean M_R value) is found to be within 20 percent in most cases. This level of variation is generally acceptable in geotechnical testing.

Some of the possible contributing factors for such variability are: (a) heterogeneous nature of aggregates, (b) non-uniformity of mixes, (c) slight deviations in sample preparation and testing techniques, (d) small variations in curing temperature and time, (e) density variation, and (f) lack of sufficient accuracy in measurement of very small displacements (Zhu et al. 1998).

It is noted that the potential factors listed above are applicable for specimens prepared, cured, and tested in the laboratory. It is expected that larger variations may be encountered in the field as a result of the difficulties associated with quality control and lack of strict uniform compaction during the construction process, among other factors. This variability should be recognized and taken into consideration in the evaluation of the properties of stabilized base aggregates.

4.7 EVALUATION OF LAYER COEFFICIENTS

Layer coefficients represent a measure of the relative ability of a unit thickness of a given material to function as a structural component in the pavement (AASHTO, 1993). Discussion of base layer coefficient a_2 of the raw aggregates together with the methodology used for computing layer coefficient values has been presented in Chapter 3 (Section 3.6). The base layer coefficient a_2 of a stabilized aggregate base is computed using equation (3-5) in a same manner as described in Section 3.6 of Chapter 3, except

that the equivalent modulus values are calculated using the k_1 and k_2 values shown in Table 4-2. The aggregate types considered in computing a_2 values include 28-day and 90-day cured aggregates stabilized with 5%, 10% and 15% CFA and FBA, as well as CKD stabilized aggregates and the raw aggregates (Meridian 1 and Meridian 2). The evaluation of a_2 was pursued here using 36 selected combinations of parameters as listed in Table 3-9. Following this approach, a total of 684 a_2 values were computed for different situations. These include 36 a_2 values for Meridian 1 and Meridian 2 raw aggregates, 36 a_2 values for CFA-, FBA- and CKD-stabilization with different amount and curing time, as listed in Tables 4-4 through 4-10. For comparison, a_2 values of good quality aggregate (Richard Spur) are also listed in Table 4-4. The range of the a_2 values are found to be -0.0852 to 0.0193 for raw Meridian 1 aggregate, 0.0511 to 0.2083 for CFA-stabilized aggregate, 0.0912 to 0.2481 for FBA-stabilized aggregate, -0.0412 to 0.0748 for raw Meridian 2 aggregate and 0.0086 to 0.1695 for CKD-stabilized aggregate, respectively.

The layer coefficients that have a negative value do not have any practical significance and therefore, should be considered as values approaching zero. Hence, layer coefficients having values approaching zero or below zero essentially mean that the material is of insignificant structural support value compared to the other materials used in the pavement system. In other words, use of that particular material would not contribute to the structural strength of the pavement system.

A multiple regression analysis was performed to correlate a_2 values with the properties of AC layer and stabilization effect as shown below. The regression equations for different stabilization cases are given as follows:

i. CFA stabilization:

$$a_2 = 0.199 - 0.00602335\ E_{ac}\ (GPa) - 1.67885 * 10^{-6}\ D_2\ (mm) - 0.00130375\ CFA\ (\%) - 0.000421345\ D_{ac}\ (mm) + 0.000606347\ Day\ (curing\ time)$$

$$R^2 = 0.85514 \qquad (4 - 2)$$

ii. FBA stabilization:

$$a_2 = 0.2604 - 0.00820612\ E_{ac}\ (GPa) - 2.30263 * 10^{-6}\ D_2\ (mm) - 3.38889 * 10^{-5}\ FBA\ (\%) - 0.000573639\ D_{ac}\ (mm) + 0.000338814\ Day\ (curing\ time)$$

$$R^2 = 0.92473 \qquad (4 - 3)$$

iii. CKD stabilization:

$$a_2 = 0.1299 - 0.00684762\ E_{ac}\ (GPa) - 1.95114 * 10^{-6}\ D_2\ (mm) + 0.00274754\ CKD\ (\%) - 0.000478938\ D_{ac}\ (mm) + 0.00040009\ Day\ (curing\ time)$$

$$R^2 = 0.9320 \qquad (4 - 4)$$

where: E_{ac} = resilient modulus of AC layer, D_2 = thickness of base layer, D_{ac} = thickness of AC layer, Day = curing periods in day.

4.7.1 Effect of Amount of Stabilizing Agent

CFA Stabilization

The a_2 values for CFA-stabilized aggregate are generally much higher than those of the raw aggregate. As shown in Tables 4-5 and 4-6, the layer coefficients for the raw

Meridian 1 aggregate vary from 0 to 0.0018, indicating the layer does not contribute structurally to the function of the pavement in a significant manner. The 28-day cured aggregate stabilized with only 5% CFA gives rise to the a_2 values in the range of 0.1678 to 0.1723, which makes an otherwise deficient aggregate base strong enough to adequately function as a structural component in the pavement system. However, the change in the amount of CFA seems to have relatively little effect on the a_2 values. This is because the a_2 value is computed using an equivalent resilient modulus which is dependent on the regression constants k_1 and k_2 values in the $M_R \sim \theta$ model as given by equation (3-2). Typical base and subbase course values (layer coefficients) are 0.10 to 0.20 (AASHTO Test 1962; Wright 1996). As discussed in Volume IV of the report (Zhu et al. 1998), the bulk stress model generally gives a low correlation coefficient (R^2) value, which means that the k_1 and k_2 values are subjected to some level of uncertainties. This limitation should be kept in mind when one uses the parameter a_2 in pavement design.

FBA Stabilization

The variation in a_2 values in this case is similar to that in the case of CFA stabilization. The addition of FBA increases a_2 values significantly with respect to the raw aggregate. For example, when the thickness of base layer is 76 mm, the a_2 values for 28-day cured aggregates are 0.2071, 0.2039 and 0.1976 for 5%, 10% and 15% FBA stabilization (Tables 4-7 and 4-8). It is noted that there is slight decrease in a_2 value when FBA amount increases. One of the possible reasons for this is that the low correlation coefficient existed in the $M_R \sim \theta$ model upon which the a_2 values are determined. In any case, the a_2 values of the FBA-stabilized aggregate base are much higher than the raw

aggregate base and this makes the FBA-stabilized aggregate base comparable with the good quality aggregate base, as discussed in Chapter 3.

CKD Stabilization

CKD stabilization was applied to raw Meridian 2 aggregate. As can be seen from Tables 4-9 and 4-10, the a_2 values increase with increasing amount of CKD. For example, at a base layer of 76 mm, the a_2 value for 7-day cured specimens is 0.0936, 0.0952 and 0.1118 for the CKD amount being 5%, 10% and 15%, respectively. Compared with the results presented in Chapter 3, the 28-day curing with 15% CKD-stabilized Meridian 2 aggregate base can achieve the same performance of a base layer as a good aggregate base layer (e.g., RS aggregate base).

4.7.2 Effect Of Curing Time

It is evident that the curing time has consistently positive effect on the layer coefficient a_2 values. As can be seen from Table 4-4, all the a_2 values increase with increasing curing periods. For example, considering a base layer having thickness of 76 mm and amount of agent being 15%, the a_2 values of 28-day and 90-day cured are 0.1453 and 0.1933 for CFA stabilization, 0.1976 and 0.2265 for FBA stabilization, 0.1334 and 0.1498 for CKD stabilization. The 90-day curing increased a_2 value up to 30% over 28-day curing. However, from a practical point of view, the curing time as long as 90 days is difficult to attain because of expensive and time-consuming nature. Since the 28-day cured stabilized aggregate base can achieve the same level of performance of a good quality aggregate base, the 28-day curing period is recommended for use in the field.

4.7.3 Effect Of Stabilizing Agent Type

To facilitate the evaluation of stabilizing agent type, the layer coefficient (a_2) values are plotted against the base thickness for different agents as shown in Figure 4-16. It is important to note that the FBA stabilization produces the highest a_2 values, followed by CFA and CKD stabilized aggregates in that order. The a_2 values obtained from the 28-day cured FBA stabilization are even higher than those produced by the 90-day cured CFA and CKD stabilization. For example, at a base thickness of 76 mm, the 28-day cured FBA stabilization has a layer coefficient (a_2) value of 0.1976, while the a_2 values for 90-day cured base are 0.1973 and 0.1498, respectively, for CFA and CKD stabilization. Therefore, on the basis of strength gain alone, the preference may be given to using FBA, followed by CFA and CKD in that order. In any case, all three stabilizing agents used in this study would significantly improve the properties of a base constructed with a marginal aggregate. It is also found from the figure that the a_2 values decrease with increasing thickness of base layer when the thickness of base layer exceeds 228 mm. This is understandable because the a_2 value reflects a relative layer support ability of unit layer base. Although overall supporting capability of a base layer should increase with increasing thickness of the base layer, the a_2 value may decrease as a result of increase of base layer thickness. This also means that the efficiency of a base layer decreases if its thickness exceeds certain value (say 220 mm in this study).

4.8 DESIGN OF AN AASHTO FLEXIBLE PAVEMENT

Traffic loading is one of the most important considerations in pavement design. Due to a great variety of axle loads and traffic volumes and their intractable effects on

pavement performance, most of the design methods in use today are based on the fixed vehicle concept, i.e. the thickness of pavement is assumed to be governed by the number of repetitions of a standard vehicle or axle load during the design periods, called equivalent single-axle load (ESAL).

As an example, this section presents a design of a flexible pavement according to the AASHTO design guide (AASHTO 1993) to examine the effect of CFA, FBA and CKD-stabilization on the ESAL and structure number (SN). The methods used for computing the ESAL and SN values are same as that described in Chapter 3 (Section 3.7). The detailed procedure for the calculation of the ESAL and SN is described in the report volume II (Tian et al. 1998). In this study, the calculation was conducted based on Case 1, Case 4, Case 7, and Case 10 (Table 3-9) for the raw and stabilized Meridian aggregates, and the results are presented in Table 4-11.

As can be seen from Table 4-11, the raw aggregates have the lowest ESAL values with a maximum 2500 for Meridian 1 raw aggregate, and 25,400 for Meridian 2 raw aggregate. The stabilization with various agents is seen to increase the ESAL values significantly. For 28-day cured aggregate stabilized with 10% CFA, the ESAL value reaches 1,114,900, representing a 400 fold increase over the raw aggregate. For 28-day cured aggregate stabilized with 10% FBA, the ESAL value reaches 2,607,500, representing a 1000 fold increase over the raw aggregate. When the aggregate was stabilized with 15% CKD and cured for 28 days, the ESAL value reached is 1,552,400, representing a 60 fold increase over the raw aggregate.

The Asphalt Institute recommends that, for urban minor arterial and light industrial streets, the design ESAL be 1,000,000 (Huang 1993). Therefore, the raw Meridian

aggregate used in this study is considered inadequate for use as a base layer, while with the addition of 5% to 15% stabilizing agents (CFA, FBA or CKD), the aggregate becomes qualified for use as a roadway base.

Table 4-1 The Optimum Moisture Content (w_{opt})-Maximum Dry Density (γ_{dmax}) of Stabilized Meridian Aggregate and Curing Period for M_R Test

Sample Type	Optimum Moisture Content (%)	Maximum Dry Density (kN/m^3)	Curing Days for M_R Test (kN/m^3)
Meridian 1	7.3	20.9	-
Meridian 2	7.5	20.9	-
Meridian 1 + 5% CFA	7.5	20.8	7, 28, 90
Meridian 1 + 10% CFA	7.7	20.8	7, 28, 90
Meridian 1 + 15% CFA	8.0	20.5	7, 28, 90
Meridian 1 + 5% FBA	8.5	20.5	7, 28, 90
Meridian 1 + 10% FBA	9.0	20.2	7, 28, 90
Meridian 1 + 15% FBA	9.3	20.0	7, 28, 90
Meridian 2 + 5% CKD	7.9	20.8	7
Meridian 2 + 10% CKD	8.3	20.6	7
Meridian 2 + 15% CKD	8.8	20.3	7, 28, 90

Table 4-1a Range of RM Values (MPa) of the Stabilized Meridian Aggregate

Curing Time, days	Stabilizing Agent								
	CFA, %			FBA, %			CKD, %		
	5	10	15	5	10	15	5	10	15
7	88.71	101.41	93.61	66.50	88.03	100.49	65.35	72.27	80.56
	263.84	321.22	292.84	317.54	494.66	541.03	385.81	411.66	499.51
28	106.32	128.81	100.90	160.45	168.74	156.29	--	--	109.35
	532.28	592.89	637.59	928.73	1041.50	1104.76	--	--	683.15
90	134.21	160.68	175.47	175.33	194.55	207.47	--	--	126.66
	587.42	679.90	701.06	970.83	1105.24	1145.64	--	--	620.55

Table 4-2 Material Parameters k_1 and k_2 of the Raw and Stabilized Aggregates

Stabilizing Agent Type	Amount of Agent (%)	Curing Period (days)	k_1 (kPa)	k_2	R^2
Raw Meridian 1			3476.2	0.5606	0.6797
Class C Fly Ash (CFA)	5	7	10076.3	0.5044	0.8472
	10	7	20365.7	0.4193	0.7749
	15	7	15761.6	0.4191	0.6761
	5	28	33853.2	0.4220	0.5297
	10	28	17096.2	0.5258	0.7679
	15	28	9756.6	0.6238	0.8314
	5	90	37127.9	0.4192	0.6131
	10	90	38823.9	0.4248	0.6777
	15	90	41495.4	0.4234	0.7199
Fluidized Bed Ash (FBA)	5	7	10849.2	0.5097	0.7869
	10	7	5753.1	0.6775	0.8333
	15	7	4177.3	0.7691	0.8919
	5	28	16132.4	0.6373	0.8126
	10	28	13418.4	0.6681	0.8339
	15	28	10565.07	0.7044	0.8511
	5	90	19045.8	0.6151	0.8165
	10	90	19177.8	0.6280	0.8512
	15	90	21842.4	0.6127	0.8550
Raw Meridian 2			4166	0.6230	0.6722
Cement Kiln Dust (CKD)	5	7	9182	0.5278	0.5600
	10	7	12468	0.4711	0.4347
	15	7	15211	0.4732	0.4234
	15	28	12354	0.5546	0.5250
	15	90	13922	0.5610	0.7377

Table 4-3 Unconfined Compressive Strength and the Elastic Modulus of the Stabilized Aggregates

			UC Strength		Elastic Modulus	
Stabilizing Agent Type	Amount of Agent (%)	Curing Period (days)	Mean UC (kPa)	Standard Deviation (kPa)	Mean EM (Mpa)	Standard Deviation (MPa)
Raw Meridian 1			177.91	14.45	38.03	4.71
Class C Fly Ash (CFA)	5	7	630.78	53.85	119.1	28.17
	10	7	1121.25	58.34	163.17	22.43
	15	7	1420.25	73.73	213.8	29.75
	5	28	1352.4	78.79	208.48	42.39
	10	28	1817.0	69.09	290.29	22.52
	15	28	1984.9	90.67	325.08	20.7
	5	90	1590.45	82.89	229.41	33.87
	10	90	1994.1	88.79	313.5	41.7
	15	90	2213.75	77.99	354.86	32.6
Fluidized Bed Ash (FBA)	5	7	941.85	72.86	205.31	27.64
	10	7	1449	85.18	298.26	21.51
	15	7	1658.3	81.02	315.51	29
	5	28	1635.3	91.85	361.64	35.26
	10	28	3243	114.13	514.57	41.74
	15	28	3881.25	101.48	596.74	39.39
	5	90	2266.65	112.09	488.6	37.34
	10	90	4211.3	99.67	753.73	21.7
	15	90	4910.5	101.66	846.13	45.19
Raw Meridian 2			216	24.01	31.50	7.18
Cement Kiln Dust (CKD)	5	7	959	322.27	115.00	16.85
	10	7	1143	130.79	163.80	29.55
	15	7	1566	260.53	211.20	16.03
	15	28	2163	226.93	344.20	46.08
	15	90	2810	297.91	439.20	59.57

Table 4-4 Layer Coefficients (a_2) for Raw Meridian 1 Aggregates and Richard Spur Aggregates

E_{ac}	Base Thickness	Meridian 1			Richard Spur		
	D_2	D_{ac} (mm)			D_{ac} (mm)		
		76	152	228	76	152	228
(kPa)	(mm)	a_2	a_2	a_2	a_2	a_2	a_2
1725000	76	0.0141	-0.0335	-0.0623	0.1255	0.0823	0.0561
	152	0.0169	-0.0335	-0.0642	0.1280	0.0823	0.0544
	228	0.0193	-0.0315	-0.0691	0.1302	0.0840	0.0500
	304	0.0111	-0.0365	-0.0674	0.1227	0.0795	0.0515
3450000	76	-0.0005	-0.0527	-0.0797	0.1122	0.0648	0.0403
	152	-0.0004	-0.0521	-0.0791	0.1123	0.0653	0.0409
	228	0.0018	-0.0548	-0.0766	0.1143	0.0629	0.0432
	304	-0.0042	-0.0594	-0.0742	0.1089	0.0588	0.0453
5175000	76	-0.0141	-0.0647	-0.0852	0.0999	0.0539	0.0353
	152	-0.0107	-0.0663	-0.0822	0.1029	0.0525	0.0381
	228	-0.0076	-0.0668	-0.0796	0.1058	0.0520	0.0404
	304	-0.0121	-0.0655	-0.0773	0.1017	0.0532	0.0425

Table 4-5 Layer Coefficients (a_2) for 28-day Cured CFA Stabilized Meridian Aggregate

E_{ac}	Base Thickness	5% CFA			10% CFA			15% CFA		
	D_2	D_{ac} (mm)			D_{ac} (mm)			D_{ac} (mm)		
		76	152	228	76	152	228	76	152	228
(kPa)	(mm)	a_2	a_2	a_2	a_2	a_2	a_2	a_2	a_2	a_2
1725000	76	0.1816	0.1458	0.1240	0.1666	0.1220	0.0949	0.1616	0.1087	0.0765
	152	0.1837	0.1458	0.1226	0.1692	0.1220	0.0932	0.1647	0.1087	0.0745
	228	0.1855	0.1472	0.1189	0.1715	0.1238	0.0886	0.1674	0.1108	0.0690
	304	0.1793	0.1435	0.1202	0.1638	0.1191	0.0902	0.1582	0.1053	0.0709
3450000	76	0.1706	0.1313	0.1110	0.1529	0.1039	0.0787	0.1453	0.0872	0.0572
	152	0.1706	0.1317	0.1114	0.1530	0.1045	0.0792	0.1454	0.0879	0.0579
	228	0.1723	0.1297	0.1133	0.1550	0.1020	0.0816	0.1479	0.0849	0.0607
	304	0.1678	0.1263	0.1151	0.1495	0.0977	0.0838	0.1412	0.0798	0.0633
5175000	76	0.1604	0.1222	0.1068	0.1402	0.0927	0.0735	0.1302	0.0738	0.0511
	152	0.1629	0.1210	0.1091	0.1433	0.0912	0.0763	0.1340	0.0721	0.0544
	228	0.1652	0.1207	0.1110	0.1463	0.0907	0.0787	0.1375	0.0716	0.0573
	304	0.1619	0.1216	0.1128	0.1421	0.0920	0.0809	0.1325	0.0730	0.0599

Table 4-6 Layer Coefficients (a_2) for 90-day Cured CFA Stabilized Meridian Aggregate

E_{ac}	Base Thickness	5% CFA			10% CFA			15% CFA		
	D_2	D_{ac} (mm)			D_{ac} (mm)			D_{ac} (mm)		
		76	152	228	76	152	228	76	152	228
(kPa)	(mm)	a_2	a_2	a_2	a_2	a_2	a_2	a_2	a_2	a_2
1725000	76	0.1900	0.1544	0.1328	0.1980	0.1619	0.1401	0.2044	0.1684	0.1466
	152	0.1921	0.1544	0.1314	0.2001	0.1619	0.1386	0.2065	0.1684	0.1452
	228	0.1938	0.1558	0.1277	0.2019	0.1634	0.1349	0.2083	0.1699	0.1415
	304	0.1877	0.1521	0.1290	0.1957	0.1596	0.1362	0.2021	0.1661	0.1428
3450000	76	0.1790	0.1400	0.1198	0.1869	0.1473	0.1269	0.1933	0.1539	0.1335
	152	0.1791	0.1404	0.1203	0.1870	0.1478	0.1273	0.1934	0.1543	0.1340
	228	0.1807	0.1384	0.1222	0.1886	0.1457	0.1293	0.1951	0.1523	0.1359
	304	0.1763	0.1350	0.1239	0.1841	0.1423	0.1311	0.1906	0.1489	0.1377
5175000	76	0.1689	0.1310	0.1157	0.1766	0.1382	0.1227	0.1831	0.1448	0.1294
	152	0.1714	0.1298	0.1180	0.1792	0.1370	0.1250	0.1856	0.1436	0.1316
	228	0.1737	0.1295	0.1199	0.1815	0.1367	0.1270	0.1880	0.1433	0.1336
	304	0.1704	0.1304	0.1216	0.1781	0.1377	0.1287	0.1846	0.1443	0.1353

Table 4-7 Layer Coefficients (a_2) for 28-day Cured FBA Stabilized Meridian Aggregate

E_{ac}	Base Thickness	5% FBA			10% FBA			15% FBA		
	D_2	D_{ac} (mm)			D_{ac} (mm)			D_{ac} (mm)		
		76	152	228	76	152	228	76	152	228
(kPa)	(mm)	a_2	a_2	a_2	a_2	a_2	a_2	a_2	a_2	a_2
1725000	76	0.2237	0.1696	0.1367	0.2212	0.1645	0.1301	0.2160	0.1562	0.1199
	152	0.2268	0.1696	0.1346	0.2245	0.1645	0.1279	0.2195	0.1562	0.1176
	228	0.2295	0.1717	0.1291	0.2274	0.1668	0.1221	0.2225	0.1586	0.1114
	304	0.2202	0.1661	0.1310	0.2176	0.1609	0.1241	0.2122	0.1524	0.1136
3450000	76	0.2070	0.1477	0.1170	0.2038	0.1416	0.1094	0.1976	0.1320	0.0981
	152	0.2071	0.1483	0.1177	0.2039	0.1423	0.1101	0.1977	0.1327	0.0988
	228	0.2096	0.1453	0.1206	0.2065	0.1391	0.1131	0.2005	0.1293	0.1020
	304	0.2028	0.1401	0.1233	0.1994	0.1336	0.1160	0.1930	0.1236	0.1050
5175000	76	0.1916	0.1340	0.1107	0.1876	0.1272	0.1029	0.1805	0.1169	0.0912
	152	0.1954	0.1322	0.1142	0.1916	0.1253	0.1064	0.1848	0.1149	0.0950
	228	0.1990	0.1317	0.1171	0.1954	0.1248	0.1096	0.1887	0.1143	0.0982
	304	0.1939	0.1331	0.1197	0.1900	0.1263	0.1123	0.1831	0.1159	0.1011

Table 4-8 Layer Coefficients (a_2) for 90-day Cured FBA Stabilized Meridian Aggregate

E_{ac}	Base Thickness	5% FBA			10% FBA			15% FBA		
	D_2	D_{ac} (mm)			D_{ac} (mm)			D_{ac} (mm)		
		76	152	228	76	152	228	76	152	228
(kPa)	(mm)	a_2	a_2	a_2	a_2	a_2	a_2	a_2	a_2	a_2
1725000	76	0.2290	0.1768	0.1451	0.2371	0.1838	0.1514	0.2425	0.1904	0.1589
	152	0.2321	0.1768	0.1431	0.2402	0.1838	0.1494	0.2455	0.1904	0.1569
	228	0.2347	0.1789	0.1377	0.2429	0.1859	0.1439	0.2481	0.1925	0.1515
	304	0.2257	0.1735	0.1396	0.2337	0.1804	0.1458	0.2391	0.1871	0.1534
3450000	76	0.2130	0.1557	0.1261	0.2207	0.1622	0.1320	0.2265	0.1694	0.1399
	152	0.2131	0.1563	0.1267	0.2208	0.1629	0.1326	0.2266	0.1700	0.1406
	228	0.2155	0.1534	0.1295	0.2232	0.1598	0.1355	0.2290	0.1671	0.1433
	304	0.2089	0.1484	0.1321	0.2166	0.1547	0.1382	0.2224	0.1621	0.1459
5175000	76	0.1981	0.1425	0.1200	0.2055	0.1487	0.1258	0.2116	0.1563	0.1339
	152	0.2017	0.1407	0.1233	0.2092	0.1470	0.1292	0.2153	0.1545	0.1372
	228	0.2052	0.1402	0.1262	0.2128	0.1464	0.1321	0.2187	0.1540	0.1401
	304	0.2003	0.1416	0.1287	0.2077	0.1479	0.1347	0.2138	0.1554	0.1426

Table 4-9 Layer Coefficients (a_2) of the Raw and CKD Stabilized Meridian Aggregate

E_{ac} MPa [ksi]	Base Thickness D_2 mm [in]	Meridian 2			5% CKD, 7-day			10% CKD, 7-day		
		D_{ac} (mm)			D_{ac} (mm)			D_{ac} (mm)		
		76	152	228	76	152	228	76	152	228
1725	76 [3]	0.0691	0.0162	-0.0158	0.1074	0.0626	0.0354	0.1101	0.0615	0.0320
[250]	152 [6]	0.0722	0.0163	-0.0179	0.1100	0.0626	0.0337	0.1130	0.0615	0.0300
	228 [9]	0.0748	0.0184	-0.0233	0.1122	0.0644	0.0291	0.1154	0.0634	0.0250
	304 [12]	0.0658	0.0129	-0.0214	0.1045	0.0597	0.0307	0.1070	0.0583	0.0268
3450	76 [3]	0.0529	-0.0051	-0.0351	0.0936	0.0445	0.0191	0.0952	0.0418	0.0142
[500]	152 [6]	0.0530	-0.0045	-0.0345	0.0937	0.0450	0.0196	0.0953	0.0424	0.0147
	228 [9]	0.0554	-0.0075	-0.0316	0.0958	0.0425	0.0220	0.0975	0.0396	0.0174
	304 [12]	0.0488	-0.0125	-0.0290	0.0902	0.0382	0.0243	0.0914	0.0350	0.0199
5175	76 [3]	0.0378	-0.0185	-0.0412	0.0809	0.0331	0.0139	0.0813	0.0295	0.0086
[750]	152 [6]	0.0415	-0.0202	-0.0379	0.0840	0.0317	0.0167	0.0847	0.0279	0.0116
	228 [9]	0.0450	-0.0208	-0.0350	0.0870	0.0312	0.0192	0.0879	0.0274	0.0143
	304 [12]	0.0400	-0.0193	-0.0325	0.0827	0.0325	0.0213	0.0833	0.0287	0.0166

Table 4-10 Layer Coefficients (a_2) of the 15% CKD Stabilized Meridian Aggregate Cured for Different Periods

E_{ac},	Base	15% CKD, 7-day			15% CKD, 28-day			15% CKD, 90-day		
MPa	Thickness	D_{ac}, (mm)			D_{ac}, (mm)			D_{ac}, (mm)		
[ksi]	D_2 mm [in]	76	152	228	76	152	228	76	152	228
1725	76 [3]	0.1241	0.0840	0.0596	0.1479	0.1008	0.0723	0.1644	0.1168	0.0879
[250]	152 [6]	0.1265	0.0840	0.0580	0.1506	0.1008	0.0704	0.1672	0.1168	0.0860
	228 [9]	0.1285	0.0856	0.0539	0.1529	0.1027	0.0655	0.1695	0.1187	0.0811
	304 [12]	0.1216	0.0814	0.0553	0.1448	0.0978	0.0672	0.1614	0.1137	0.0828
3450	76 [3]	0.1118	0.0677	0.0450	0.1334	0.0817	0.0551	0.1498	0.0975	0.0706
[500]	152 [6]	0.1119	0.0682	0.0454	0.1335	0.0823	0.0556	0.1499	0.0981	0.0711
	228 [9]	0.1137	0.0660	0.0476	0.1356	0.0797	0.0582	0.1521	0.0954	0.0737
	304 [12]	0.1087	0.0621	0.0496	0.1297	0.0752	0.0605	0.1461	0.0909	0.0761
5175	76 [3]	0.1003	0.0576	0.0403	0.1200	0.0698	0.0496	0.1362	0.0855	0.0651
[750]	152 [6]	0.1032	0.0563	0.0428	0.1233	0.0683	0.0526	0.1395	0.0839	0.0680
	228 [9]	0.1058	0.0558	0.0451	0.1264	0.0678	0.0552	0.1427	0.0834	0.0707
	304 [12]	0.1020	0.0569	0.0469	0.1219	0.0691	0.0574	0.1382	0.0848	0.0729

Table 4-11 Comparison of SN and ESAL of the Raw and Stabilized Aggregate Bases

Case No.	Raw Meridian 1		Raw Meridian 2		10% CFA, 28-day Cured		10% FBA, 28-day Cured		15% CKD, 28-day Cured	
	SN	ESAL	SN	ESAL	SN	ESAL	SN	ESAL	SN	ESAL
Case 1	1.03	1400	1.2	2900	1.52	12,000	1.61	19,400	1.43	7,300
Case 4	1.07	1700	1.43	7300	2.03	79,400	2.21	151,400	1.89	34,800
Case 7	1.12	2100	1.67	17,100	2.18	316,700	2.98	740,400	2.36	133,100
Case 10	1.16	2500	1.79	25,400	3.09	1,114,900	3.47	2,607,500	3.56	1,552,400

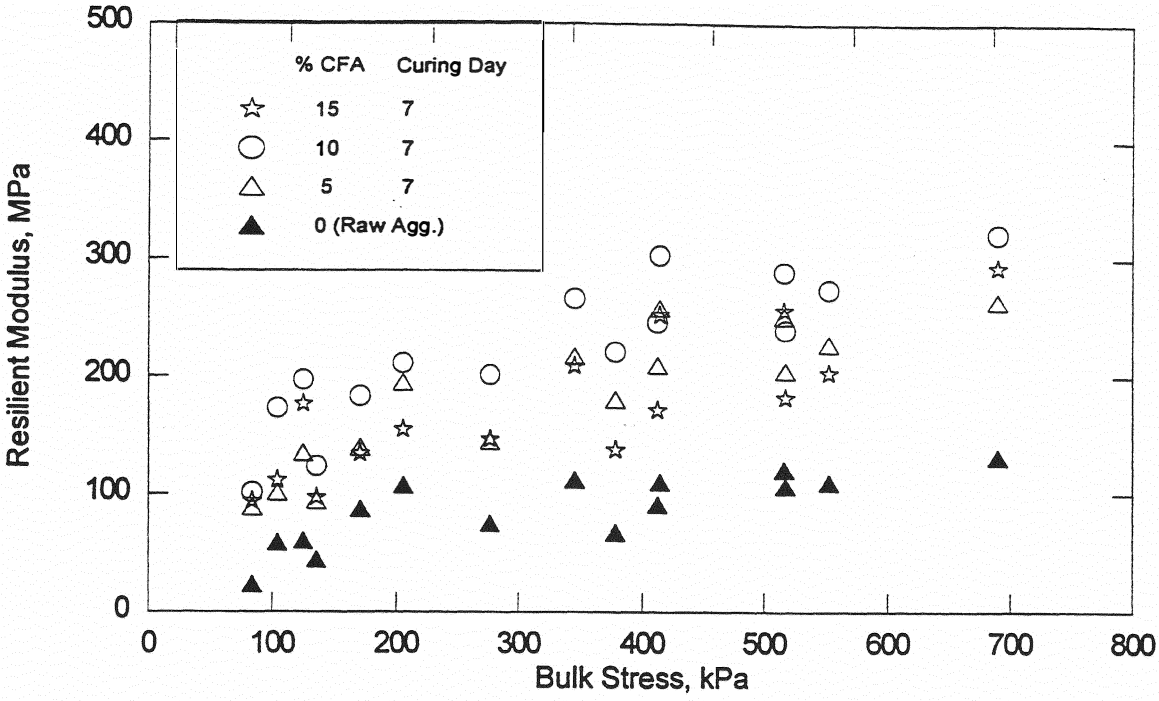

Figure 4-1 Mean M_R Values of Raw and 7-day Cured CFA Stabilized Aggregate

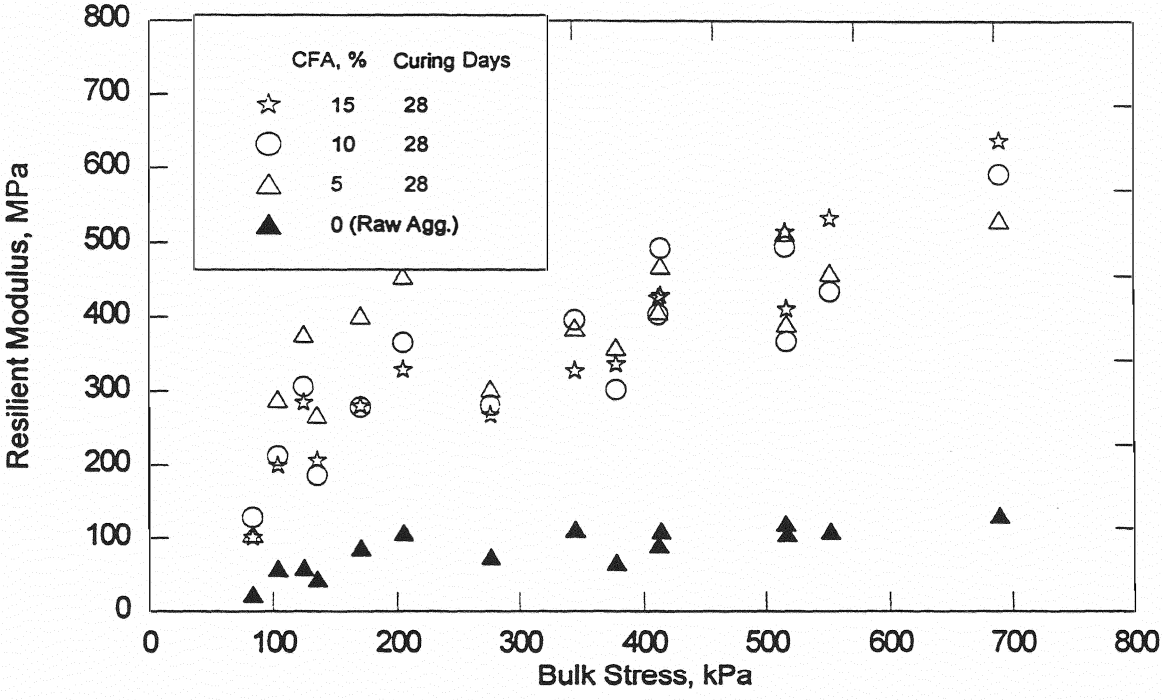

Figure 4-2 Mean M_R Values of Raw and 28-day Cured CFA Stabilized Aggregate

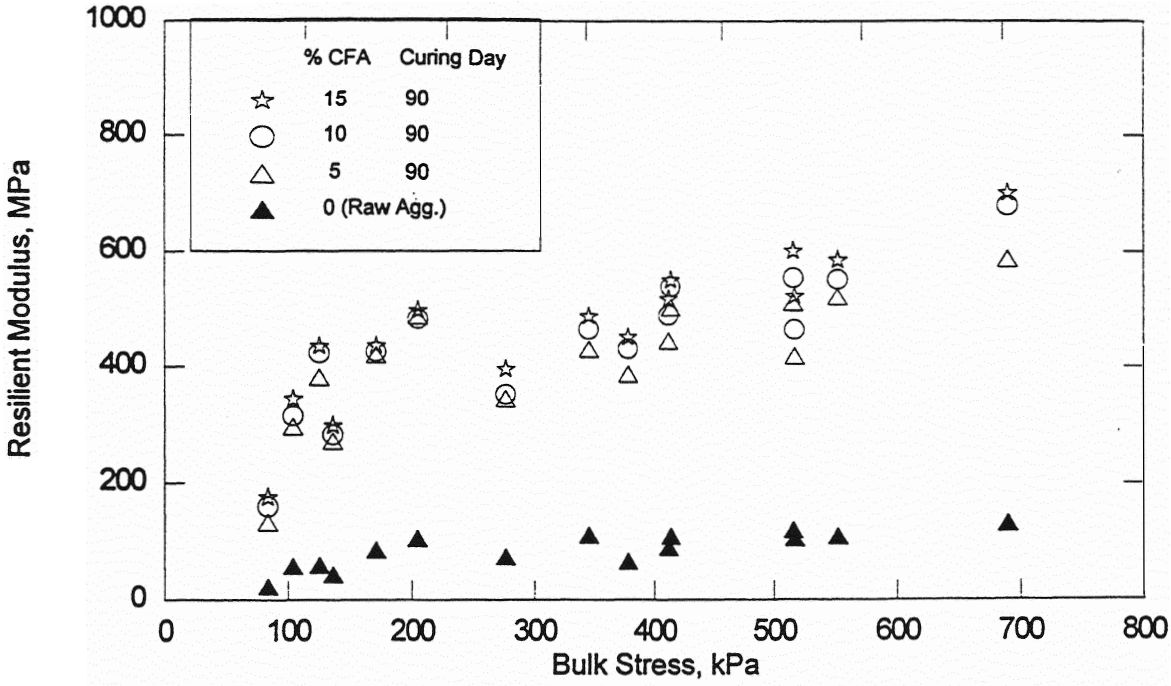

Figure 4-3 Mean M_R Values of Raw and 90-day Cured CFA Stabilized Aggregate

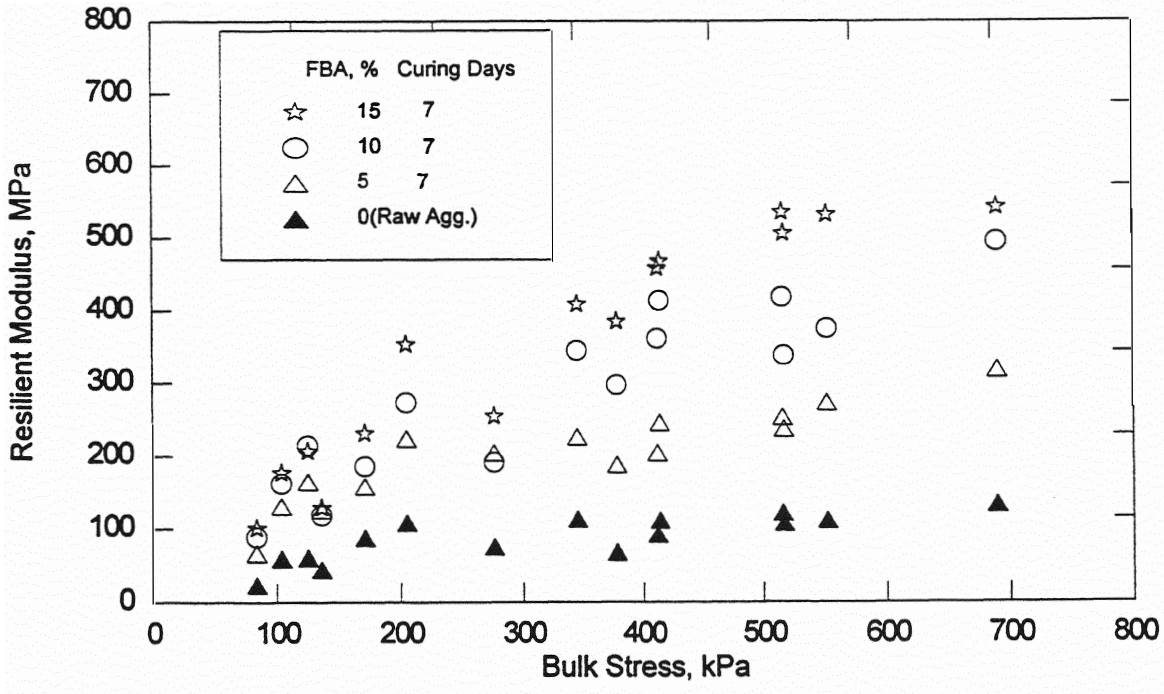

Figure 4-4 Mean M_R Values of Raw and 7-day Cured FBA Stabilized Aggregate

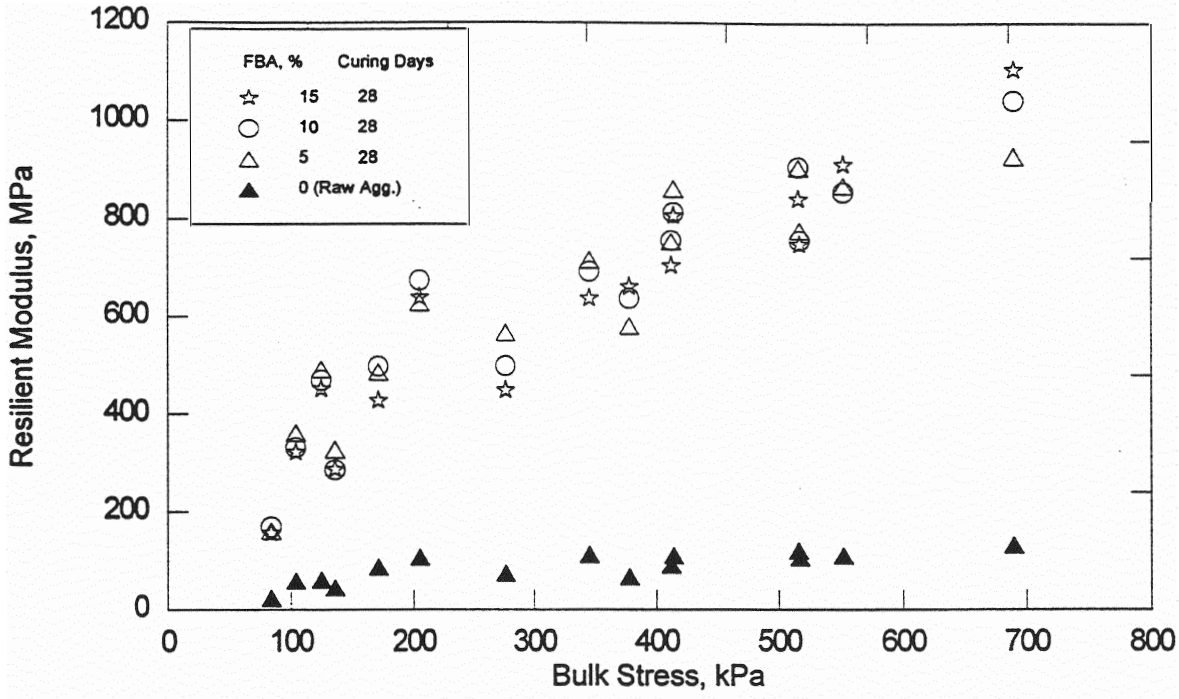

Figure 4-5 Mean M_R Values of RAw and 28-day Cured FBA Stabilized Aggregate

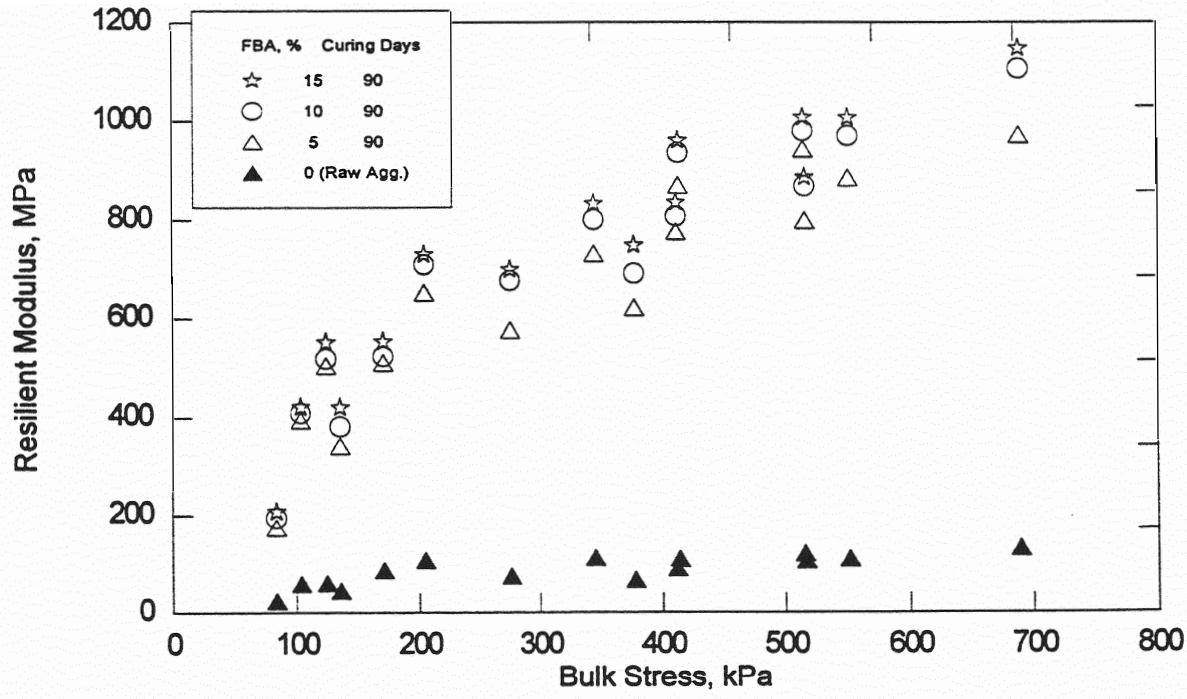

Figure 4-6 Mean M_R Values of Raw and 90-day Cured FBA Stabilized Aggregate

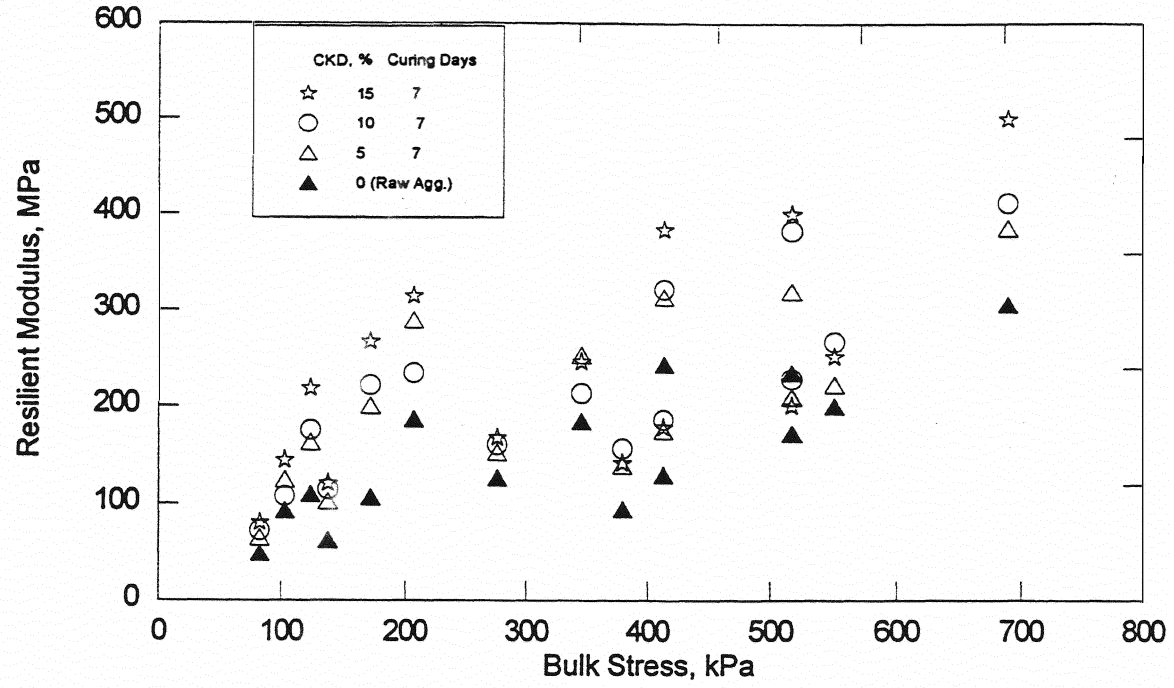

Figure 4-7 Mean M_R Values of Raw and 7-day Cured CKD Stabilized Aggregate

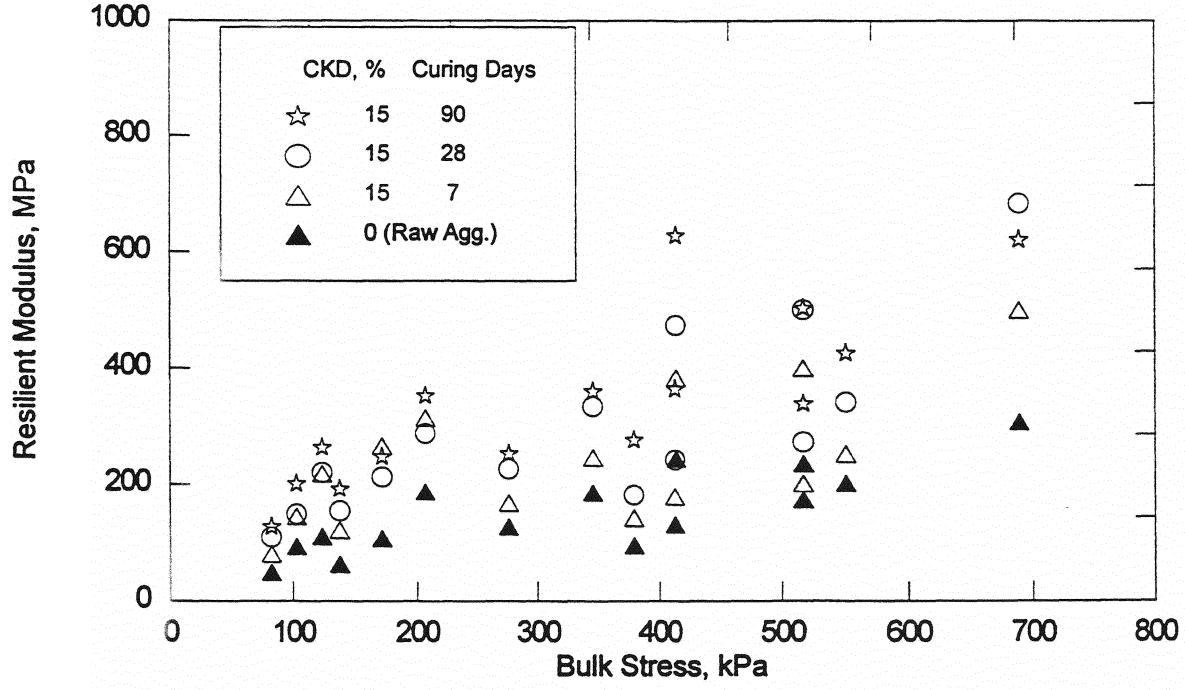

Figure 4-8 Mean M_R Values of Raw and 15-day Cured CKD Stabilized Aggregate

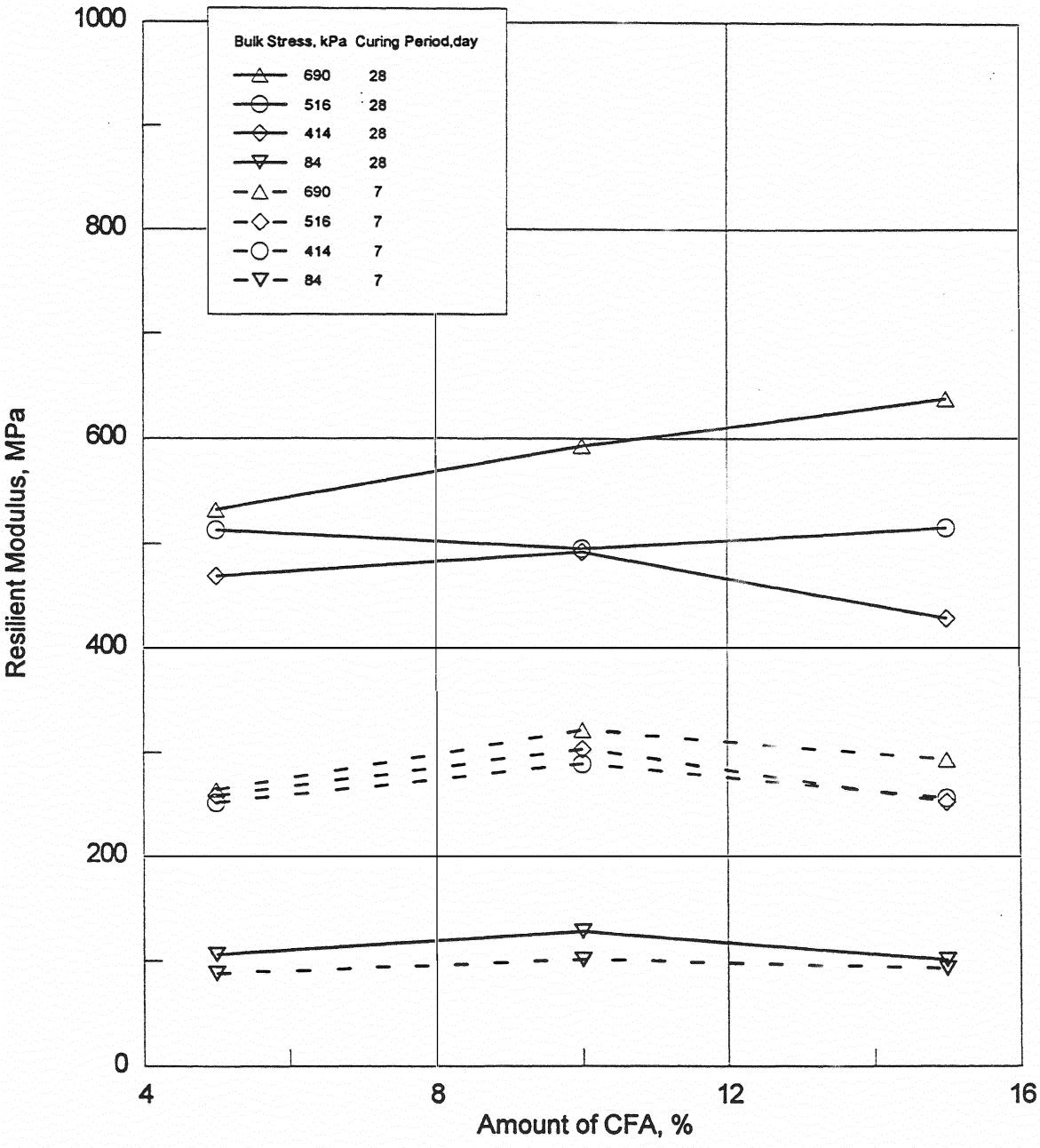

Figure 4-9 Relationship Between Resilient Modulus and Amount of CFA

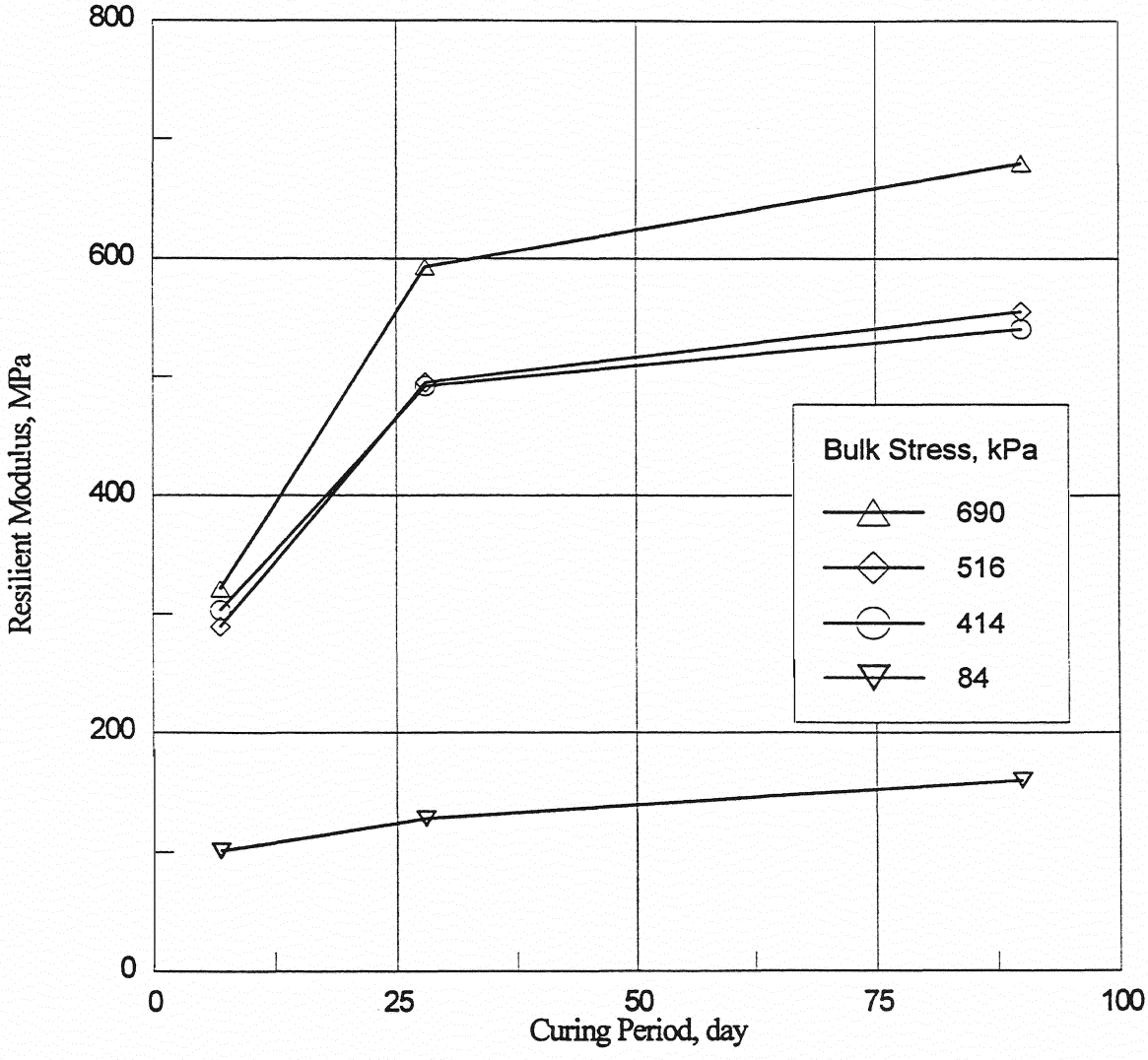

Figure 4-10 Relationship between Resilient Modulus and Curing Period for 10% CFA-Stabilized Aggregate

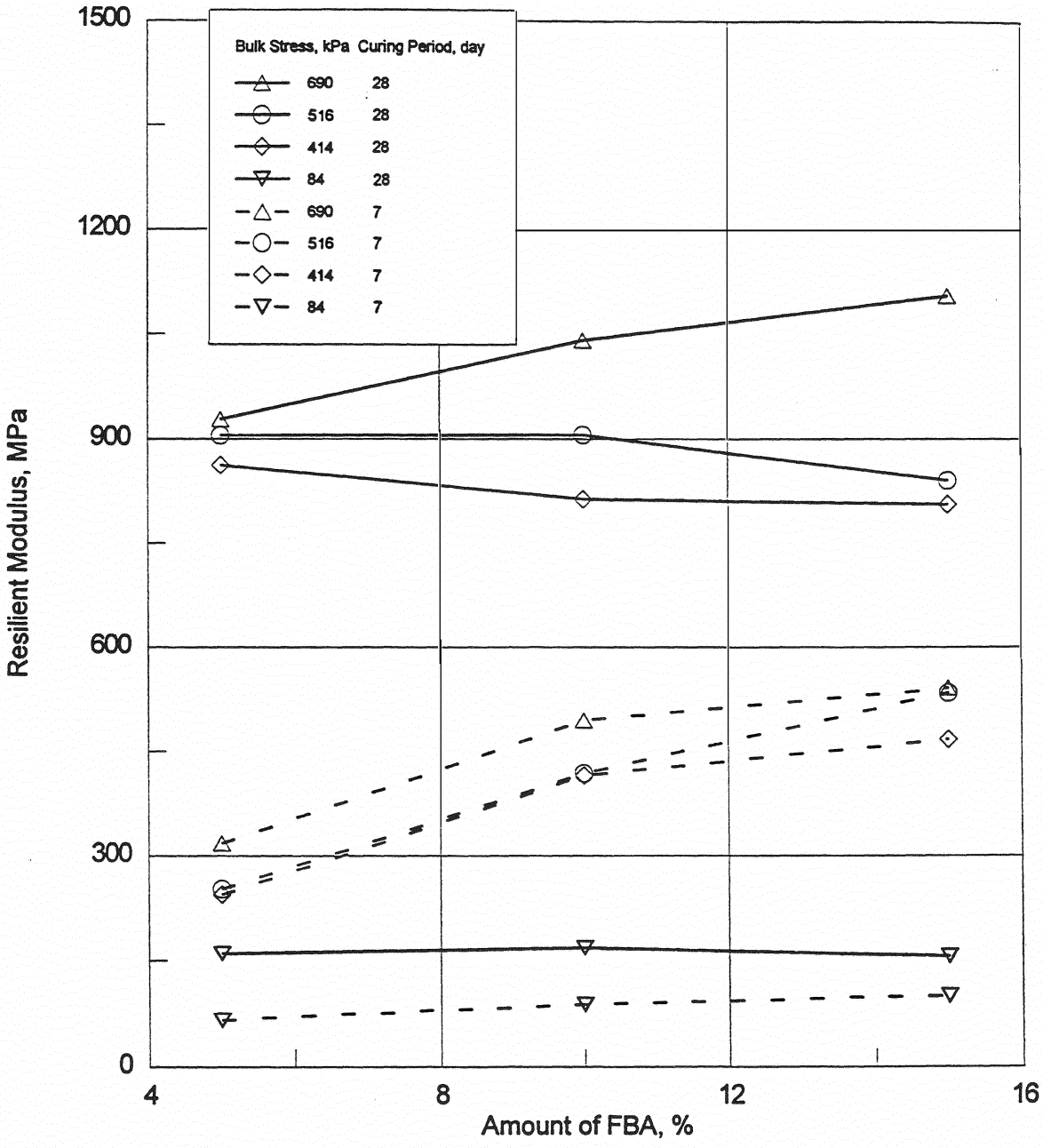

Figure 4-11 Relationship between Resilient Modulus and Amount of FBA

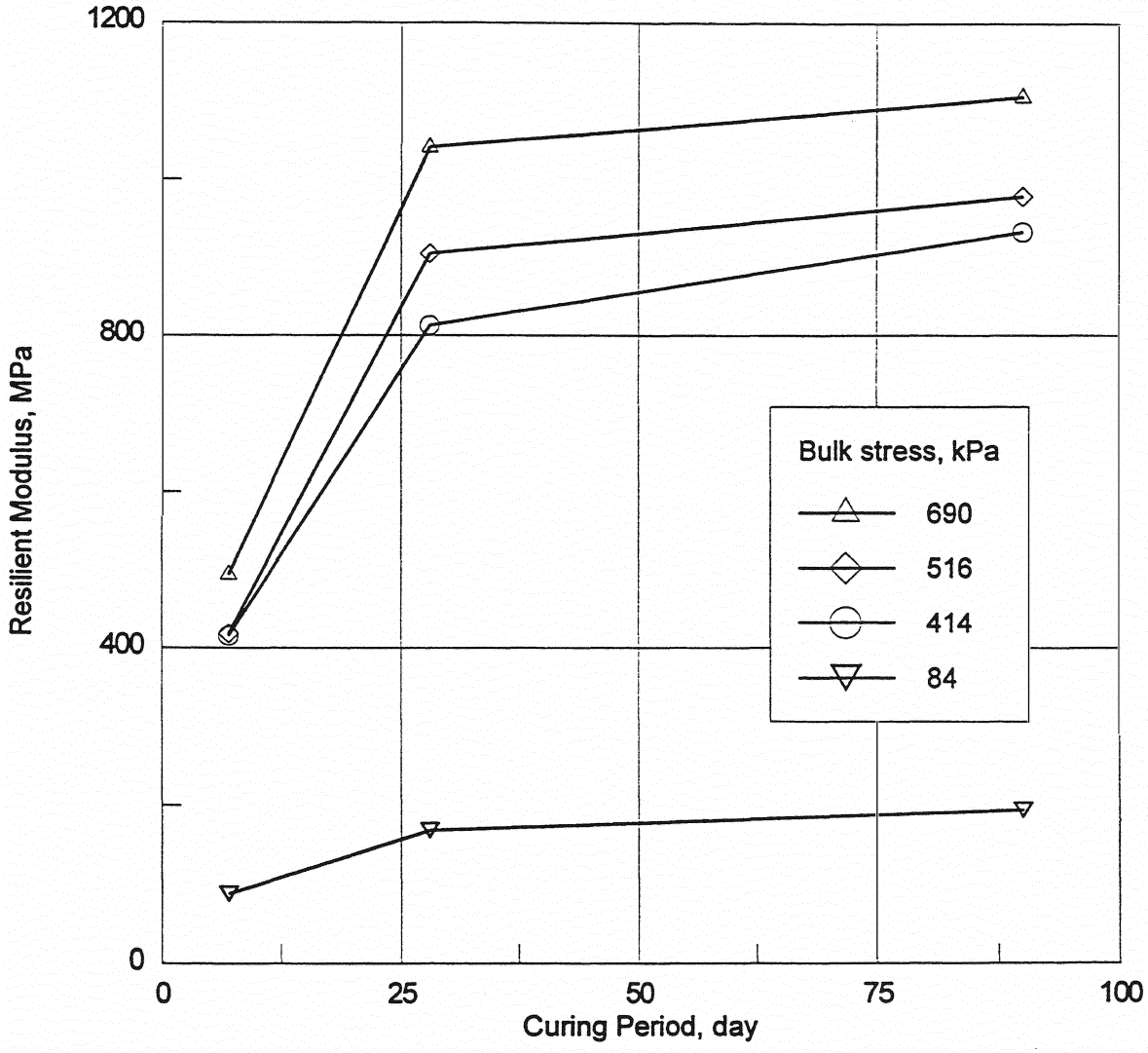

Figure 4-12 Relationship between Resilient Modulus and Curing Period for 10% FBA-Stabilized Aggregate

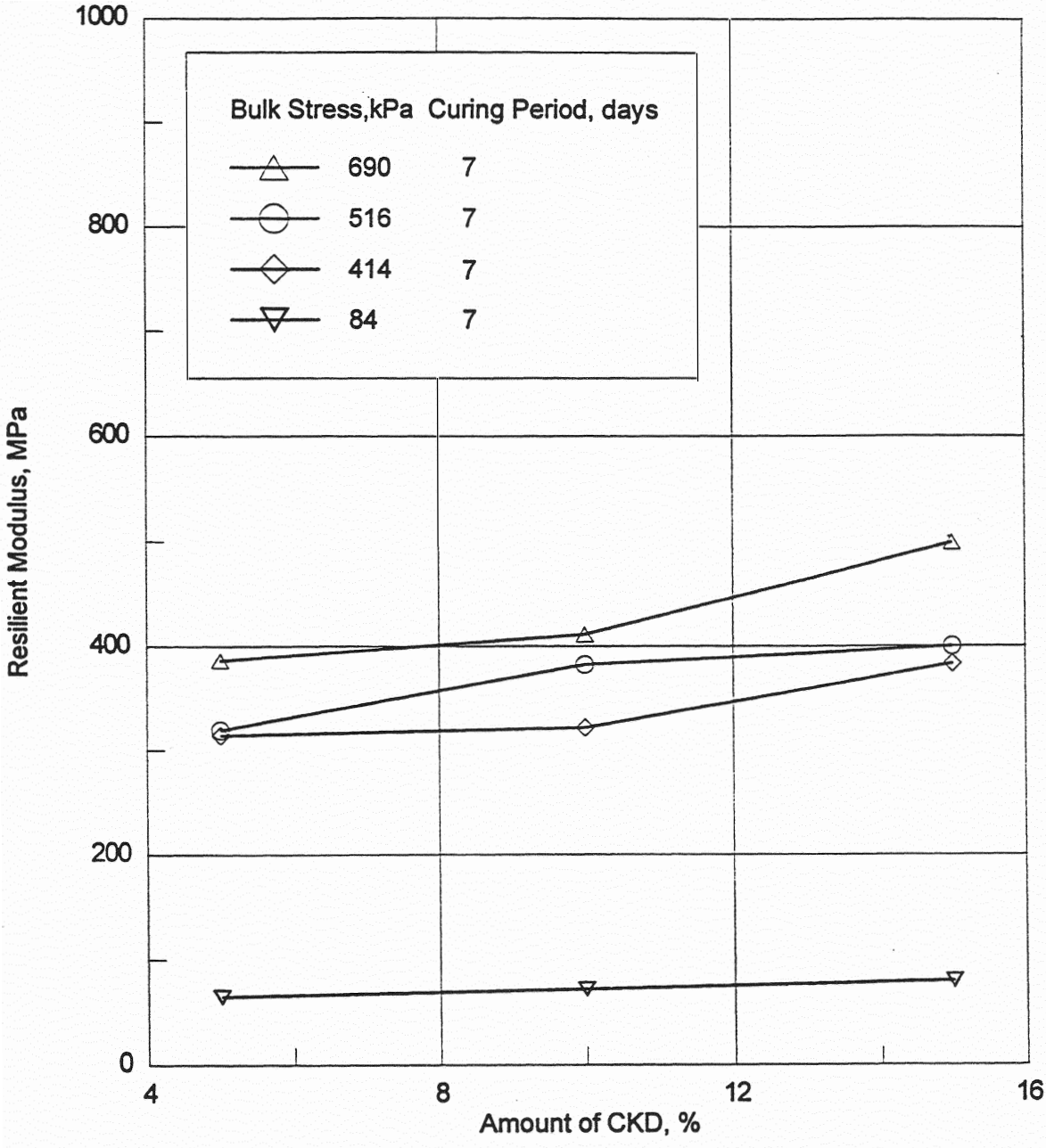

Figure 4-13 Relationship Between Resilient Modulus and Amount of CKD

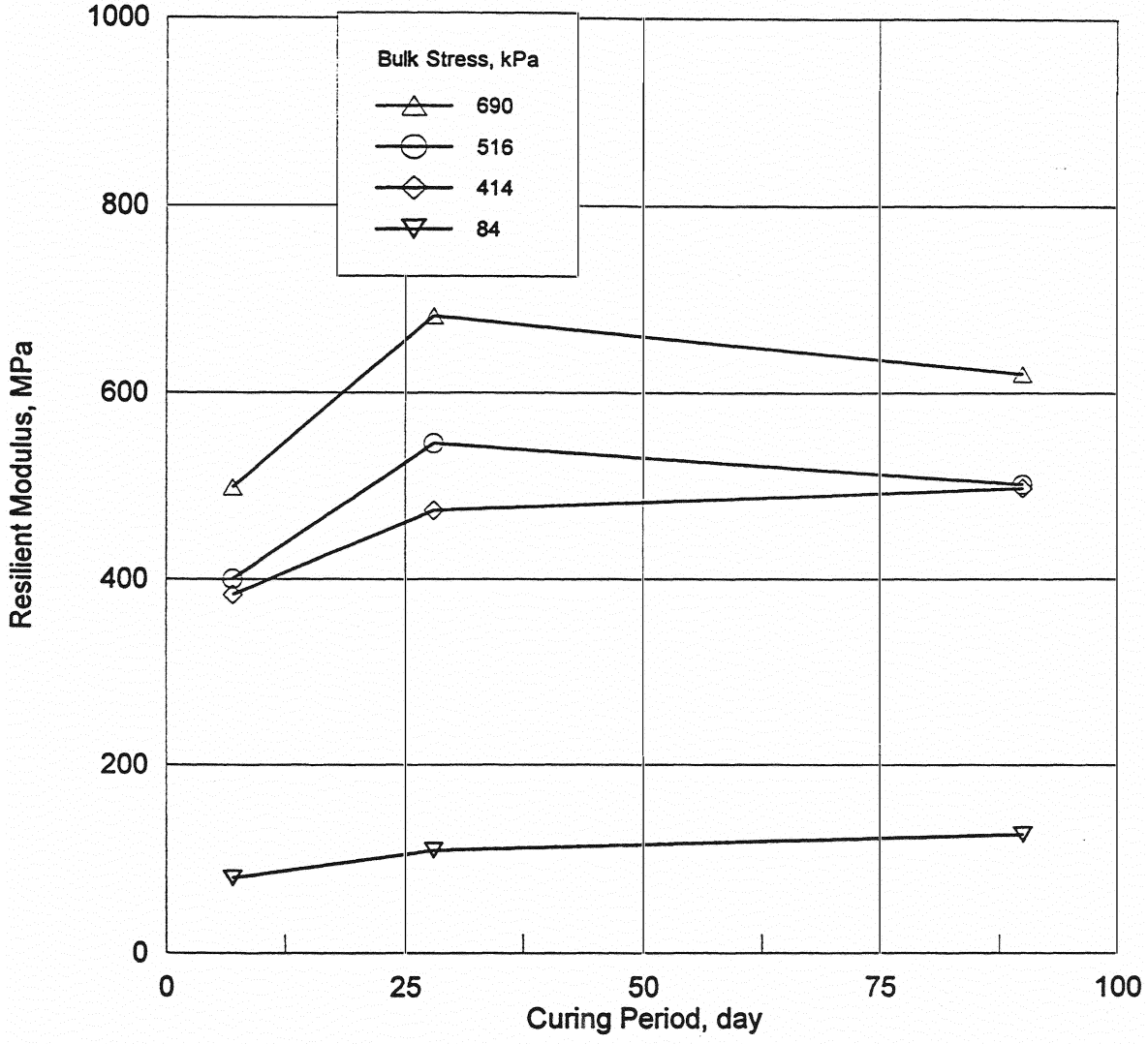

Figure 4-14 Relationship between Resilient Modulus and Curing Period for 15% CKD-Stabilized Aggregate

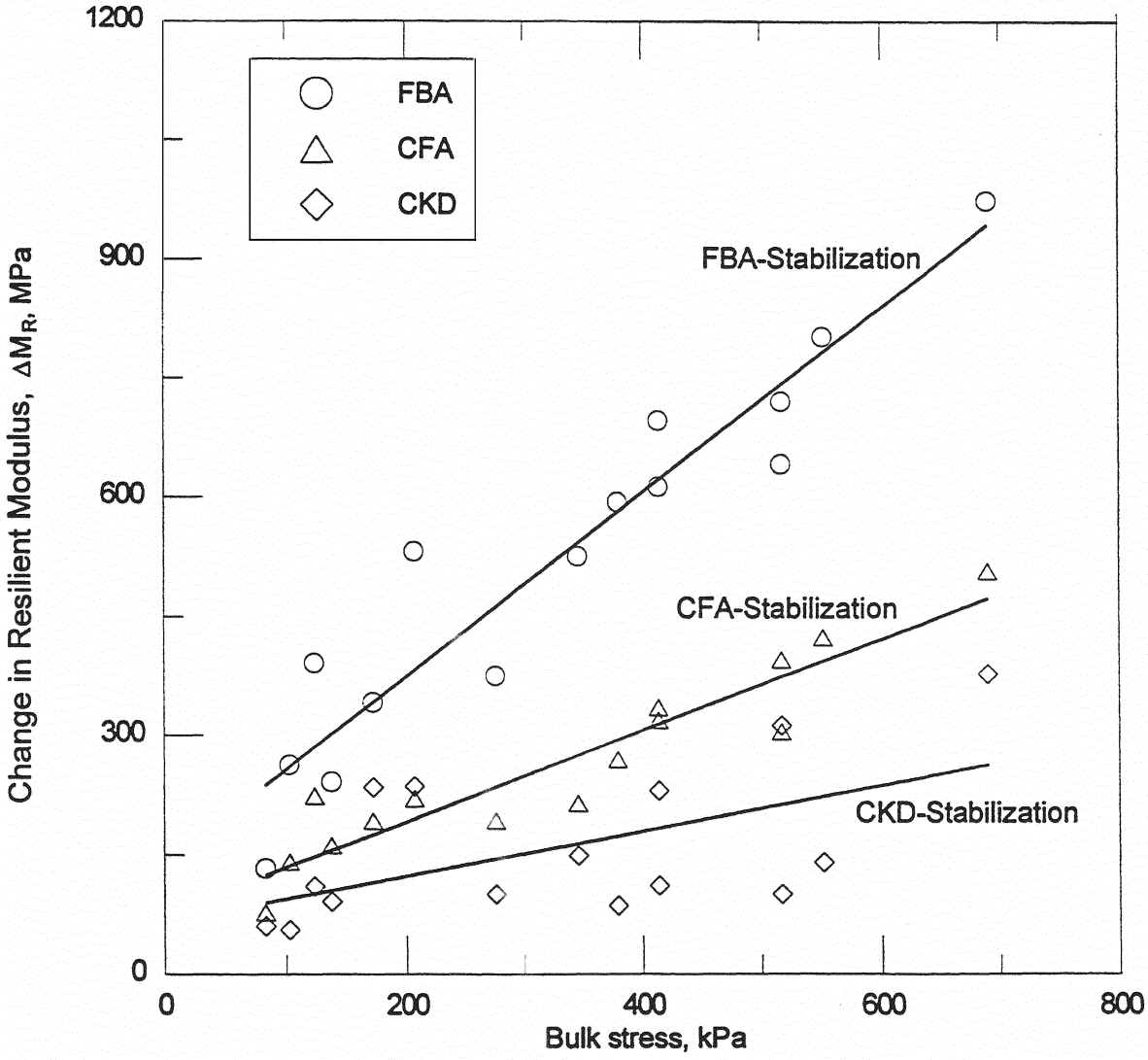

Figure 4-15 Relationship between Increase in Resilient Modulus and Bulk Stress for 28-day Cured Aggregate Stabilized with Different Agents (15%)

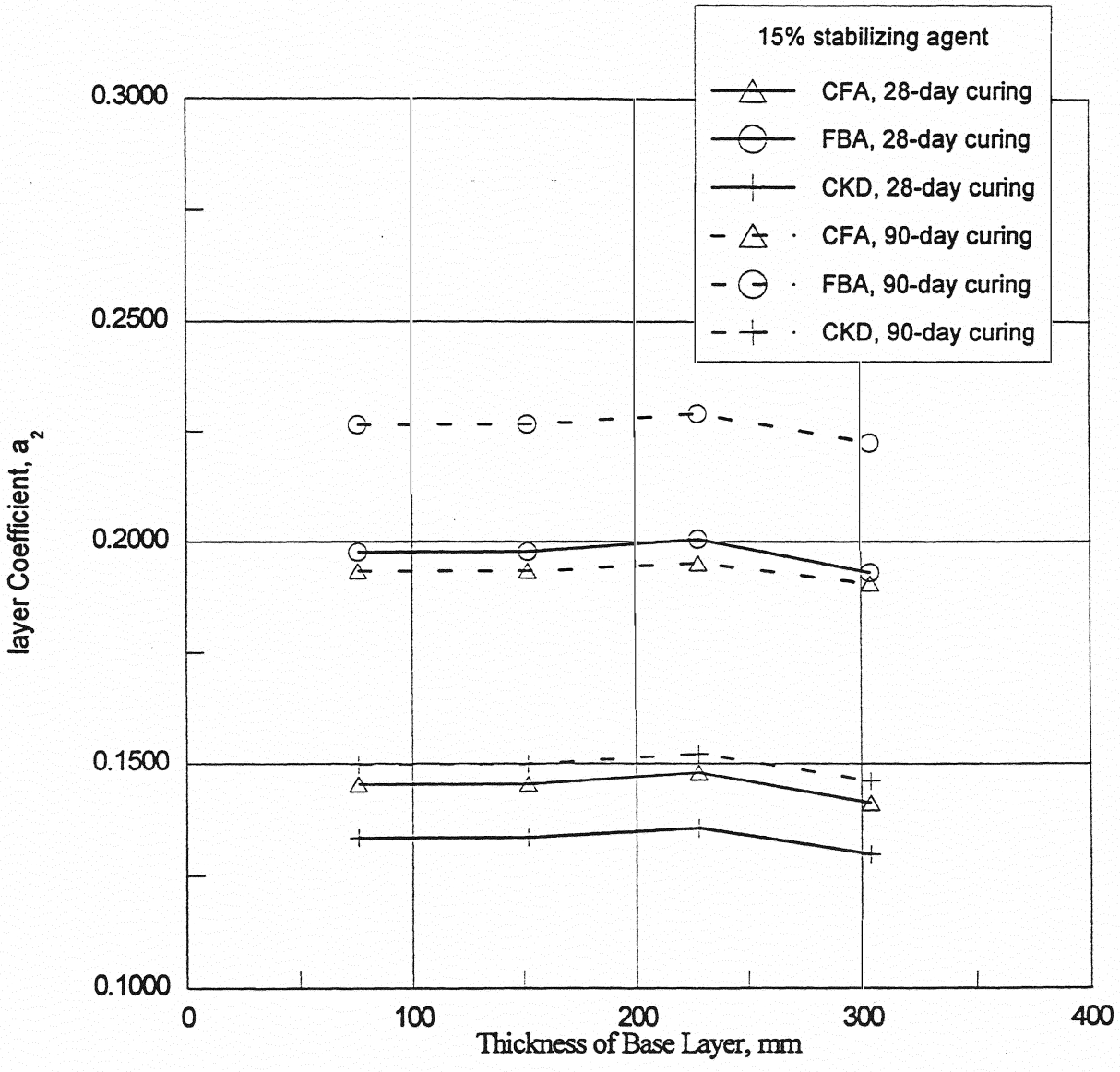

Figure 4-16 Layer Coefficient Versus Thickness of Base Layer for Different Stabilizing Agents

CHAPTER 5

MICROANALYSIS OF CHEMICALLY STABILIZED AGGREGATES

5.1 INTRODUCTION

The XRD analysis was employed to examine the mineralogical content of the raw aggregate, additives (stabilizing agent) and stabilized aggregates. To identify the reaction products over the various curing periods and to study the microstructure development in the stabilized aggregate matrix, specially prepared specimens were microscopically examined by SEM. The testing procedure and methodology of XRD are similar to that reported before (Laguros and Zenieris, 1987). Processing samples for SEM analyses are similar to that reported by Baker and Laguros (1985).

5.2 MICROANALYSIS RESULTS

5.2.1 X-ray Diffraction

XRD tests were conducted on the raw Meridian aggregate, fly ash and CKD stabilized aggregate which yielded diffractograms (Pandey et al. 1998; Zhu et al. 1998). The minerals identified by XRD analyses are presented in Table 5-1. A typical diffractogram is presented for raw aggregate and 28-day cured aggregate stabilized with 10% FBA (Figures 5-1a and b). The diffractograms indicate the presence of quartz (SiO_2) (Q) in the raw Meridian aggregate, along with tricalcium aluminate ($3CaO.Al_2O_3$) (T), lime (CaO) (L) and anhydrite ($CaSO_4$) (A). Similar patterns, in terms of mineral identification, are observed on the diffractograms of CFA, FBA and CKD, but the intensities differ. However, the diffractograms of the stabilized aggregates show an

abundance of calcite (Calcium carbonate: $CaCO_3$) (C) and quartz (SiO_2) (Q) and also the presence of tricalcium aluminate, ettringite, and gismondine (a calcium aluminum silicate hydrate) which are compounds of hydration products. The lime available in the CFA, FBA and CKD most likely underwent chemical changes to produce the compounds, calcite, ettringite, and gismondine. However, it should be noted that the calcium oxide (CaO) (L) present in the aggregate and stabilizers, termed as lime in this study, should not be confused with hydrated lime ($Ca(OH)_2$) (P) or quick lime. It is calcium oxide present in the aggregate and stabilizers and only part of it from the stabilized agent may be available for hydration reaction.

It is noted that ettringite is the only hydration product in CKD stabilized aggregate, which may be attributed to low content of free lime (2% - 3%) and high Loss on Ignition (LOI) (28% - 30%) of CKD. It is observed that FBA stabilization produces more hydration products which include tricalcium aluminate, ettringite, and gismondine than CKD stabilization. This confirms the resilient modulus test results that FBA stabilization increases the M_R value most and CKD stabilization least. The high volume of hydration products in FBA stabilization can be attributed to the fact that FBA has higher content of free lime (18.2%) and low LOI (5.34%) than CKD does.

The amount of ettringite is small and with curing time it tends to disappear (e.g. 90-day cured CKD-stabilized aggregate). This is explained as the change from ettringite ($3CaO{\cdot}Al_2O_3{\cdot}3CaSO_4{\cdot}32H_2O$) (E) to monosulfoaluminate ($3CaO{\cdot}Al_2O_3{\cdot}CaSO_4{\cdot}13H_2O$).

5.2.2 Scanning Electron Microscopy

The visual examination of micrographs of the stabilized aggregates demonstrates evidence of crystal formation in the matrix of stabilized aggregates. These crystals which

are absent in the micrographs of the raw aggregate and additives are formed as a result of hydration. Figures 5-2 and 5-3 present typical micrographs taken from raw aggregate and a typical stabilized form, i.e. 10% FBA.

It is observed that the raw aggregate is essentially composed of granular particles that lack a definite form, some are rounded, but the majority are angular. There is no connection between the aggregate particles in a point of micro-view, i.e., there are abundant gaps, or voids, existing between the individual particles. This micro-void can only be observed with a magnification of several thousands.

For stabilized aggregate, the crystal formation and paste surrounding the individual structures were observed and increased with the prolongation of the curing period. Some changes in the void domain characteristics are observed in the stabilized aggregate. The overall size (area) of voids decreases with increasing curing time. This relationship is more macroscopic than quantitative and no attempt has been made to numerically associate the rate of strength gain to changes in crystal formation or reduction in void area. Nevertheless, it may be reasoned that the gain in strength is associated with the crystal formation and the void-size reduction. The presence of the calcium silicate hydrate (CSH) crystals (ettringite) in the stabilized aggregate, as observed in the micrographs, confirms the chemical changes that took place within the matrix with time. The results of M_R tests on the stabilized aggregate indicate that M_R values increase with the increase in ash/dust content and curing period duration.

Table 5-1 Minerals Identified by X-ray Diffraction Analysis

Mineral Name	Chemical Formula	Symbol	Raw Material				Stabilized Aggregate		
			Aggregate	CFA	FBA	CKD	CFA	FBA	CKD
Anhydrite	$CaSO_4$	A	Yes	Yes	Yes	Yes			
Lime	CaO	L	Yes	Yes	Yes	Yes			
Tricalcium Aluminate	$3CaO.Al_2O_3$	T	Yes	Yes	Yes		Yes	Yes	
Portlandite	$Ca(OH)_2$	P	Yes	Yes				Yes	Yes
Quartz	SiO_2	Q	Yes	Yes	Yes	Yes	Yes	Yes	Yes
Calcite	$CaCO_3$	C				Yes	Yes	Yes	Yes
Calcium Aluminium Oxide Sulfate	$3CaO.3Al_2O_3.CaSO_4$	X	Yes	Yes					
Gismondine	$CaO.2SiO_2.Al_2O_3.4H_2O$	G					Yes	Yes	
Ettringite	$3CaO.Al_2O_3.3CaSO_4.32H_2O$	E					Yes	Yes	Yes

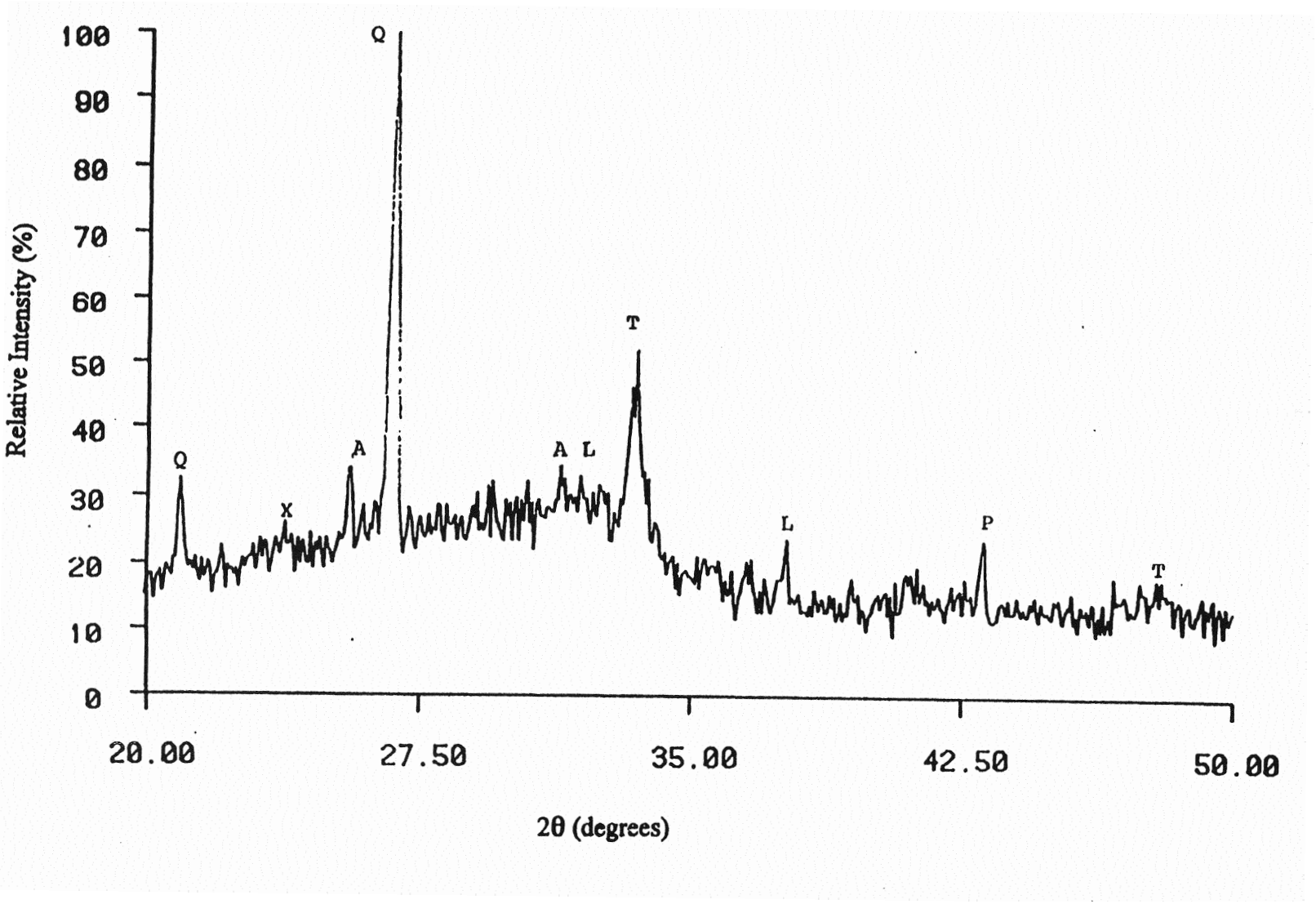

Figure 5-1 (a) X-Ray Diffractogram of the Raw Meridian Aggregate

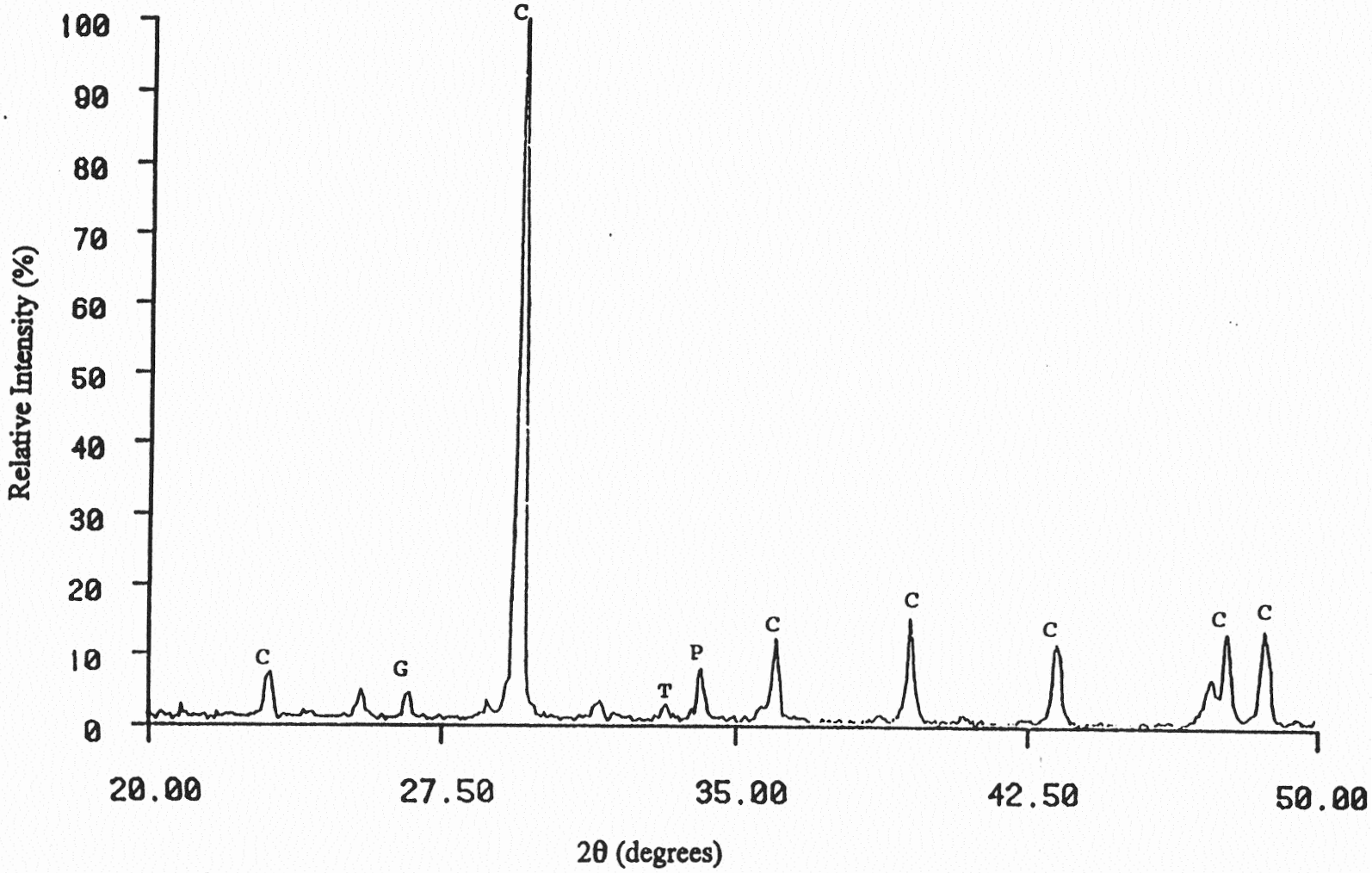

Figure 5-1 (b) X-Ray Diffractogram of the 28-day Cured Aggregate Stabilized with 10% FBA

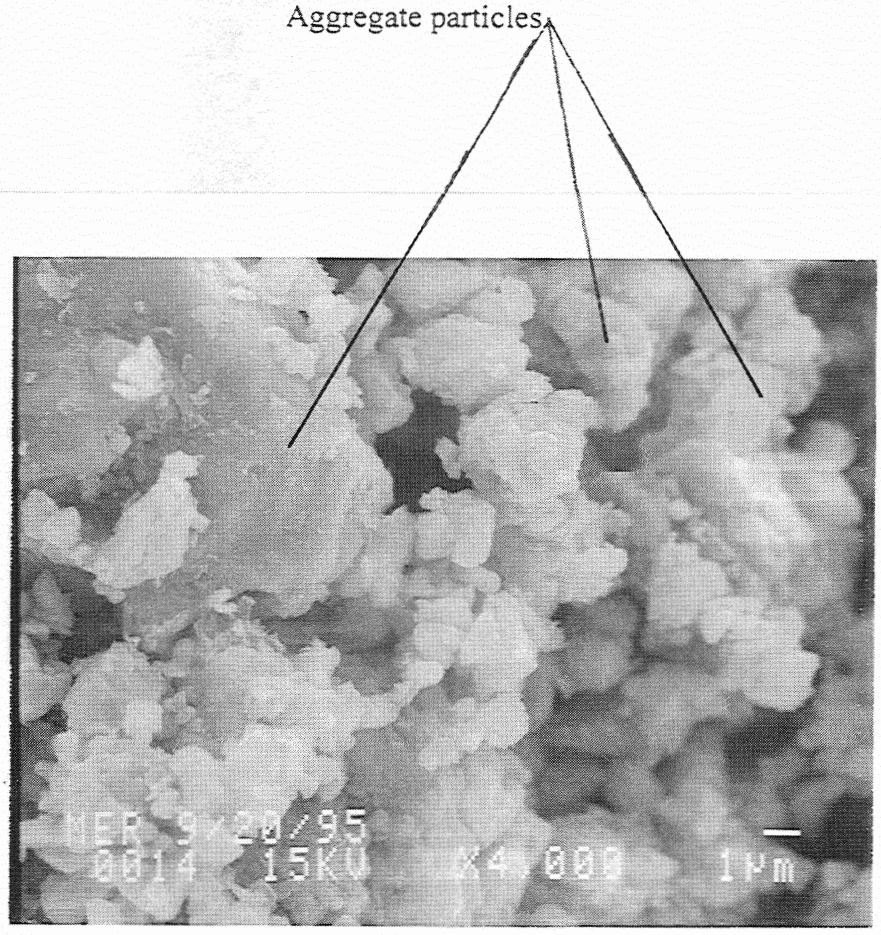

Figure 5-2 Micrograph of the Raw Meridian Aggregate

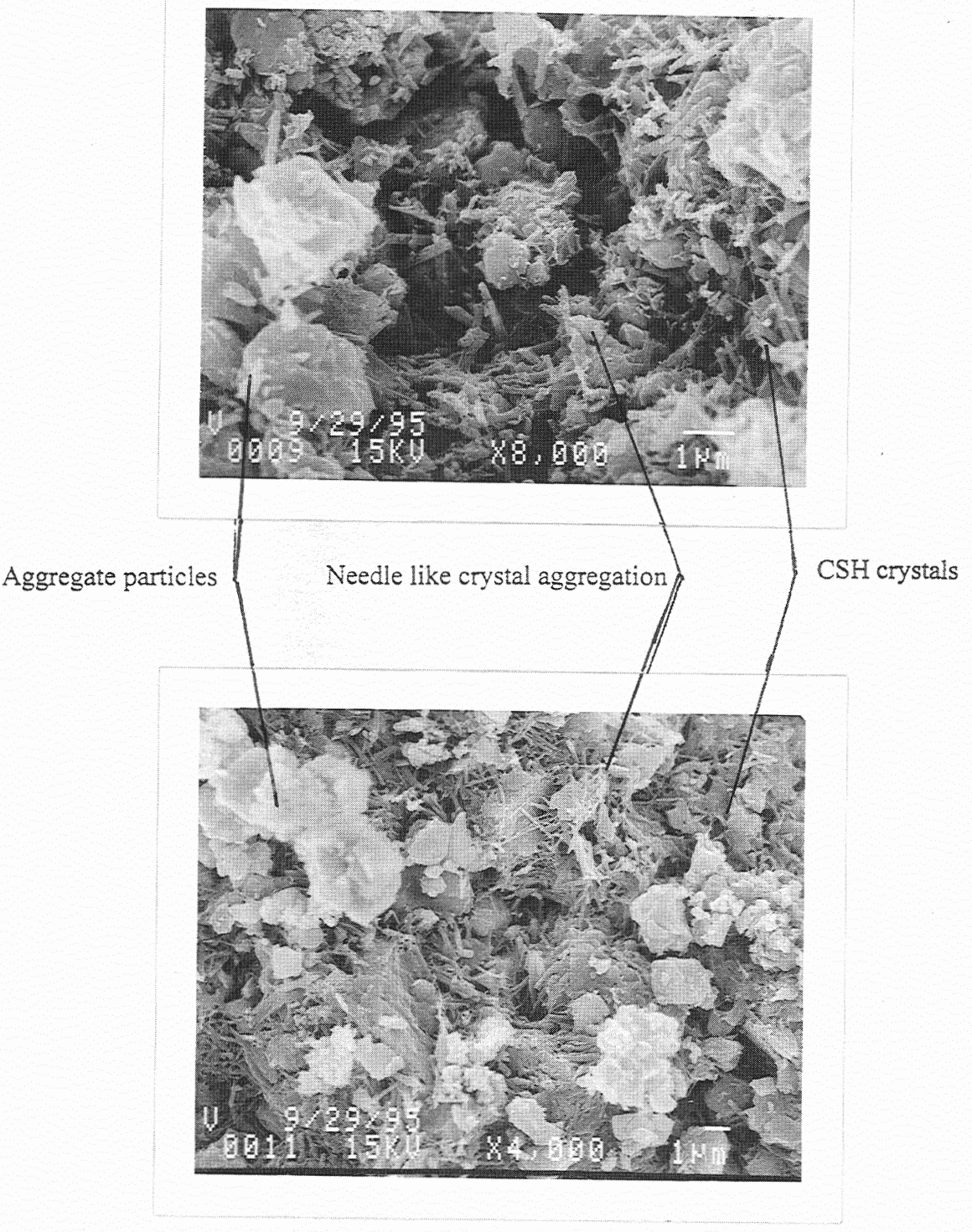

Figure 5-3 Micrographs of the 28-day Cured Aggregate Stabilized with 10% FBA

CHAPTER 6

CONCLUSIONS AND RECOMMENDATIONS

6.1 CONCLUSIONS

From the data obtained and the analysis of the results presented in the preceding chapters, the following observations and conclusions are made.

1. The M_R values obtained from the AASHTO T 294-94 method are nearly 32 to 122% higher than those from the AASHTO T 292-91I method due to the different stress sequences and loading waveforms used in the two testing procedures. The haversine waveform used in the AASHTO T 294-94 method produces higher M_R values than those from the triangular and rectangular waveforms due to the different loading durations, rest periods, and loading frequency used in these waveforms.

2. The variabilities of the M_R values due to the three different gradations, namely, the median, finer limit, and coarser limit, as specified by Oklahoma DOT, are found to be different for the two aggregates studied. For the RS aggregate, the median gradation produces substantially higher M_R values (41 to 129% higher) than the finer limit gradation but only slightly higher values (0 to 26% higher) than the coarser limit gradation. However, for the Sawyer aggregate, the coarser limit gradation produces the highest M_R values (nearly 10 to 36% higher than the finer limit and the median gradations), and the M_R values of the median and the finer limit gradations are nearly the same.

3. An increase in moisture content leads to a decrease in M_R values. The variations of the M_R values between 2% below the OMC and the OMC are nearly -13 to

27% (RS aggregate) and 11 to 37% (Sawyer aggregate), while the variations between the OMC and 2% above the OMC are more than 25 to 80% (RS aggregate) and 18 to 71% (Sawyer aggregate), respectively. Therefore, it is expected that the M_R values will decrease significantly when the specimens reach the state of saturation.

4. The M_R values obtained from the drained tests are 34 to 97% and 25 to 58% higher than those from the undrained tests for the RS and the Sawyer aggregates, respectively. This may be due to (i) the increased density and decreased moisture content in the specimens used in the drained tests; (ii) the pore pressure generated in the specimens used in the undrained tests.

5. As the design of a pavement moves from a moisture content below OMC to higher moisture contents – which is likely to be the case in the field because of frequent rainfall – its service life is expected to be reduced.

6. As M_R values changed due to different factors, the k_1 values were significantly influenced. However, the variation of k_2 value for different cases was not significant. Generally, assuming the k_2 value as 0.5 is a safe assumption for design purposes. The k_1 value, however, should be carefully selected in the design practice, since the variation of k_1 value is significant for different conditions.

7. As the fines increased in a gradation, the k_1 value decreases. However, the k_2 value remains unchanged (near 0.5). On the other hand, as the moisture increased, generally, the k_1 value decreases and the k_2 value slightly increases. As M_R values decrease from the drained to the undrained conditions, the k_1 value decreases and

the k_2 value remains nearly the same for both aggregates. Drainage condition has a significant effect on the k_1 value.

8. The M_R values of the CFA, FBA and CKD stabilized Meridian aggregates increased with an increase in the amount of stabilizing agent and curing time. This is expressed only as a general statement because resilient modulus, and therefore its increase, is highly dependent on the bulk stress and there were instances where instead of an increase a slight decrease of the M_R values was observed.

9. Within the bulk stress range of 84 to 690 kPa and on the basis of range, rather than individual values, the M_R strength gain from 5% to 10% CFA is higher than that from 10% to 15% CFA. The same holds true for FBA. Similarly, curing time indicates that the strength gain from 7 days to 28 days is greater than from 28 days to 90 days although slightly higher values were attained at the end of 90 days.

10. On the basis of 7-day strength it was initially decided to use 15% CKD and therefore only those values which show that they are comparable to 10% CFA and 10% FBA are reported.

11. Curing time has a substantial influence on the increases in M_R of CKD-stabilized aggregate. The 28-day curing period provides sufficient time for major completion of hydration and other chemical reactions helpful for the strength gain. Therefore, a remarkable increase in M_R is observed in the 28-day specimens. With respect to the raw aggregate, the M_R values of 15% CKD-stabilized aggregate increase from a range of 49.42 - 306.59 MPa to 109.35 - 683.15 MPa.

12. The U_C values increased with increasing CFA, FBA, and CKD content and curing

period. The aggregate stabilized with CFA and FBA produced U_C values that are considerably higher than the U_C value of the raw Meridian aggregate. Again, as in conclusion No. 9, the strength gain from 5% to 10% is greater than the 10% to 15% stabilizing agents used. The aggregate stabilized with 15% CKD produced 28-day U_C values of 2163 kPa and the corresponding values for CFA and FBA are 2223 and 3881 kPa, respectively. The 90-day U_C values are 2810 kPa for CKD, 2213 for CFA, and 4910 kPa for FBA.

13. The EM values of the Meridian aggregate also increase significantly as a result of stabilization wherein the beneficiation is proportional to the increase in ash content and curing period in much the same way as the U_C values.

14. The M_R values of the 28-day cured stabilized aggregate are all higher than the M_R values of the good quality (RS) aggregate. Hence, from a comparative point of view, 5% ash content is sufficient to make the marginal aggregate as good as RS aggregate, but higher practical values are attained at 5 to 10% CFA.

15. Cement-kiln-dust, an industrial by-product, is an effective stabilizing agent to strengthen base/subbase aggregate. There is a continuous increase in M_R within the range of addition of CKD. For 7-day curing time, the increased M_R values can be up to 33%, 60% and 73% for the aggregate stabilized with 5%, 10% and 15% CKD, respectively. Considering strength gain and compaction preference, 15% CKD-stabilized aggregate is considered to be most appropriate.

16. Microstructure analysis using SEM techniques reveals that crystals formed during the hydration process contribute to the cementing of particles as an integral body, while the filling of the intracluster voids of the fine particles minimizes possible

elastic deformation of the aggregate. More crystals and less voids are observed with the stabilized specimens having higher amount of CFA, FBA, and CKD and longer curing time.

17. The XRD analyses show the result of chemical activity within the aggregate matrix as a result of stabilization. The analyses lead to the conclusion that the hydration of CFA, FBA, and CKD was followed by crystal formation of ettringite within the matrix observed in the micrographs. The results of the XRD analyses conform with the results of the SEM analyses and M_R and U_C tests.

18. The layer coefficients of the stabilized aggregates are significantly higher than those of the raw aggregates. The layer coefficients of the 90-day cured aggregate stabilized with 10% CFA are as high as 10 times those of the raw Meridian and 1.5 times those of the raw RS aggregate. Similarly, 90-day cured aggregate stabilized with 10% FBA have layer coefficients as high as 12 times than those of the raw Meridian aggregate and 1.8 times those of raw RS aggregate. The FBA stabilized aggregate consistently yielded higher layer coefficients values than the CFA stabilized aggregate. The layer coefficients of the 28-day cured aggregate stabilized with 15% CKD are more than double those of the raw aggregate.

6.2 RECOMMENDATIONS

In view of analyses and conclusions drawn, the following recommendations are made for further studies.

1. To evaluate the effectiveness of chemically stabilized aggregates, particularly durability, as a result of freezing/thawing and wetting/drying action, it is

recommended that a detailed study be carried out including these environmental factors. The effect of freezing/thawing and wetting/drying cycles on resilient behavior is expected to provide valuable information on pavement performance when subjected to such conditions. There is a general perception and exploratory test data indicate that the resilient modulus of stabilized aggregates may significantly reduced due to freezing/thawing and wetting/drying actions, but no previous studies have quantified such effects although they are extremely important from design considerations.

2. A comparison between field and laboratory M_R values of aggregate materials should be pursued. Such a study could involve falling weight deflectometer (FWD) tests to obtain the backcalculated field moduli. Any deviation between the field and the laboratory moduli, if any, is essential to formulate more realistic design procedures and specifications.

3. The drainage condition appears to have a significant effect on M_R values. In the present study, the undrained M_R test was conducted with aggregate having the ODOT median gradation. The influence of undrained condition on M_R values could be different if the different aggregate gradations are used. Hence, the drainage effect should be studied at gradations corresponding to the ODOT coarser limit and the finer limit gradations. Also, to evaluate the drainage capability of stabilized aggregate base, permeability tests (e.g., flexible wall triaxial permeability test) should be performed on various stabilized aggregate specimens. Such a test can take into account the effect of vehicle load-induced stresses on the hydraulic conductivity.

4. Test results from this study indicate that aggregate material is very sensitive to moisture content. Further studies should be conducted to investigate the moisture sensitivity of aggregate materials at different gradations, particularly for the gradations with different percentages of fine particles. Also, gradation analyses should be conducted after the sample preparation and M_R testing processes to investigate (i) if the segregation of particles is produced due to the vibration and compaction used in the sample preparation; and (ii) if the particles are broken down due to the sample compaction and cyclic triaxial testing. These analyses are important in terms of the cyclic behavior of aggregate materials.

5. The marginal aggregate used in the present study is a limestone-type aggregate. Marginal aggregates of other types (e.g. sandstone) should be studied to investigate the effect of stabilization. Also, further cost analysis of the application of different stabilizing agents (e.g. fly ash, lime, cement and CKD) should be conducted to determine the most cost-effective method of chemical stabilization of base/and subbase aggregates.

REFERENCES

American Association of State Highway and Transportation Officials (AASHTO). (1972). *AASHTO interim guide for design of pavement structures.* AASHTO, Washington, D.C.

American Association of State Highway and Transportation Officials (AASHTO). (1982). "Suggested method of test for resilient modulus of subgrade soils, AASHTO DESIGNATION: T 274-82," Washington, D.C.

American Association of State Highway and Transportation Officials (AASHTO). (1991). "Interim method of test for resilient modulus of subgrade soils and untreated base/subbase materials, AASHTO DESIGNATION: T 292-91I," Washington, D.C.

American Association of State Highway and Transportation Officials (AASHTO). (1992). "Interim method of test for resilient modulus of unbound base/subbase materials and subgrade soils - SHRP Protocol P46, AASHTO DESIGNATION: T 294-92I," Washington, D.C.

American Association of State Highway and Transportation Officials (AASHTO) (1993). *AASHTO guide for design of pavement structures.* AASHTO, Washington, D.C.

American Association of State Highway and Transportation Officials (AASHTO). (1993a). "Sieve analysis of fine and coarse aggregates, AASHTO DESIGNATION: T 27-93," Washington, D.C.

American Association of State Highway and Transportation Officials (AASHTO). (1993b). "Moisture-density relations of soils using a (4.55-kg) 10-lb rammer and an (457-mm) 18-in. Drop, AASHTO DESIGNATION: T 180-93," Washington, D.C.

American Association of State Highway and Transportation Officials (AASHTO). (1994a). "Standard method of test for resilient modulus of unbound base/subbase materials and subgrade soils - SHRP Protocol P46, AASHTO DESIGNATION: T 294-94," Washington, D.C.

American Association of State Highway and Transportation Officials (AASHTO). (1994b). "Resistance to degradation of small-size coarse aggregate by abrasion and impact in the Los Angeles machine, AASHTO DESIGNATION: T 96-94," Washington, D.C.

American Association of State Highway and Transportation Officials (AASHTO). (1994c). "Specific gravity and absorption of fine aggregate, AASHTO DESIGNATION: T 84-94," Washington, D.C.

Azad, S. (1998), "Soil stabilization of three different soils using cement kiln dust." *Master Thesis*, School of Civil Engineering and Environmental Science, University of Oklahoma.

Baghdadi, Z. A. and Rahman, A. (1990). "The potential of cement kiln dust for the stabilization of dune sand in highway construction." *J. Build. and Envir.*, Oxford, England, 25(4), 285-289.

Barksdale, R.D. and Itani, S.Y. (1989). "Influence of aggregate shape on base behavior," *Transportation Research Record, No. 1227*, Transportation Research Board, Washington, D.C., 173-182.

Boynton, R. S. (1980), *Chemistry and Technology of Lime and Limestone*, 2nd. Edn., John Wiley & Sons, Inc., New York, N.Y.

Cross, S.A. and Fager, G.A. (1995). "Fly ash in cold recycled bituminous pavements," *Transportation Research Record, No. 1486*, Transportation Research Board, Washington, D.C., 49-56.

Chen, D.H. (1994). "Resilient modulus of aggregate bases and a mechanistic-empirical methodology for flexible pavements," PhD dissertation, School of Civil Engineering and Environmental Science, University of Oklahoma, Norman, Oklahoma.

Das, B.M. (1990). *Principles of Geotechnical Engineering*. Second Edition. PWS Publishers.

Elliott, R.P. and Thornton, S.I. (1988). "Resilient modulus and AASHTO pavement design," *Transportation Research Record, No. 1196*, Transportation Research Board, Washington, D.C., 116-124.

Gerrity, D.M, Metcalf, J.B., and Seals, R.K. (1994). "Estimating the design life of a prototype cement-stabilized phosphogypsum pavement" *Transportation Research Record, No. 1440*, Transportation Research Board, Washington, D.C., 32-36.

Gould, C. N. (1930). "Oklahoma geological survey," *Oil and Gas in Oklahoma,* Volume III, Norman, Oklahoma.

Gray, D.H., Tons, E., and Thiruvengadam, T.R. (1994). "Performance evaluation of a cement-stabilized fly ash base," *Transportation Research Record, No. 1440*, Transportation Research Board, Washington, D.C., 8-15.

Harichandran, R.S., Yeh, M.S., and Baladi G.Y. (1989). "MICH-PAVE user's manual," *Final Report, FHWA-MI-RD-89-032*, Department of Civil and Environmental Engineering, Michigan State University, East Lansing, Michigan.

Haynes, J.H. and Yoder, E.J. (1963). "Effects of repeated loading on gravel and crushed stone base course materials used in the AASHTO road test," *Highway Research Record No. 39*, Highway Research Board, Washington, D.C., 82-96.

Hicks, R.G. (1970). "Factors influencing the resilient properties of granular materials," Ph.D. dissertation, University of California at Berkeley, California.

Hopkins, T.C., Hunsucker, D.Q., and Beckham, T. (1994). "Selection of design strengths of untreated soil subgrades and subgrades treated with cement and hydrated lime," *Transportation Research Record, No. 1440*, Transportation Research Board, Washington, D.C., 37-52.

Huang, Y.H. (1993). *Pavement analysis and design.* Prentice-Hall, Inc., Englewood Cliffs, N.J.

Huffman, G.G., Alfonsi, P.P., Dalton, R.C., Duarte-Vivas, A., and Jeffries, E.L. (1975). *Geology and mineral resources of Choctaw county, Oklahoma.* Bulletin 120, Oklahoma Geological Survey.

Johnson, E.G. and Hicks, R.G. (1987). "Evaluation of effect of uncrushed base layers on pavement performance," *Transportation Research Record, No. 1117*, Transportation Research Board, Washington, D.C., 11-20.

Kamal, M.A., Dawson, A.R., Farouki, O.T., Hughes, A.B., and Sha'at, A.A. (1993). "Field and laboratory evaluation of the mechanical behavior of unbound granular materials in pavements," *Paper presented at 72nd Annual Meeting of the Transportation Research Board*, Washington, D.C., January 12, 1993.

Khedr, S. (1985). "Deformation characteristics of granular base course in flexible pavements," *Transportation Research Record, No. 1043*, Transportation Research Board, Washington, D.C., 131-138.

Ksaibati, K. and Conklin, T.L. (1994). "Field performance evaluation of cement-treated bases with or without fly ash," *Transportation Research Record, No. 1440*, Transportation Research Board, Washington, D.C., 16-21.

Laguros, J.G. and Zenieris, P. (1987). "Feasibility of using fly ash as a binder in coarse and fine aggregates for bases," *Final Report, ORA 155-404, FHWA/OK 86(8)*, Office of Research Administration, University of Oklahoma, Norman, Oklahoma.

Lary, J.A. and Mahoney, J.P. (1984). "Seasonal effects on the strength of pavement structures," *Transportation Research Record, No. 954*, Transportation Research Board, Washington, D.C., 41-49.

Lee, S.W. and Fishman, K.L. (1992). "Improved resilient modulus realized with waste product mixtures," *Geotechnical Special Publication, Vol. 2, No. 30*, American Society of Civil Engineers, New York, N.Y., 1356-1367.

Lofti, H. A. and Witczak, M. W. (1985), "Dynamic characterization of cement-treated base and subbase materials." *Transportation Research Record 1031,* TRB, National Research Council, Washington, DC., 41-48.

McManis, K. L. and Arman, A. (1989). "Class C fly ash as a full or partial replacement for Portland cement or lime." *Transportation Research Record 1219,* TRB, National Research Council, Washington, D.C., 68-81.

Mendenhall, W. and Sincich, T. (1992). *Statistics for engineering and the sciences*. Third Edition, Dellen Publishing Company, San Francisco, California.

Miller, G. A., Azad, S. and Dhar, B., (1997), "The effect of kiln dust on the collapse potential of compacted shale." *Testing Soil Mixed with waste or Recycled Materials, ASTM STP 1275.* Mark A. Wasemiller, Keith B. Hoddinott, Eds., American Society for Testing and Materials.

Mitchell, J. K. (1981), " Soil improvement - state of the art report." *Proc., 11th ICSMFE*, Vol. 4, 509-565.

Monismith, C. L. (1992), "Analytically based asphalt pavement design and rehabilitation: Theory and practice, 1962-1992," *Transportation Research Record 1354,* TRB, National Research Council, Washington, D.C., 5-26.

Oklahoma Department of Transportation (ODOT) (1996). *Standard Specifications for Highway Construction.* 1996 Edition, Oklahoma City, Oklahoma.

Pandey, K.K., Zaman, M.M., and Laguros, J.G. (1998). "Resilient moduli of raw and stabilized aggregate bases and evaluation of layer coefficients for AASHTO flexible pavement design," Final Report Volume III (Coal Ash Stabilized Aggregates), the University of Oklahoma, Norman, Oklahoma.

Pezo, R.F., Claros, G., Hudson, W.R., and Stoke, K. H. (1992). "Development of a reliable resilient modulus test for subgrade and non-granular subbase materials for use in routine pavement design," *Research Report 1177-4f*, Center for Transportation Research, Bureau of Engineering Research. The University of Texas at Austin.

Rada, G. and Witczak, M. (1981). "Comprehensive evaluation of laboratory moduli results for granular material," *Transportation Research Record, No. 810*, Transportation Research Board, Washington, D.C., 23-33.

Rowland, T.L. (1972). *General Survey of Carbonate Mineral Deposits in Oklahoma.* Oklahoma Geology Notes, Vol. 32, No. 3, Oklahoma Geological Survey.

Sayah, A. I. (1993), "Stabilization of expansive clay using cement dust," M.Sc. Thesis, Graduate College, University of Oklahoma, Norman.

Spangler M.G. and Handy R.L. (1973). *Soil Engineering*. Intext Educational Publishers, New York, NY.

Thompson, M.R. (1989). "Factors affecting the resilient moduli of soil and granular materials," Workshop on Resilient Modulus Testing, Oregon State University, Corvallis, Oregon, March 28-30, 1989.

Tian, P., Zaman, M.M., and Laguros, J.G. (1998). "Resilient moduli of raw and stabilized aggregate bases and evaluation of layer coefficients for AASHTO flexible pavement design," Final Report Volume II (Raw Aggregates), the University of Oklahoma, Norman, Oklahoma.

Usmen, M. and Baradan, B. (1991). "Properties and environmental impact of stabilized fly ash," *Proceedings, Specialty Conference: Energy in the 90's*, March 10-13, Sponsored by the Energy Division of the American Society of Civil Engineers, New York, N.Y., 208-214.

Van Til, C.J., McCullough, Vallerga, B.A., and Hicks, R.G. (1972). "Evaluation of AASHO interim guides for design of pavement structures," *NCHRP Report No. 128*, Highway Research Board, Washington, D.C.

Wright, P. "Highway Engineering," John Wiley, New York, N.Y., 1996, 6th Ed., p. 469.

Yi L. P. (1995), "Resilient moduli of fly ash stabilized aggregates." Master's thesis, University of Oklahoma, Norman.

Zaman, M., Laguros, J. G. and Sayah, A. (1992), " Soil stabilization using cement kiln dust," *Proc. 7th Int. Conf. On Expansive Soils*, Dallas, Texas, 1-5.

Zaman, M.M., Chen, D.H., and Laguros, J. (1994). "Resilient modulus of granular materials," *Journal of Transportation Engineering*, Vol. 120, No. 6, American Society of Civil Engineers, New York, N.Y., 967-988.

Zenieris, P. E. and Laguros, J. G. (1988). "Fly Ash as a binder in aggregate base courses", Materials Research Society, Fly Ash and Coal Conversion By-Products: Characterization, Utilization, and Disposal IV, Symposium Proceeding, Vol. 113, 231-241.

Zhu, J.H., Zaman, M.M., and Laguros, J.G. (1998). "Resilient moduli of raw and stabilized aggregate bases and evaluation of layer coefficients for AASHTO flexible pavement design," Final Report Volume IV (Cement-Kiln-Dust Stabilized Aggregates), the University of Oklahoma, Norman, Oklahoma.